MPR ASSOCIATES, INC.

NINE MILE POINT UNIT 1

LEAK-BEFORE-BREAK ANALYSIS OF HIGH ENERGY PIPING SYSTEMS

MPR-820, Rev. 2

Prepared for:

Niagara Mohawk Power Corporation
Syracuse, New York

May 1984
Rev. 1, July 1984
Rev. 2, August 1984

1050 CONNECTICUT AVENUE, N.W. WASHINGTON, D.C. 20036 202-659-2320

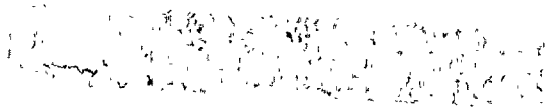

TABLE OF CONTENTS

I. INTRODUCTION

Analyses have been performed to evaluate the likelihood of unstable ruptures in high energy piping at the Nine Mile Point Unit 1. Specifically, the analyses demonstrate that, for representative high energy piping systems in the reactor and turbine buildings, leaks will develop before flaws can grow to unstable sizes, and that the resulting leakage can be detected and appropriate action taken before the risk of unstable piping failure develops.

The objectives of this study are to:

- Identify for analysis representative high energy piping systems, fabricated from both carbon steel and stainless steel and carrying both subcooled water and steam.
- Evaluate existing leakage detection capability at Nine Mile Point Unit 1, and establish a leak rate for both the reactor building and turbine building that is clearly detectable.
- Develop, and benchmark against existing test data, a thermo-hydraulic model for prediction of leak rates through tight cracks in pipes and establish flaw sizes for each piping system that will, under pressure loading only, result in the established detectable leak rate.
- Perform finite element stress analyses of each piping system and evaluate the stresses from deadweight, pressure and safe shutdown earthquake loads, i.e., ASME Code Service Level D loads.
- Perform elastic and elastic-plastic fracture mechanics evaluations of each piping system to determine if postulated through-wall axial and circumferential flaws will not show substantial growth as a result of Service Level D loadings. Further, show that large (one-quarter circumference) circumferentially oriented, through-wall flaws are stable under fully plastic loads.

- Establish leakage monitoring requirements to assure the postulated detectable leak rate is detected.

The general methodology for performing the fracture mechanics analyses has been developed by nuclear steam system suppliers, utilities, the NRC and NRC consultants, and has been used in numerous operating plant applications, including Systematic Evaluation Program evaluations. Appropriate analysis guidelines and acceptance criteria were outlined in the enclosures to the NRC letter, Reference 1.

II. SUMMARY

Stress analyses and fracture mechanics evaluations have been performed for the main steam, reactor feedwater, emergency condenser steam supply and condensate return and reactor water cleanup piping described in Section III of this report. The evaluations were performed using conservative values of crack extension resistance, axial and circumferential postulated through-wall flaw size, and ASME Code Service Level D axial and bending loads. Flaw sizes for linear elastic analyses were selected as those through-wall flaw sizes (axial and circumferential) which will produce leak rates which can be reliably detected by leakage detection systems currently being monitored at Nine Mile Point Unit 1. The flaw size for the extreme plastic load analysis (90° circumferential) was established by the NRC guidelines in Reference 1.

The specific objectives for the fracture mechanics analyses were the following:

- Using linear elastic or elastic-plastic methods, show that insignificant flaw growth occurs under Service Level D loads for flaw sizes dictated by leakage detection capabilities.
- For extreme plastic loads, show that 90° through-wall circumferential flaws display no unstable tearing behavior.

The results of the evaluations show that no growth of the postulated flaw occurs under Service Level D loads in the main steam, reactor water cleanup, reactor feedwater and emergency condenser condensate return piping. The flaw growth in the emergency condenser steam supply piping is

insignificant (0.17 inches with a 7.94 inch initial flaw). Further, no unstable tearing occurs in any of the piping systems with a postulated 90° flaw under Service Level D loadings. Loads resulting in unstable tearing or plastic collapse range from 1.26 to 2.10 times the conservative Service Level D loads assumed in the analysis. Loads resulting in plastic collapse for the postulated 90° flaw are often more limiting than the loads required for unstable tearing when piping system compliance effects are considered. Because of the conservatism with which flaw size and Level D service loads were established, and the acceptable results obtained using these conservative criteria, it is concluded that the probability for a catastrophic pipe failure is insignificantly small. Therefore, a full double-ended pipe break need not be postulated as a design basis for defining loads at Nine Mile Point Unit 1.

III. METHODOLOGY AND RESULTS OF ANALYSES

A. Piping Systems

Leak-before-break analyses were performed for piping systems in the Nine Mile Point Unit 1 Reactor and Turbine Buildings: Main Steam, Reactor Feedwater, Emergency Condenser and Reactor Water Cleanup. These systems are considered to have the highest potential for unacceptable break consequences and represent both large and small diameter piping, carbon and stainless steel material, and carry both steam and subcooled water.

B. NRC Guidelines for Analyses

The NRC, as part of its resolution of high energy line break safety issues, provided general guidelines, Reference 1, for using fracture mechanics methods to evaluate leak-before-break conditions in piping in nuclear facilities in the Systematic Evaluation Program. These guidelines can be summarized as follows:

- Demonstrate the capability to detect a 2t (two times the wall thickness) flaw under normal operating conditions.
- Show, using elastic or elastic-plastic fracture mechanics methods, that longitudinal or circumferential through-wall flaws 4t in length will not extend when subjected to ASME Code Service Level D loads. If extension is predicted, show it is insignificant.
- Show that there is margin against unstable growth for a 90° circumferentially oriented flaw subjected to extreme loads.

- Show that there is a positive tendency for part-through wall cracks to grow radially through-wall rather than to grow around the pipe circumference.

The methods used to perform leak-before-break evaluations of the four piping systems at Nine Mile Point Unit 1 differ in one respect from these guidelines. The detection of leakage from a 2t flaw may be impossible for small pipe, as in the reactor water cleanup system, where the 2t flow rate could be hundredths of a gallon per minute. Requirements for finding such small leaks by sensitive local leak detection methods may be complicated and unnecessary, especially when considering that larger flaws could be tolerated safely. Therefore, it was concluded that the postulated flaw size in each piping system should be based on the leakage rate which can be readily detected by existing leak detection and other methods. As will be shown in Section III.C., a leak rate of one gallon per minute is easily detected by existing floor drain sump pump monitoring methods. Therefore, the flaw size for crack extension studies was established as the one gallon per minute flaw size plus 2t, in accordance with the intent of the NRC guidelines to provide some flaw size margin in the analysis. While this approach differs from the NRC guidelines, it results in the evaluation of substantially larger postulated flaws which can be readily detected. Subsequent fracture mechanics analyses, which are intended to demonstrate stable behavior of these postulated flaws, are therefore more conservative than required by NRC guidelines.

C. Leak Detection

An evaluation of the reactor building and turbine building floor drain sump logs taken in January and February 1984, indicates that a leak rate of one gallon per minute or greater would be easily detected from sump pump run time data, which is taken daily. Table 1 shows sump pump flow rate data for this period. These flow rates are all less than the 1440 gallons per day that would result from a 1 gallon per minute leak.

TABLE 1

SUMP PUMP FLOW RATES
JANUARY-FEBRUARY 1984

Sump Identification	Location	Average Flow Rate (gal/day)	Maximum Flow Rate (gal/day)
R-11	Reactor Building	31.0	42.9
R-12	Reactor Building	5.4	9.4
R-13	Reactor Building	1.1	8.6
R-14	Reactor Building	0.0	0.0
R-15	Reactor Building	412.7	744.4
R-16	Reactor Building	1.5	10.3
T-11	Turbine Building	186.9	336.0
T-13	Turbine Building	20.1	103.9
T-14	Turbine Building	215.8	550.7
T-16	Turbine Building	273.2	783.7
T-17	Turbine Building	14.8	25.1
T-18	Turbine Building	50.0	231.4

Further, an evaluation of existing crack growth rate data indicates that flaw growth does not significantly affect leak-before-break safety margins over a period of several weeks after the one-gallon-per-minute rate is reached. Therefore, no special leak detection equipment is required to detect such a leak before flaw growth becomes significant. On this basis, a one-gallon-per-minute leak rate was established for flaw size calculations in each system.

D. Leak Rate Modeling

The correlation between crack size and leak rate was calculated using CRACKFLO, a specialized computer code developed for this purpose. This computer model assumes that the pressure loss through the crack can be described by a typical fL/D loss mechanism. Choking is evaluated using a homogeneous choking model which depends on local stagnation pressure and stagnation enthalpy at the choke point. The flow area caused by opening of the crack due to internal pressure was determined from formulas given in NRC guidelines in Reference 1. CRACKFLO results compare favorably to measured flows through small slits reported in Reference 2. Conservative estimates of flow through tight cracks were obtained by using a friction factor based on a relative roughness of 0.1. Similar flows are predicted by this model for tight cracks as were reported by the LEAKS 01 model developed for EPRI in Reference 3. A more detailed description of CRACKFLO, and its technical bases, is provided in Appendix A.

E. Stress Analysis

Finite-element stress analyses were performed for each piping system using the ANSYS computer code. The carbon steel main steam system was modeled from the anchors at the external main steam line isolation valves to the inlets to the turbine stop and control valve manifold. A large portion of the turbine bypass line was also modeled since it affects stresses in the main steam line. The carbon steel high pressure reactor feedwater piping was modeled from the exits of the fifth stage feedwater heaters to the external feedwater isolation valves. The west bank emergency condenser stainless steel steam supply and condensate return lines were modeled in their entirety, between the reactor vessel (steam supply), recirculation line (condensate return) and emergency condensers #111 and #112. Finally, the carbon steel reactor water cleanup piping was modeled from the external reactor water cleanup isolation valve to the first regenerative heat exchanger, including the branch to the inlet of auxiliary cleanup pump No. 1. The five models are shown in Figures 1 through 5. Normal operating conditions and pipe material for each system are shown in Table 2.

The four representative piping systems were analyzed for ASME Service Level D loads: pressure, deadweight, and safe shutdown earthquake. Amplified floor response spectra for seismic analyses were obtained from the bounding analyses of Reference 4. These floor response spectra are based on a Reg. Guide 1.60 ground motion spectra anchored at 0.11g ZPA. This ZPA is in

TABLE 2

OPERATING CONDITIONS

Piping System	Material	Normal Operating Pressure (psi)	Normal Operating Temperature (°F)	Fluid State
Reactor Water Cleanup	Carbon Steel	1030	530	Water
Main Steam	Carbon Steel	1030	550	Steam
Reactor Feedwater	Carbon Steel	1050	360	Water
Emergency Condenser Steam Supply	Stainless Steel	1030	550	Steam
Emergency Condenser Condensate Return	Stainless Steel	1030	530*	Water

* Value for the system in service.

accordance with the NMP-1 design basis given in the FSAR. More realistic response spectra are now being developed for Nine Mile Point Unit 1. The spectra used in the leak-before-break analysis are upper-bound values enveloping the expected finalized spectrum. Damping values for the seismic analyses were chosen in accordance with Regulatory Guide 1.61, and are also considered to be very conservative, particularly for the relatively severe Level D loads.

A more detailed description of the piping system models, loads and stress results is given in Appendix B.

F. Fracture Mechanics Methodology

Elastic and elastic-plastic fracture mechanics analyses were performed for Service Level D loads and extreme loads to evaluate the stability of crack extension in each piping system. The various methodologies are discussed below, and are described in more detail in Appendices C, D and E.

1. Crack Extension - Crack extension under Service Level D loads for the 1 gpm plus 2t flaw was calculated by means of the crack driving potential, or J-integral, as recommended in the Reference 1 guidelines. The calculated value of J at the cracked section is compared to the critical value of J for the material, J_{IC}, to determine if the crack will grow. The determination of J_{IC} for

carbon and stainless steels is discussed in Section 3 below.

When stresses are low, the value of J is related to the more traditional stress intensity factor by the relation

$$J = K_I^2/E.$$

Elastic K_I solutions are available in Reference 1. Suitable plastic zone corrections for ductile materials were applied to calculate an effective crack length, as outlined in Reference 5.

As stresses increase, the net section at the postulated crack can become plastic before J_{IC} is reached. In this case, the more generalized expression for J was used:

$$J = Je + Jp,$$

where Je is the plastic zone corrected value of J discussed above and Jp is the plastic contribution to J. The plastic contribution to J has been studied in detail by General Electric Company in References 6, 7, 8 and 9. The analysis procedure uses methodology for a single edge cracked plate (representing 1/2 the pipe) modified to account for pipe curvature. The plastic contribution to J is expressed in the form

$$Jp = \alpha \varepsilon_o \sigma_o ch_1(a/b,n)[M/M_o]^{n+1}$$

where

α,n are the strain hardening fitting coefficient and exponent for the material

σ_o is the yield strength, psi

ε_o is σ_o/E

c is the remaining uncracked length on the pipe circumference (for 1/2 the pipe)

a is half the crack length

b is half the pipe circumference (c = b - a)

h_1 is a tabulated function of a/b and n

M is the effective applied moment for Service Level D loads (for 1/2 the pipe)

M_o is the moment at which the remaining uncracked section becomes fully plastic (for 1/2 the pipe)

The plastic contribution to the cracked section hinge angle, φ_c, can be calculated in a similar manner to J:

$$\varphi_c = \alpha \varepsilon_o h_3(a/b,n) [M/M_o]^n$$

This function is needed for tearing stability analyses, discussed below.

2. Tearing Stability Analysis - The cracked section resistance to unstable tearing is determined by examining the moment carried by the crack and mathematically perturbing the assumed flaw size. Paris, in Reference 10, states that stability is assured if the moment lost from the cracked section due to an increase in crack length is less than the moment that is picked up by the piping

system via the increase in cracked section hinge angle. A stable condition then is represented by:

$$\left| \frac{dM}{d\varphi_c} \right|_{\text{crack}} < \left| \frac{dM}{d\varphi_c} \right|_{\text{piping}}$$

The expression on the right can be evaluated directly from the piping finite element model by inserting into the model a ball joint at the cracked node and applying a moment couple on the joint. In Paris' notation, this is the system residual stiffness. The system residual stiffness is often equated to the stiffness of a cantilever beam of length L with the same area moment of inertia, I, and radius, R, of the pipe. The ratio, L/R, of the equivalent cantilevered pipe will be used to report system residual stiffnesses (or compliances) in this report.

The expression on the left can be evaluated in terms of the partial derivatives of J and φ_c with respect to crack size, a, and applied moment, M, and a material property called the tearing modulus which is defined as

$$T_{MAT} = E/\sigma_o^2 \frac{dJ}{da}$$

T_{MAT} is determined directly from the slope of J vs Δa test data for the material of interest. In terms of these parameters, the stability criterion becomes:

$$T_{MAT} > \frac{E}{\sigma_o^2} \frac{1}{t} \left[\left(\partial\varphi_c/\partial a \right)_M / \left(\partial\varphi_c/\partial M \right)_a \right]^2 \times$$

$$\times \left[\left| \frac{dM}{d\varphi_c} \right|_{pipe} + 1/\left(\partial\varphi_c/\partial M \right)_a \right]^{-1} +$$

$$+ \frac{E}{\sigma_o^2} \left\{ \left(\frac{\partial J}{\partial a} \right)_M - \left[\left(\partial\varphi_c/\partial a \right)_M / \left(\partial\varphi_c/\partial M \right)_a \right] \left(\frac{\partial J}{\partial M} \right)_a \right\}$$

Since the expressions on the right side of the inequality are all functions of the ratio M/Mo, actual margins to tearing instability can be directly calculated in terms of applied moment.

3. Material Properties - The main steam, reactor feedwater and reactor water cleanup systems of Nine Mile Point Unit 1 are fabricated from A106, Gr.B carbon steel. The emergency condenser steam supply and condensate return lines are A376, type 304 stainless steel.

Strain hardening coefficients for carbon steel were reported for A212 material (similar to A106) in the annealed and also the normalized conditions in Reference 11. Data for A106 material are not available. A conservative upper bound value for n was chosen from among the normalized A212 data. The coefficient, α was determined from large strain stress strain data for carbon steel in Reference 12.

Large strain stress-strain data are available for Type 304 stainless steel at elevated temperatures in Reference 13. The strain hardening exponent, n, and also α were determined from these data.

The data used to define the J_{IC} and tearing modulus values for A106 Gr.B material were selected as lower bound values from all available data at 550°F, the reactor nominal operating temperature. A strong effect of plate rolling direction on J_{IC} and T_{MAT} was noted, and worst case data were used. Values of J_{IC} and T_{MAT} used

in the analysis were determined from data in Reference 14. The determination of J_{IC} and T_{MAT} is shown in Appendix F.

The data base used to define J_{IC} and T_{MAT} for Type 304 stainless steel was obtained from stainless steel weld material test data at 550°F in Reference 14. The weld material has lower crack initiation and growth resistance than the base material, and provides a lower bound estimate of material properties. Appendix F shows the determination of J_{IC} and T_{MAT} for stainless steel.

The material property values used in the analyses are presented in Table 3. In this table, tensile properties for A106 GrB material are based on ASME Code minimum values. The same is true for Type 304 stainless steel except for yield strength, where the value taken is that of the material in Reference 12 whose strain hardening behavior was quantified.

TABLE 3

MATERIAL PROPERTIES

	A106 Gr. B	A376, Type 304
Elastic Modulus, E (ksi)	27.0×10^3	25.6×10^3
Yield Stress, σ_o (ksi)	27.1	23.0
Flow Stress, σ_f (ksi)	43.6	42.0
J_{IC} (in-lb/in^2)	903	992
T_{MAT}	214	182
α	1.94	2.13
n	4.42	3.79

4. Net Section Plastic Collapse - The presence of the postulated 90°, circumferential, through-wall flaw will reduce the ultimate load carrying capacity of the pipe section. To ensure that the cracked section has adequate margin against net section plastic collapse, limit load calculations were performed to define the margin against collapse for extreme bending loads compared to the load at tearing instability.

The limit moment was determined from Reference 9 and is expressed as

$$M_f = 4\sigma_f R^2 t \left(\cos\frac{\gamma}{2} - \tfrac{1}{2}\sin\gamma\right)$$

where:

R = the mean pipe radius,

t = the pipe wall thickness,

γ = half crack angle,

σ_f = flow stress (values given in Table 3).

5. Through-Wall Crack Development - The purpose of this evaluation is to demonstrate that assumed through-wall flaws are appropriate bounding flaws for analysis purposes. Since part through flaws cannot be found by leak detection methods, such flaws must demonstrate a propensity to grow radially and leak before becoming large circumferentially and posing a sudden pipe rupture threat. The preference for radial growth can be demonstrated under normal operating conditions and under conditions of large axial or bending loads.

For normal operating conditions, a large body of operating history data exist that show that cracks in BWR and PWR primary and secondary systems tend to grow radially and leak before becoming a break threat (References 15 to 17). These data cover various initiation and growth mechanisms and exposure to various stress conditions.

For large axial and bending loads the crack driving force, J, for a part-through wall crack is always larger in the radial direction than in the circumferential direction (Reference 18). This variation is shown in Figure 6, taken from Reference 18. On the basis that crack driving force will determine the direction of flaw growth, it can be assumed that flaws will grow radially and leak under severe load conditions.

G. Results

Through-wall longitudinal and circumferential flaw sizes corresponding to a 1 gpm leak rate were determined for each pipe size in each system and are presented in Table 4. Flaw sizes for use in fracture mechanics evaluations were increased by two times the wall thickness to provide margin for flaw growth, consistent with NRC guidelines in Reference 1.

Numerical calculations were performed to determine stresses in each system resulting from deadweight, pressure and seismic loads. These stresses were combined and the most highly stressed areas in each system were identified.

TABLE 4

ONE GPM CRACK LENGTHS

PIPING SYSTEM	OD (in)	1 GPM CIRCUMFERENTIAL CRACK LENGTH A (in)	1 GPM LONGITUDINAL CRACK LENGTH A (in)
Main Steam	16	8.5	6.0
	18	9.5	5.7
	24	8.9	5.0
Reactor Water Cleanup	6.625	4.1	2.5
Reactor Feedwater	14	4.8	3.1
	16	4.9	3.1
	18	5.1	3.2
Emergency Condenser Steam Supply	12.75	6.7	3.8
Emergency Condenser Condensate Return	10.75	3.4	2.1

Linear elastic and elastic-plastic fracture mechanics analyses were performed to determine if assumed initial 1 gpm + 2t flaws are likely to grow under Service Level D loads. Results for these analyses are shown in Tables 5 and 6. In these tables, it can be seen that $J < J_{IC}$ in every case except for the emergency condenser steam supply piping where a small growth, 0.17 inch, is expected in a circumferentially oriented flaw. This is only 2% of the initial flaw size and is considered insignificant.

The margin to instability of a 90° circumferential flaw was investigated by varying the applied moment and comparing the moment at instability to the moment resulting from Level D Service loads. This was done conservatively by assuming infinite piping compliance ($L/R = \infty$). In some cases, actual system L/R values were evaluated at the locations of highest stress, conservatively assuming all snubbers and seismic constraints are inoperable, as recommended in Reference 1. The relation between system residual stiffness, K_φ, and L/R is:

$$L/R = \frac{EI}{K_\varphi R}, \text{ where } K_\varphi = \left.\frac{dM}{d\varphi_c}\right| \text{pipe},$$

E is the modulus of elasticity and I is the area moment of inertia.

Results of this evaluation are shown in Table 7. It is apparent that the margin between the load required for tearing instability or plastic collapse and the conservative Level D Service loads is adequate (> 1.25) in all cases. It is notable that, when system compliance

effects (L/R) were considered, the limiting condition was determined to be plastic collapse rather than tearing instability.

TABLE 5

CIRCUMFERENTIAL FLAWS

SYSTEM	OUTSIDE DIAMETER (in)	WALL THICKNESS (in)	MATERIAL	TOTAL STRESS @ FLAW[1] (psi)	A_o[2] (in)	J (in-lbs/in^2)	J/J_{IC}[3]	LEAKAGE FLOW (gpm)	Δa[4] (in)
Reactor Cleanup	6.625	0.432	CS	13,947	5.0	210	0.23	1.6	0
Main Steam	16.0	1.031	CS	16,817	10.56	520	0.58	1.8	0
	18.0	1.156	CS	16,388	11.81	537	0.59	1.9	0
	24.0	1.219	CS	17,708	11.34	470	0.52	2.1	0
Reactor Feedwater	14.0	0.937	CS	24,439	6.67	879	0.97	2.5	0
	16.0	1.031	CS	19,832	6.96	375	0.43	2.7	0
	18.0	1.156	CS	25,342	7.41	534[5]	0.59	3.0	0
Emer. Cond. - Condensate	10.75	0.522	SS	21,336	4.44	417	0.42	2.0	0
Emer. Cond. - Steam	12.75	0.622	SS	23,201	7.94	1,317[5]	1.33	1.7	0.17

NOTES:

(1) Total Stress = Bending Stress + Axial Stress + Pressure Stress under Deadweight + Safe Shutdown Earthquake Loading

(2) One gpm flaw size + 2T

(3) Carbon Steel: J_{IC} = 903 in-lb/in^2

Stainless Steel: J_{IC} = 992 in-lb/in^2

(4) Crack growth resulting from applied J.

(5) Calculated with elastic-plastic theory.

TABLE 6

LONGITUDINAL FLAWS

SYSTEM	OUTSIDE DIAMETER (in)	WALL THICKNESS (in)	MATERIAL	CIRCUMFERENTIAL PRESSURE STRESS (psi)	A_o (1) (in)	J (in-lbs/in^2)	J/J_{IC} (2)	LEAKAGE FLOW (gpm)
Reactor Cleanup	6.625	0.432	CS	6868	3.36	69	0.07	2.2
Main Steam	16.0	1.031	CS	7097	8.06	130	0.14	3.4
	18.0	1.156	CS	7125	8.01	101	0.11	4.0
	24.0	1.219	CS	9286	7.44	126	0.14	2.7
Reactor Feedwater	14.0	0.937	CS	6794	4.97	36	0.04	4.9
	16.0	1.031	CS	7097	5.16	37	0.04	4.9
	18.0	1.156	CS	7125	5.51	38	0.05	5.2
Emer. Cond. - Condensate	10.75	0.522	SS	9576	3.14	80	0.08	3.4
Emer. Cond. - Steam	12.75	0.622	SS	9527	5.04	Note (3)	Note (3)	2.2

NOTES:

(1) One gpm flaw size + 2T

(2) Carbon Steel: J_{IC} = 903 in-lb/in^2

Stainless Steel: J_{IC} = 992 in-lb/in^2

(3) Plasticity effects precluded a linear elastic calculation. Value of J expected to be similar to condensate line.

TABLE 7

ELASTIC-PLASTIC RESULTS

SYSTEM	OUTSIDE DIAMETER (in)	WALL THICKNESS (in)	MATERIAL	APPLIED TEARING MODULUS T (1)	LEVEL D STRESS (psi)	MARGIN TO INSTABILITY (2) (3)
Reactor Cleanup	6.625	0.432	CS	27	13,947	2.10
Main Steam	16.0	1.031	CS	28	16,817	1.75
	18.0	1.156	CS	28	16,388	1.80
	24.0	1.219	CS	31	17,708	1.62
Reactor Feedwater	14.0	0.937	CS	17	24,439	1.29(4)
	16.0	1.031	CS	10	19,832	1.61(5)
	18.0	1.156	CS	30	25,342	1.26(6)
Emer. Cond. - Condensate	10.75	0.522	SS	49	21,336	1.43(7)
Emer. Cond. - Steam	12.75	0.622	SS	55	23,201	1.32(8)

NOTES:

(1) Carbon Steel: $T_{mat} = 215$
Stainless Steel: $T_{mat} = 182$

(2) Moment required to unstably tear a 90° flawed pipe divided by the equivalent moment resulting in Level D stress in an unflawed pipe.

(3) Unless otherwise indicated, $L/R = \infty$.

(4) L/R = 73. For L/R = 73, instability is controlled by plastic collapse rather than unstable tearing. For $L/R = \infty$, Margin = 1.20.

(5) L/R = 63. For L/R = 63, instability is controlled by plastic collapse rather than unstable tearing. For $L/R = \infty$, Margin = 1.49.

(6) L/R = 110. For L/R 110, instability is controlled by plastic collapse rather than unstable tearing. For $L/R = \infty$, Margin = 1.06.

(7) L/R = 262. For L/R 262, instability is controlled by plastic collapse rather than unstable tearing. For $L/R = \infty$, Margin = 1.15.

(8) L/R = 178. For L/R 178, instability is controlled by plastic collapse rather than unstable tearing. For $L/R = \infty$, Margin = 1.05.

MPR ASSOCIATES
F-85-45-3
6/13/84

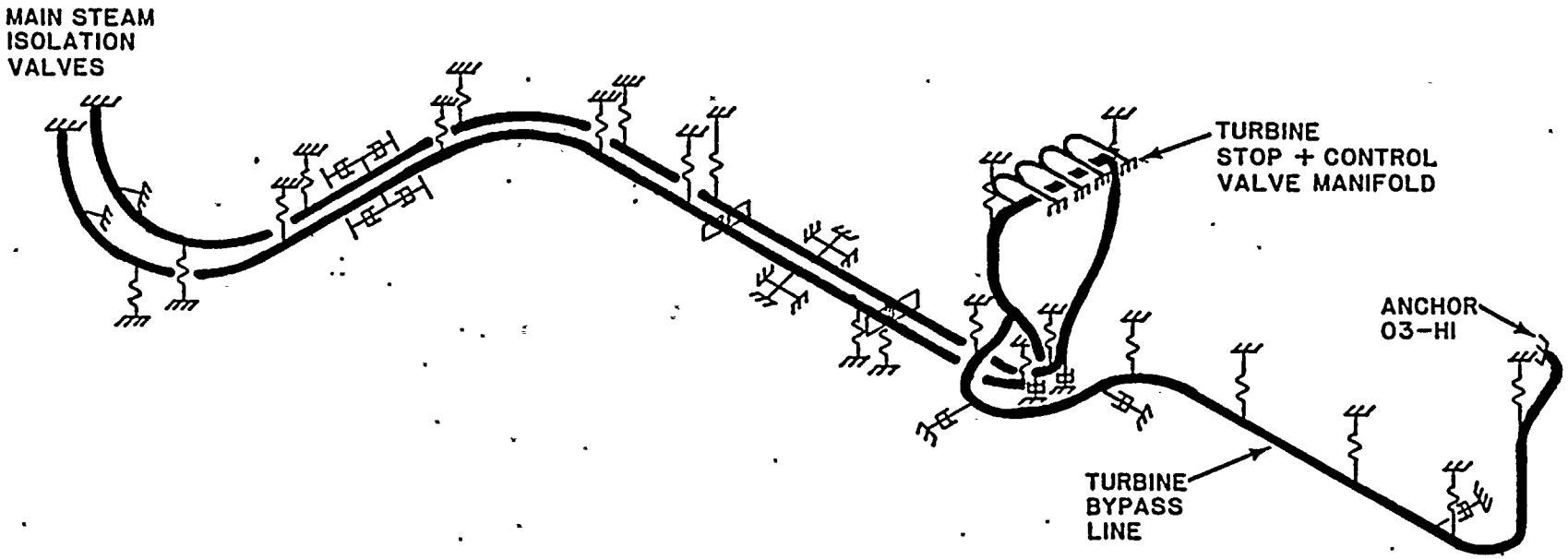

MAIN STEAM

FIGURE 1

MPR ASSOCIATES
F-85-45-1
6/13/64

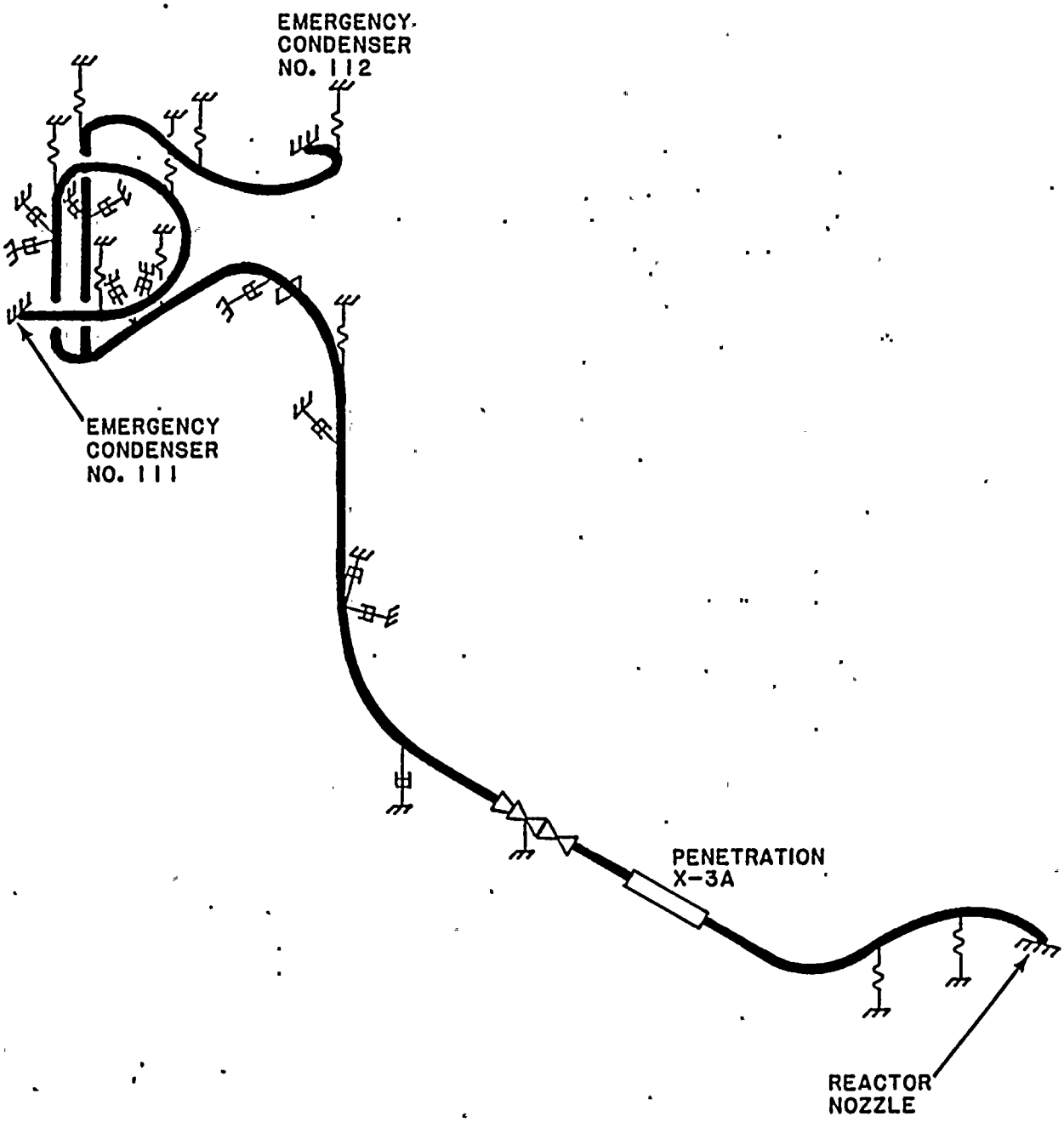

EMERGENCY CONDENSER STEAM SUPPLY

FIGURE 2

MPR ASSOCIATES
F-85-45-2
6/13/84

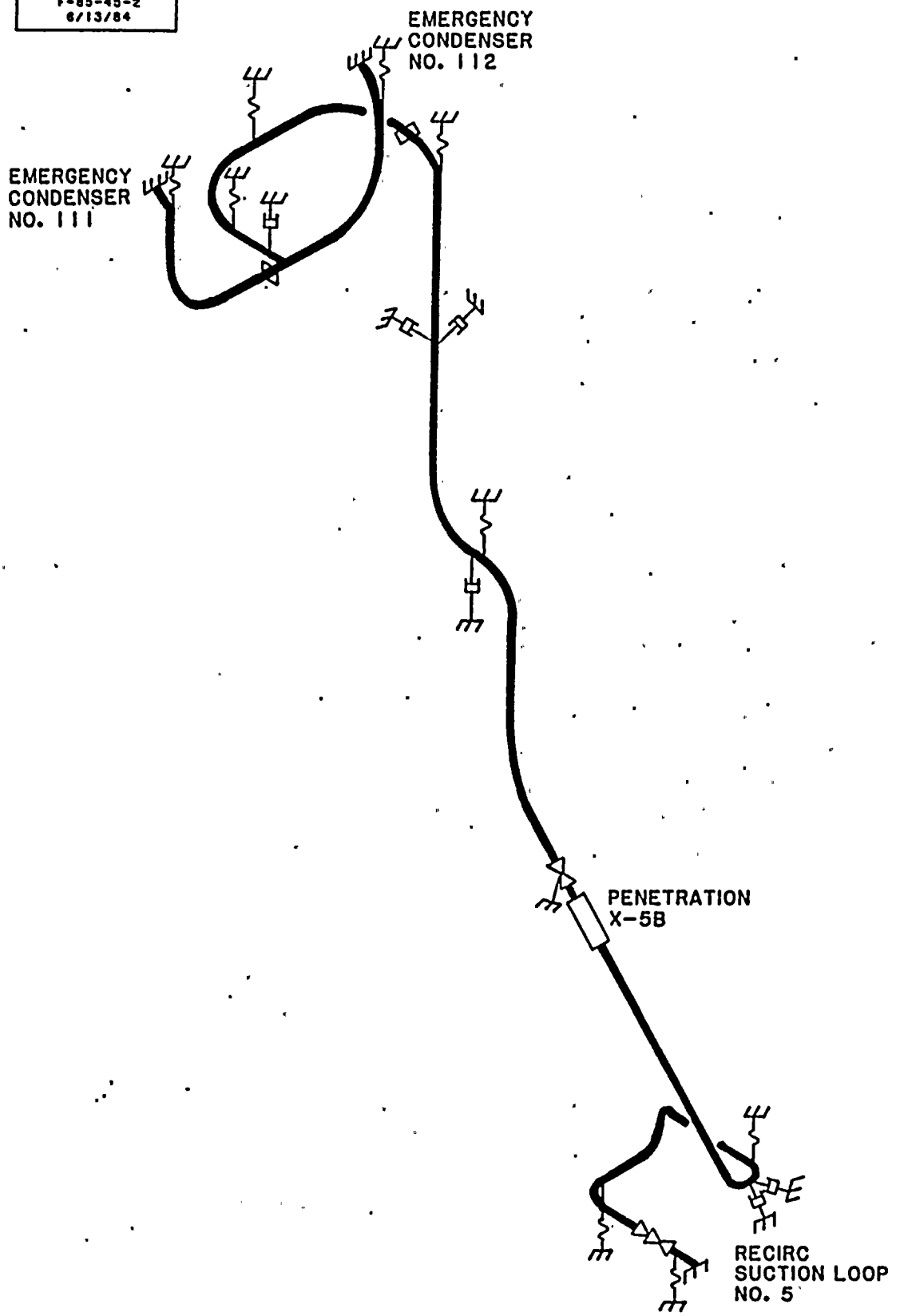

EMERGENCY CONDENSER CONDENSATE RETURN

FIGURE 3

MPR ASSOCIATES
F-85-45-4
6/13/84

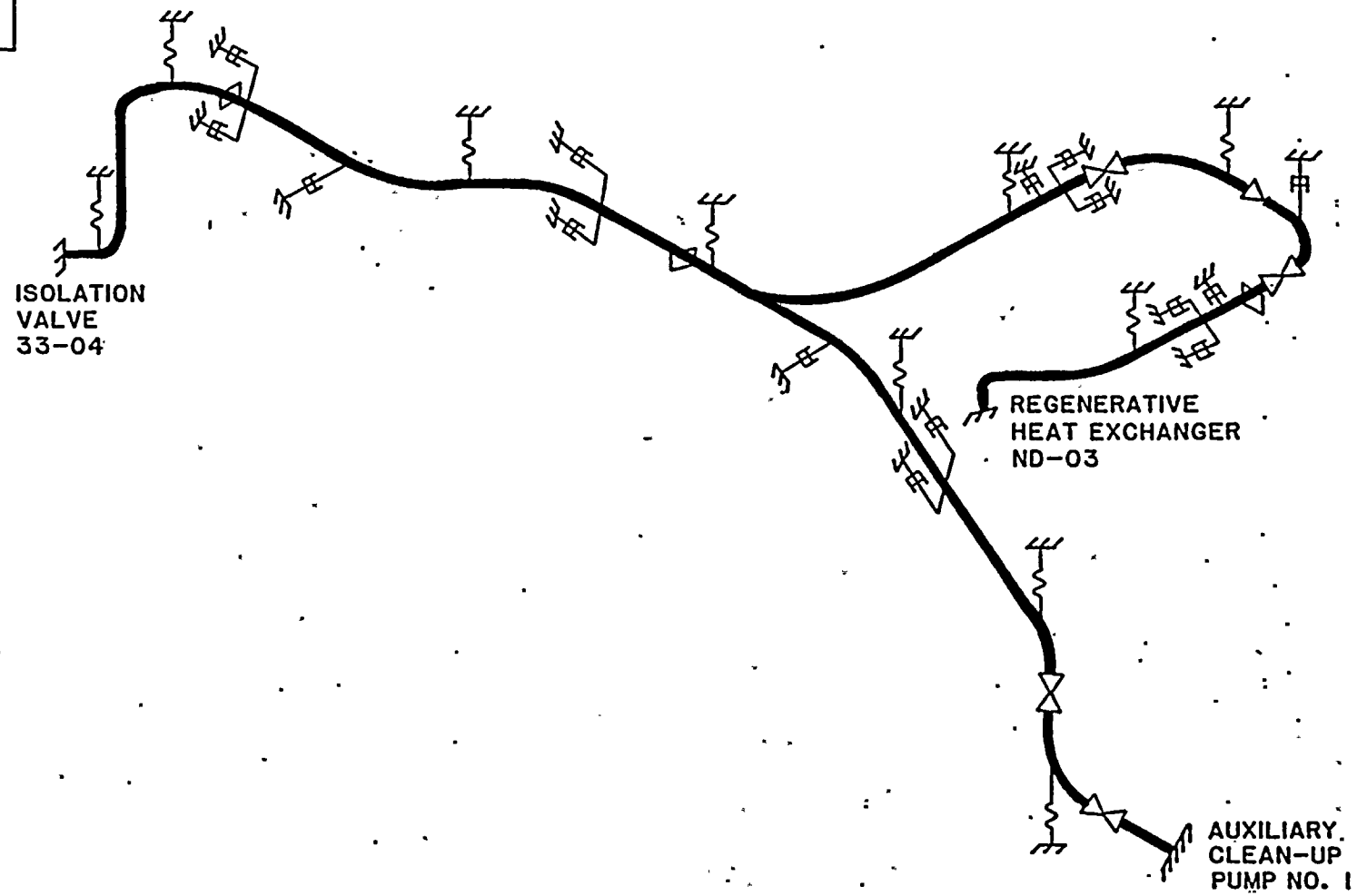

REACTOR WATER CLEAN-UP

FIGURE 4

MPR ASSOCIATES
F-85-45-5
6/13/84

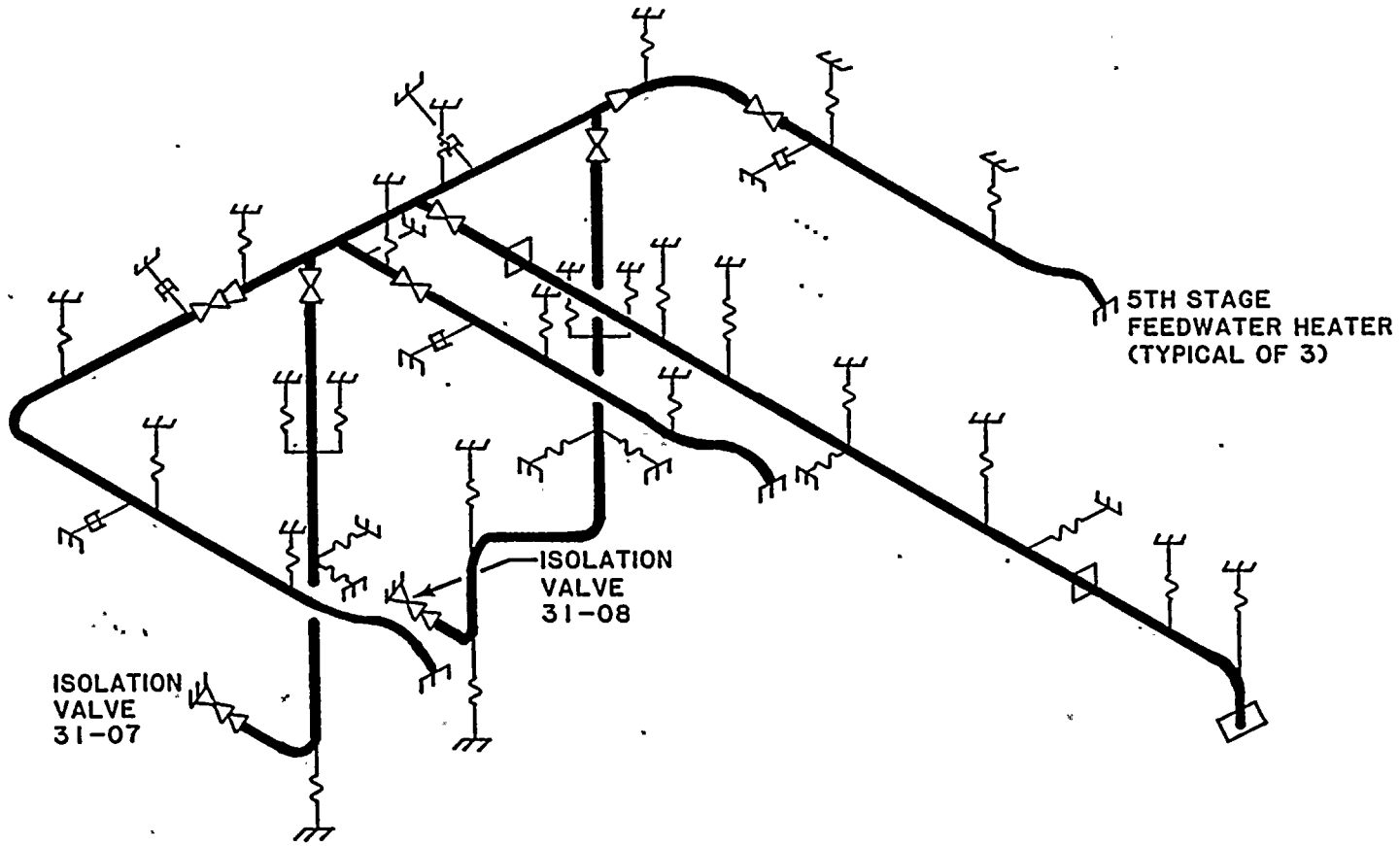

REACTOR FEEDWATER

FIGURE 5

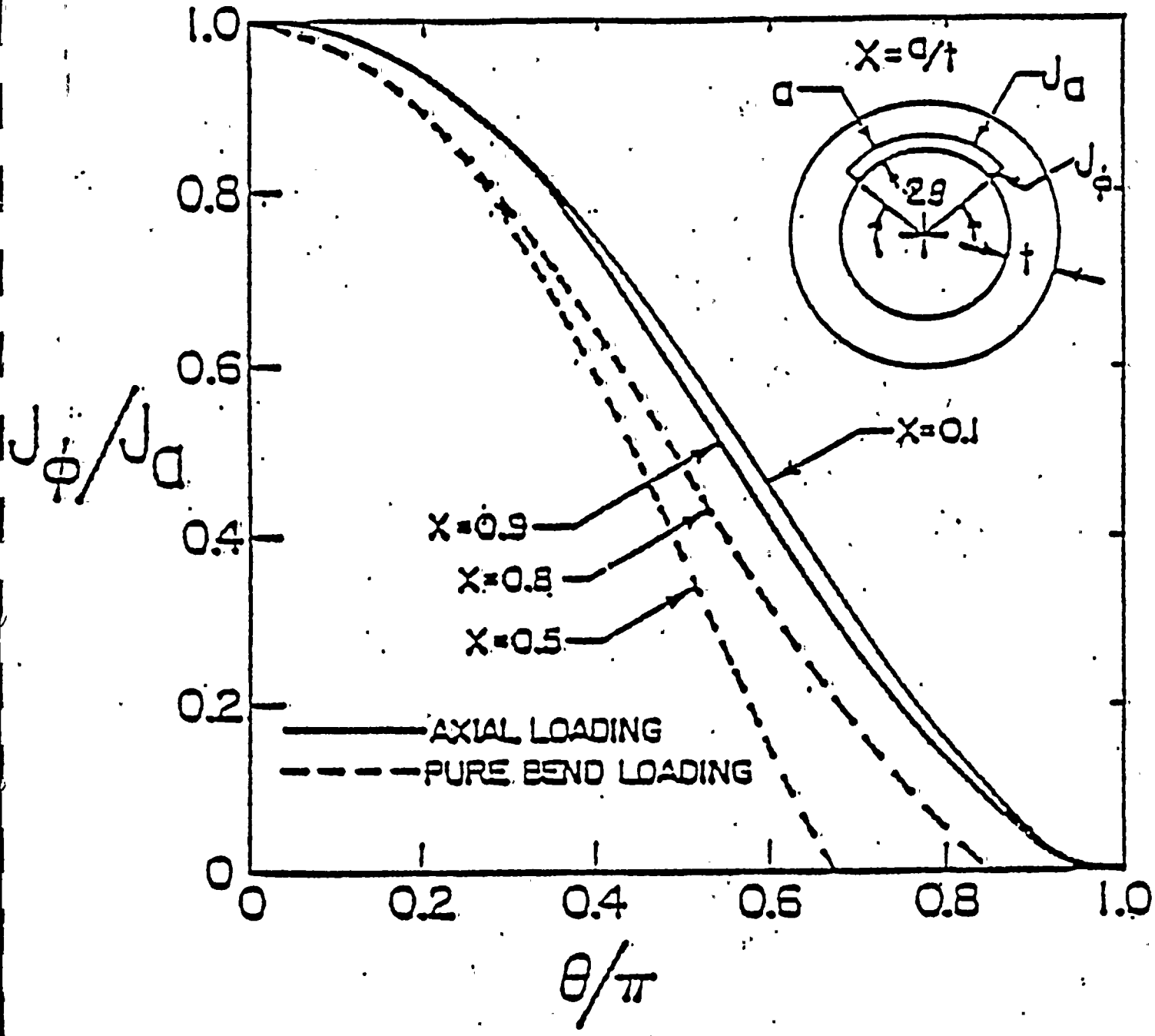

Figure 6

Relative Tendency for Part Through Wall

Cracks to Become Through Wall Cracks

(Reproduced from Reference 18)

IV. REFERENCES

1. NRC letter L505-81-12-015 dated December 4, 1981 to Consumers Power Corporation.

2. "Critical Discharge of Initially Subcooled Water Through Slits," NUREG/CR-3475, September, 1983.

3. "Calculation of Leak Rates Through Cracks In Pipes and Tubes," EPRI NP-3395, December 1983.

4. URS/JAB and Associates Report URS/JAB 8250, "Generation of Floor Acceleration Response Spectra for Reactor, Turbine and Administration Buildings, NMP Nuclear Station, Unit 1," September 1983 (3 Vols).

5. Hiroshi Tada, "The Effects of Shell Correlations on Stress Intensity factors and Crack Opening Area of a Circumferential and a Longitudinal Through-Crack in a Pipe," NUREG CR-3464, September 1983.

6. J. W. Hutchinson and P. C. Paris, "Stability Analysis of J-Controlled Crack Growth" ASTM STP 668, 1979, p. 37.

7. V. Kumar, M. D. German and C. F. Shih, "An Engineering Approach to Elastic-Plastic Fracture Analysis," EPRI NP-1931, July 1981.

8. M. D. German, W. R. Andrews, V. Kumar, C. F. Shih, H. G. deLorenzi and D. F. Mowbray, "Elastic-Plastic Fracture Analysis of Flawed Stainless Steel Pipes," EPRI NP-2608LD, Final Report September, 1982.

9. V. Kumar, W. W. Wilkening, W. R. Andrews, M. D. German, H. G. deLorenzi and D. F.Mowbray, "Estimation Technique for the Prediction of Elastic-Plastic Fracture of Structural Components of Nuclear Systems," Contract RP1237-1 (EPRI) Combined Fifth and Sixth Semiannual Report, February 1, 1981 to January 31, 1982.

10. Paul C. Paris, Hirashi Tada and Richard Marcek, "Fracture Proof Design and Analyses of Nuclear Piping," NUREG CR-3464, September 1983.

11. R. D. Stout and A. W. Pense, Journal of Basic Engineering, June, 1965, 269.

12. G. F. Carter, Principles of Physical and Chemical Metallurgy, (American Society for Metals, Metals Park, Ohio, 1979), p. 221.

13. Aerospace Structural Metals Handbook, Volume 2, Code 1303, p. 13.

14. J. P. Gudas, and D. R. Anderson, "J-R Curve Characteristics of Piping Material and Welds," 9th Water Reactor Safety Research Information Meeting, 29 October, 1981.

15. PWR Pipe Crack Study Group, 1975, "Investigation and Evaluation of Cracking in Austenitic Stainless Steel Piping of Boiling Water Reactor Plants," NUREG-CR-75-067.

16. Pipe Crack Study Group, 1979, "Investigation and Evaluation of Stress-Corrosion Cracking in Piping of Light Water Reactor Plants," NUREG-0531.

17. PWR Pipe Crack Study Group, 1980, "Investigation and Evaluation of Cracking Incidents in Piping in Pressurized Water Reactors," NUREG-0691.

18. A. Zahoor and M. F. Kanninen, Trans ASME, 103, July 1981, 194-200.

V. APPENDICES

Appendix A

CALCULATION OF LEAKAGE FLOW THROUGH PIPE CRACKS

1. Introduction

The calculation technique described below determines the mass flow rate through a crack in a piping system containing pressurized steam or water. This technique assumes that the pressure loss through the crack can be described by a typical fL/D loss mechanism. Choking is evaluated using a homogeneous choking model which depends on local stagnation pressure and stagnation enthalpy at the choke point. The flow area caused by opening of the crack due to internal pressure is determined as suggested in Reference A-1. Results obtained using this calculation technique compare favorably to measured values of flows through small slits described in Reference A-2. Also, crack opening areas obtained by finite element analysis of a crack in a plate under stress demonstrated good agreement with crack opening areas obtained using the methods presented in Reference A-1.

2. Description of Method

a. Crack Opening Area

It is conservatively assumed the only force acting to open pipe cracks is internal pressure. The longitudinal and circumferential stresses in a pipe due to internal pressure are approximately PR/2t and PR/t, respectively, where P is the internal pressure, R is the inside radius of the

pipe, and t is the wall thickness. If a through-wall crack exists, these stresses will tend to open the crack to provide a finite flow area for leakage from the pipe. Reference A-1 provides a method to determine flow areas for longitudinal and circumferential cracks in pipe.

$$A = \frac{\sigma}{E} (2\pi Rt)\ G$$

where:

- A is the flow area
- σ average stress remote from the crack
- E is Young's Modulus for the pipe material
- R is the pipe inside radius
- t is the wall thickness
- G is a geometry factor which depends on the orientation of the crack (longitudinal or circumferential), crack length and pipe size.

If the crack lies in the circumferential direction then σ and G are given by the following:

$$\sigma = PR/2t$$

$$G = \lambda^2 + 0.16\lambda^4 \text{ for } 0 \leq \lambda \leq 1$$

$$G = 0.02 + 0.81\lambda^2 + 0.30\lambda^3 + 0.03\lambda^4 \text{ for } 1 \leq \lambda \leq 5$$

where: $\lambda = \frac{a}{\sqrt{Rt}}$ and a is half the length of the crack.

If the crack lies in the longitudinal direction, σ and G are given by the following:

$$\sigma = PR/t$$

$$G = \lambda^2 + 0.625\,\lambda^4 \qquad \text{for } 0 \leq \lambda \leq 1$$

$$G = 0.14 + 0.35\lambda^2 + 0.72\lambda^3 + 0.405\lambda^4 \qquad \text{for } 1 \leq \lambda \leq 5$$

b. Leakage Mass Flow Rate

Once the opening area is known, the leak mass flow rate can be obtained iteratively from the friction loss through the crack and a critical flow expression which gives critical flow as a function of stagnation pressure and stagnation enthalpy. In this method the crack is divided into a number of control volumes through the wall thickness of the pipe, as shown in Figure A-1, and an initial estimate for mass flow through the crack is assumed. Since the geometry of the crack is known, the loss in stagnation pressure due to inlet flow into the crack and friction losses through the crack can be determined for the assumed flow rate. The stagnation pressure losses are incorporated as follows:

$$P_{on+1} = P_{on} - \frac{f\Delta L}{D} + K\,\frac{W^2}{\rho A^2}$$

$$h_{on+1} = h_{on}$$

where: P_{on} is the stagnation pressure at control volume n

f is the friction factor

ΔL is the part of the pipe wall thickness between two control volumes

K is the K factor describing entrance, exit, or extraneous losses

D is the hydraulic diameter of the crack given by twice the crack area divided by the crack length

W is the leak flow rate

ρ is the local density

A is the crack flow area

h_{on} is the stagnation enthalpy at control volume n

In this manner, the stagnation pressure at the outside wall of the crack is determined and a critical flow rate based on the homogeneous equilibrium model is obtained:

$$W_{crit} = A\, G_{crit}(P_{on}, h_o)$$

where: A is crack flow area, and
G_{crit} is the critical mass flux.

If W_{crit} is less than the assumed flow, the assumed flow was too high and must be reduced. If W_{crit} is greater than the assumed flow, the exit loss and static head are accounted for and the resulting exit static pressure is compared to the pressure outside the pipe. If a static pressure equal to

the external pressure can be found for which the flow at the crack exit plane is not yet choked, the solution is acceptable and the flow will not be choked.

However, if the outlet static pressure is too high compared to the outlet pressure, the assumed flow must be increased and the procedure repeated. Convergence is achieved when either the proper back pressure is achieved or the critical flow calculated at the choke point is equal to the assumed flow.

c. Comparison to Test Data

References A-2 and A-3 provide test data for flow of pressurized initially subcooled water through small slits or cracks. The calculational technique described above was applied to the test geometry of Reference A-2 using a friction factor for smooth pipe. Predicted flow rates for several values of initial subcooling were compared to the measured flow rates. Results of this comparison are shown in Figure A-2. These results demonstrate the validity of the calculational technique. However, the use of a smooth pipe friction factor leads to an overprediction of flow, particularly for small crack widths on the order of a few mils. Such overprediction is unconservative for leak-before-break analyses. Accordingly, a friction factor for pipe based on a relative roughness ε/D of 0.1 was used for all leak rate calculations. Calculated mass flow rates obtained

using a friction factor based on a relative roughness of 0.1 are included on Figure A-2 as dashed lines for the two cases of 0°C and 60°C subcooled water. The scatter in the data for small cracks from Reference A-3, in which the mass fluxes range from 2000 $Kg/m^2/sec$ to 52000 $Kg/m^2/sec$ for similar geometry and conditions, implies that the cracks may have plugged or opened during some of these tests. Using rough pipe assumptions underpredicts flow and is considered conservative for the leak-before-break analysis.

d. Finite Element Check of Crack Flow Area

Since the comparison of mass flow rates to test data described above does not check the effect of internal pressure on the opening flow area of the crack, a finite element analysis of a plate with a crack under uniaxial stress normal to the crack was used to determine if the crack opening area obtained using the method for a circumferential crack described in Reference A-1 gives reasonable results. The geometry used for the finite element model is shown in Figure A-3 and the corresponding crack displacement obtained for a 1000 psi uniaxial stress is shown in Figure A-4. The crack opening area obtained from finite element analysis using a 6200 psi uniaxial load equivalent to the longitudinal pressure stress for a 10.75 ID pipe with a wall thickness of .522 inches and internal pressure of 1200 psi is .033 in^2 and compares well with a value of .034 in^2 obtained using the method from Reference A-1.

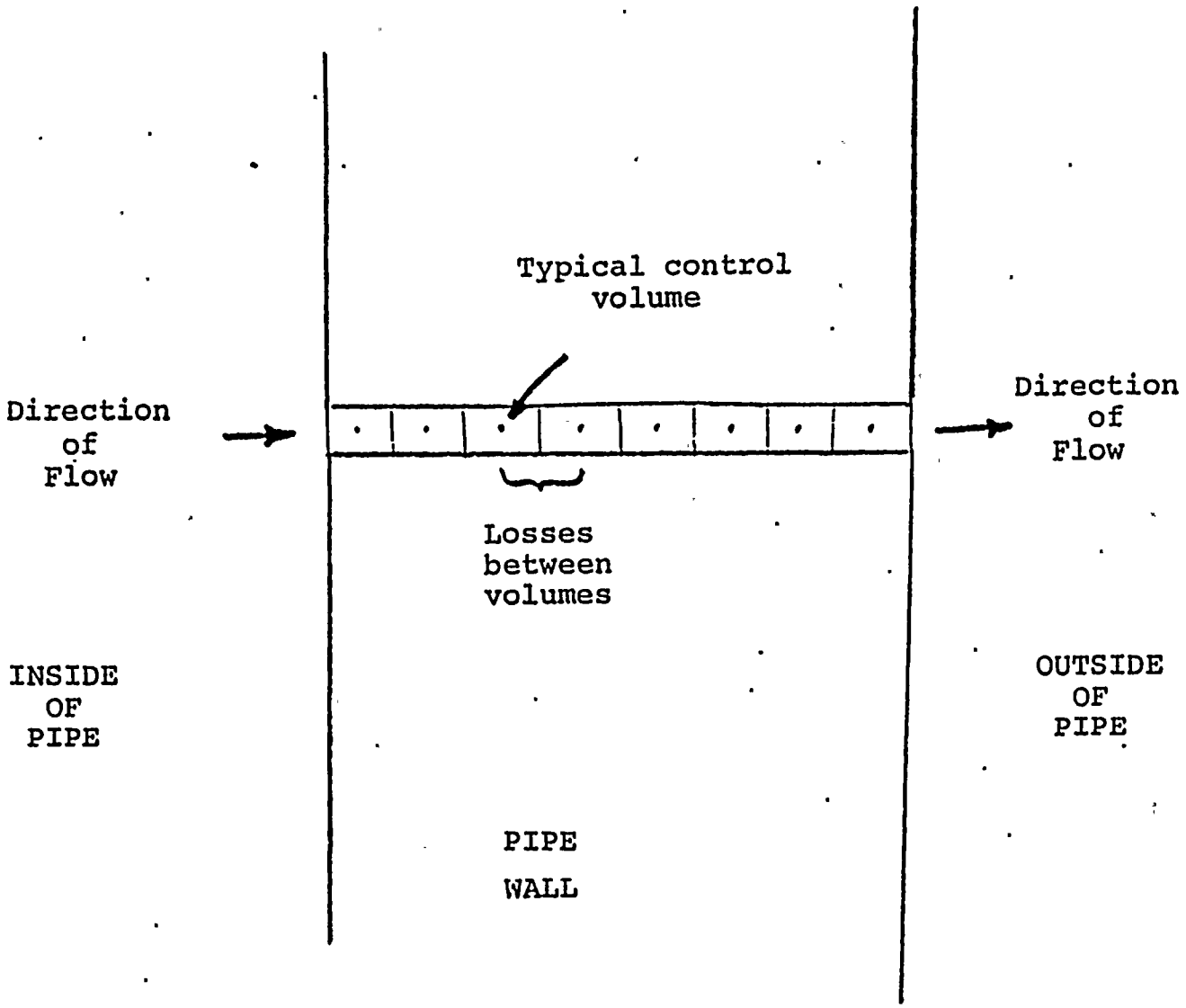

FIGURE A-1

SCHEMATIC OF CRACK DIVIDED INTO CONTROL VOLUMES

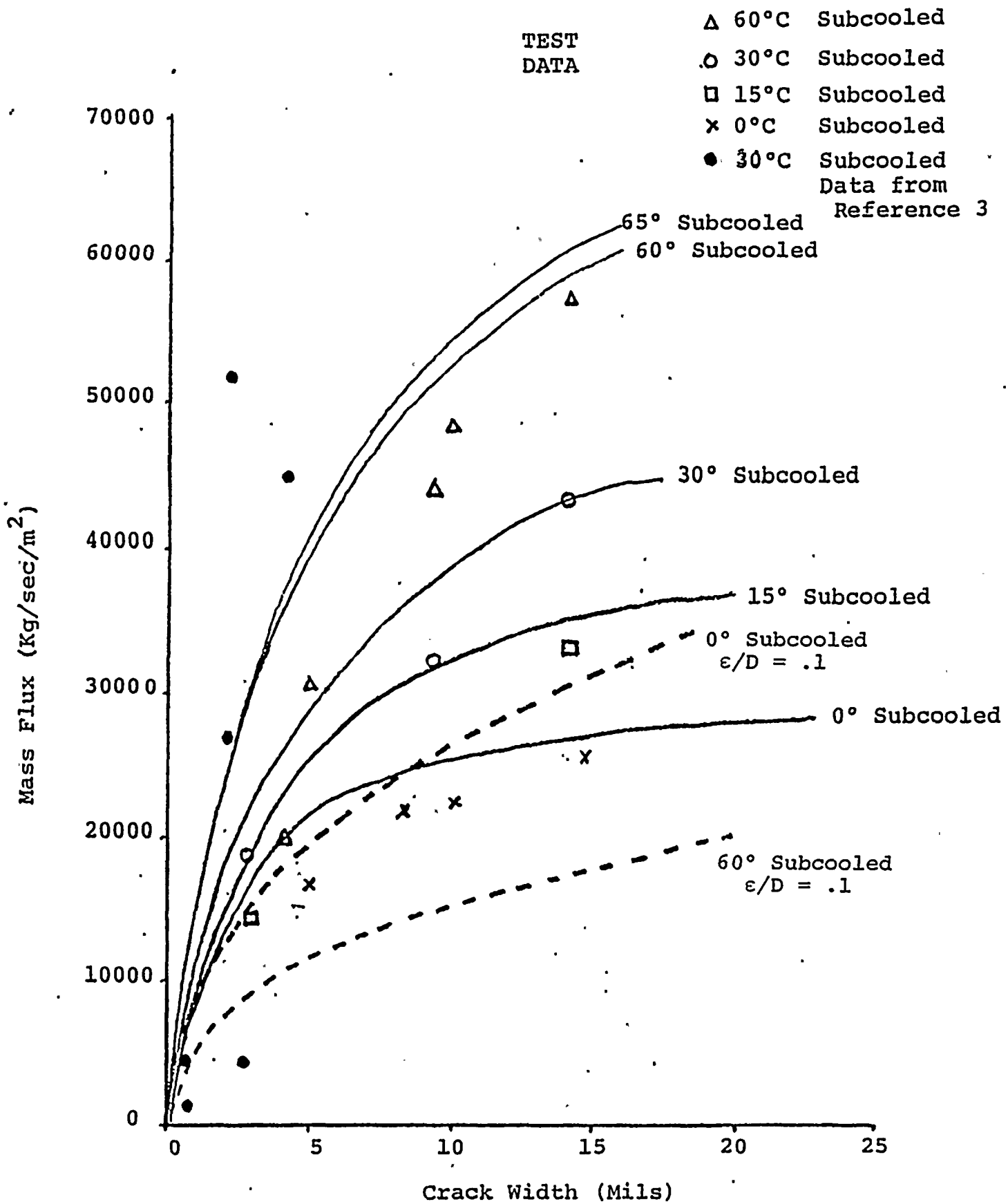

FIGURE A-2

COMPARISON OF LEAK RATE CALCULATIONS WITH TEST DATA FROM REFERENCE 2

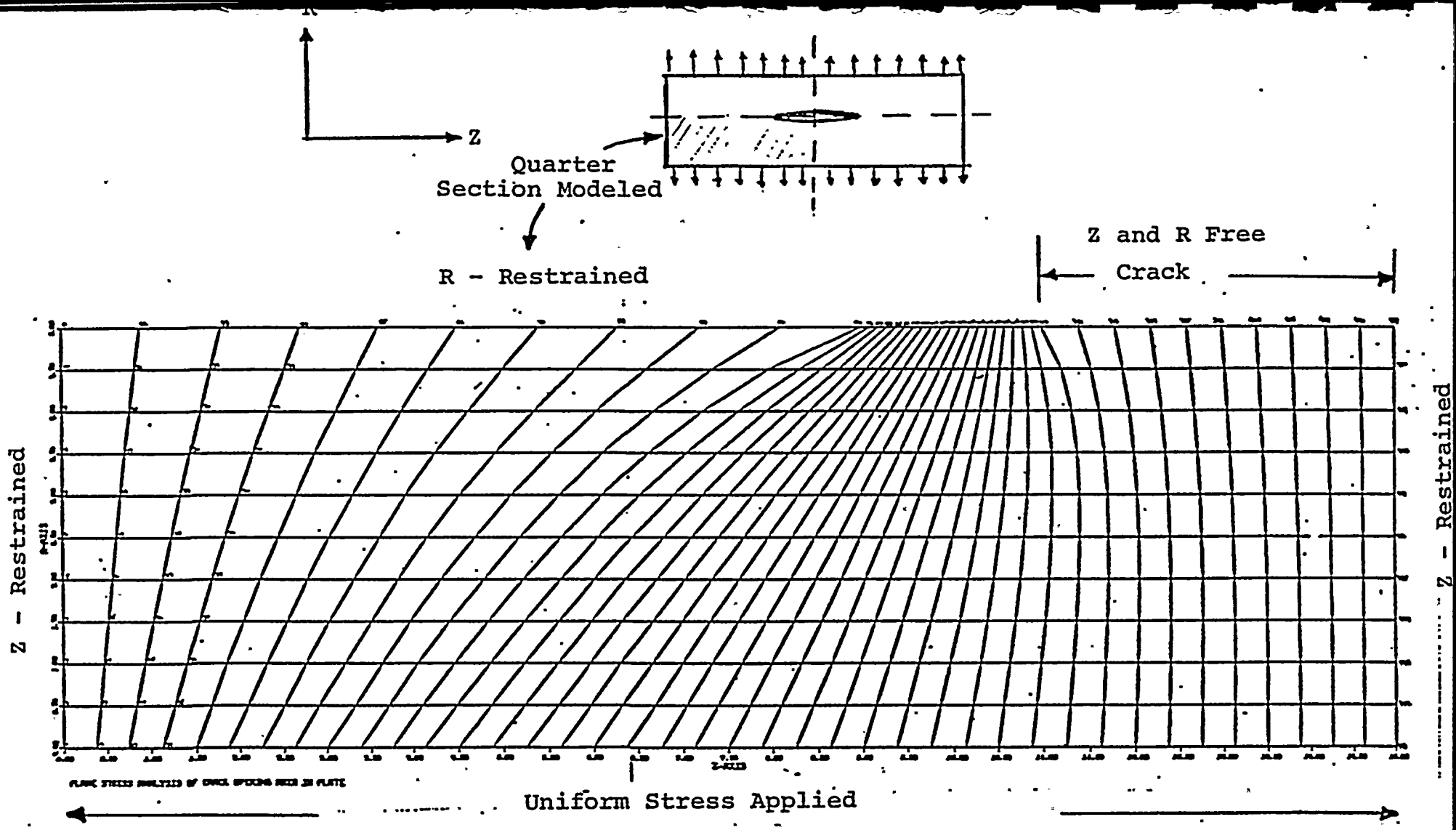

FIGURE A-3

FINITE ELEMENT MODEL
FOR PLATE WITH CRACK

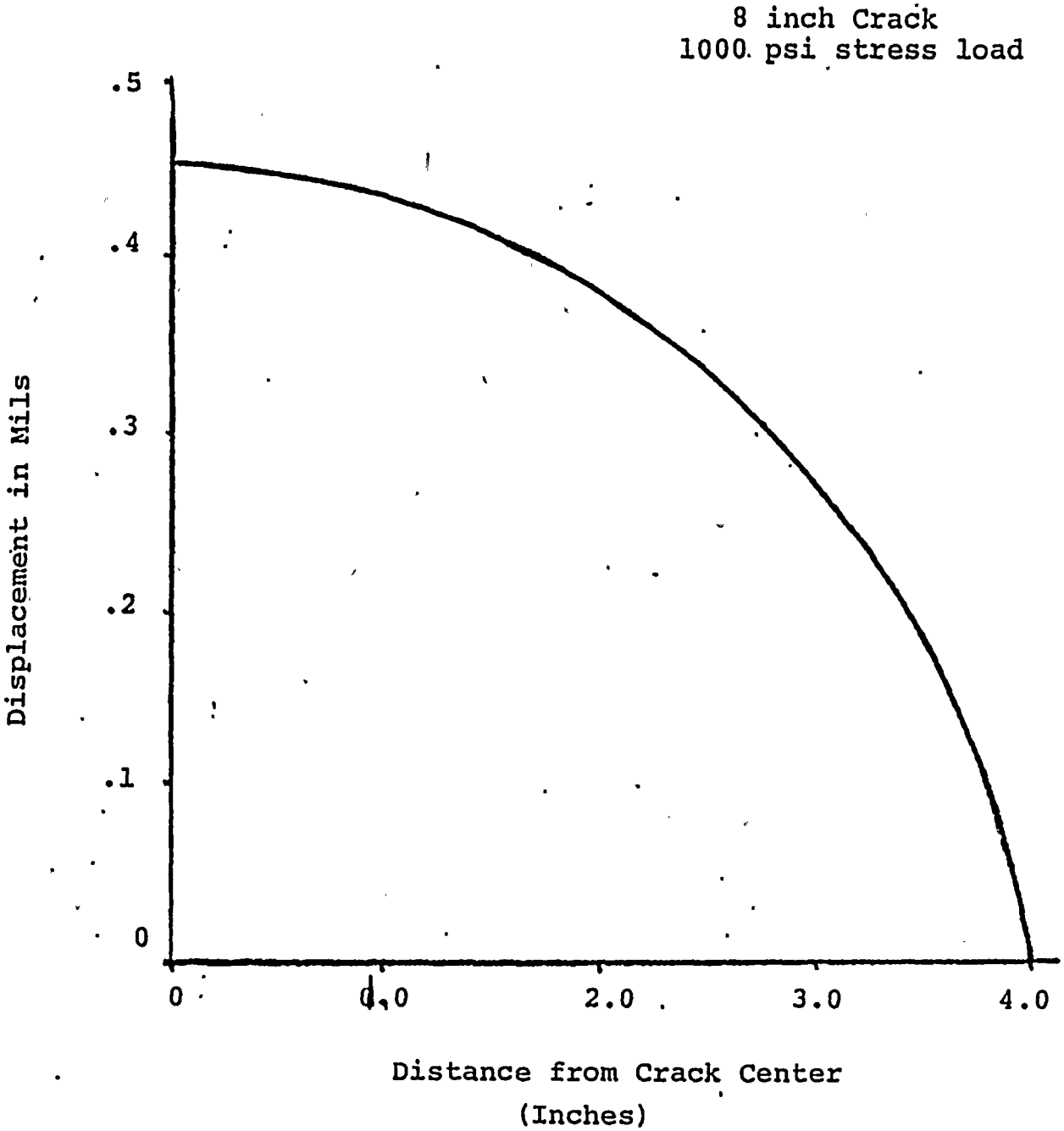

FIGURE A-4

DISPLACEMENT ALONG CRACK
FROM FINITE ELEMENT RESULTS

References

A-1 NRC letter L505-81-12-015 dated December 4, 1981 to Consumers Power Corporation, with enclosures.

A-2 C. N. Amos and V. E. Schrock, "Critical Discharge of Initially Subcooled Water Through Slits," NUREG/CR-3475, September 1983.

A-3 "A Calculation of Leak Rate Through Cracks in Pipes and Tubes," EPRI NP-3395, by S. Levy Inc., December 1983.

Appendix B

FINITE-ELEMENT STRESS ANALYSES

Finite element stress analyses were performed for four high energy piping systems at NMP-1 to obtain stress results for use in leak-before-break fracture mechanics evaluations. The four representative high energy piping systems chosen were Main Steam, Reactor Water Clean-Up, Reactor Feedwater and Emergency Condenser. In accordance with criteria in Reference B-1, these piping systems were analyzed for ASME Code service level D loads: pressure, deadweight and safe shutdown earthquake.

1. Piping Analyses Models

Finite-element models developed for the piping systems are described below:

a. Main Steam Piping (System 02) - The main steam system was modeled from the anchors just below the external main steam isolation valves to the inlets to the turbine stop and control valve manifold. The piping from the isolation valves to the branch runs to the stop and control valve manifold is 24 inch schedule 80 pipe; the branch runs connecting the 24 inch header to the turbine stop and control valves is 18 inch schedule 100 piping. A section of the turbine bypass system 03, from the main steam connection to anchor 03-H1, is also included to increase the accuracy of the model. The flexibility of the 16-inch turbine bypass line is comparable to the 24 inch main steam piping and induces restraint on the main steam piping,

decreasing the dynamic response. All main steam piping is A106 Grade B carbon steel. Figure B-1 shows the main steam system, including piping supports. Figures B-2 and B-2A show the finite element model employed.

b. Emergency Condenser Piping (System 39) - The west bank steam supply line was modeled from the reactor vessel nozzle to the inlets of emergency condensers #111 and #112. The piping inside the drywell and a small segment outside the drywell is 10.75 inch outside diameter with a wall thickness of 0.522 inches. From the gate valve located near the drywell penetration to the condensers, the pipe is 12.75 inch outside diameter and 0.622 inch wall thickness.

The west bank condensate return line was also modeled, from the outlets of emergency condensers #111 and #112 to the connection into the suction side of recirculation loop #5. Except for a very short segment of 12.75 inch diameter pipe near the recirculation loop attachment, the entire west bank condensate return system is 10.75 inch outside diameter piping with 0.522 inch wall thickness.

Figures B-3 and B-4 illustrate the steam supply and condensate return systems; Figures B-5 and B-6 show finite element models employed for stress analyses. All emergency condenser piping is A376, Type 304 stainless steel.

c. Reactor Water Clean-Up Piping (System 33.1) - The portion of the reactor water clean-up system which was modeled extends from the external reactor water clean-up isolation valve to the first regenerative heat exchanger and includes the branch to the inlet of auxiliary clean-up pump #1. This section is judged typical of the reactor cleanup piping and is also the highest energy section of the system. This pipe is 6.625 inch outside diameter, schedule 80, A106 Grade B carbon steel. Figures B-7 and B-8 show this system, including piping supports (Figure B-7) and finite element nodal locations (Figure B-8).

d. High Pressure Feedwater Piping (System 30) - The model of the high pressure feedwater system includes the sections of feedwater piping from the 5th stage feedwater heaters to the external feedwater isolation valves. Three similar 16 inch schedule 100 lines extend from the feedwater heaters to a common header. This header and the two lines decending from it to the isolation valves are 18 inch schedule 100 piping. A section of System 49, Feedwater Recirculation (14 inch Schedule 30) is included to increase the accuracy of the model. Although it is typically empty, the stiffness of the 14 inch pipe is comparable to other piping in the system. Including this line increases the accuracy of dynamic analyses. Piping material for the feedwater system is A106 Grade B carbon steel. The feedwater system and finite element model are shown in Figures B-9 and B-10.

2. Stress Calculation

All stress analyses were performed using ANSYS, a general purpose finite element code. The piping was modeled using two types of piping elements available in ANSYS, elastic straight pipe and elastic curved pipe. To improve the distribution of piping mass, long runs of straight pipe were modeled using several straight pipe elements. Unless otherwise noted on support sketches or piping drawings, all elbows were modeled as standard long radius elbows using a single elastic curved pipe element.

The physical and material properties assigned to model pipe elements are shown in Table B-1. The piping weight includes the weight of insulation, fluid in the pipe and the piping material. Valves were modeled using elastic straight-pipe elements and a lumped mass placed at the approximate center of gravity of the valve and operator (if applicable). This method models the inertial effects of the valve and operator. For the feedwater system model, pipe element wall thicknesses were increased at valve locations, and the additional mass and inertia due to operators were added at the valve midpoint. The model of the reactor water cleanup system used lumped valve weights on the pipe center-line. This is considered acceptable because of the small amount of eccentricity of that system's valves.

The systems modeled for this analysis contain four types of piping supports: anchors, spring hangers,

seismic snubbers and seismic constraints. These supports were modeled as follows:

a. Anchors - Anchor supports, in which the piping was firmly supported against displacements, were modeled with zero-displacement boundary conditions in the directions of anchor support.

b. Spring Hangers - Most piping supports in the modeled systems are constant force spring hangers. The stiffness of the spring hangers was obtained from data provided by the hanger manufacturer and was modeled using the general stiffness element available in ANSYS.

c. Seismic Snubbers - Snubbers are attached to the piping system to reduce piping deflections and stresses during dynamic loads. Under normal operating conditions, the snubbers offer negligible resistance to pipe deflections due to thermal growth or deadweight loadings. During an earthquake, the snubbers tend to "lock-up" when loaded by rapid deflections and are equivalent to stiff tension-compression rods. Except for the reactor water cleanup system, snubbers were modeled with ANSYS 3-D spar elements. These elements offer no resistance to bending and are simple tension-compression members. The cross-sectional area of the spar elements was defined such that the element axial stiffness was approximately 10^7 lb/in, a value judged typical of actual snubbers. For the reactor water clean-up system, snubbers were assumed to completely lock-up during

seismic loading and were, therefore, constrained at the pipe attachment in the direction of the snubber line of action.

d. Seismic Constraints - These constraints are structural steel boxes built around the pipe that include small gaps between the box and pipe to allow for thermal deflections. During an earthquake, the piping is restrained to move only to the limit of the gap. To model these supports, a stiffness element similar to that used for spring hangers was employed. The stiffness matrix for the support was determined by analyzing the support structure surrounding the pipe in each of the supported directions. In several cases the gap between the pipe and support was sufficiently large that it was judged to offer no support during a seismic event (i.e., the pipe would not deflect through the entire gap). In these cases the support was conservatively neglected. The seismic constraints constructed on the reactor water clean-up system have relatively small gaps between the support and piping and the support steel is stiff compared to the small 6.625 inch pipe. For these reasons, seismic constraints on this system were modeled by constraining the pipe at the support location in two orthogonal directions perpendicular to the pipe axis.

3. Loading

Criteria B.1 of Reference B-1, requires fracture mechanics evaluations for level D loading conditions.

Service level D loading consists of only mechanical loads: internal pressure, deadweight and safe shutdown earthquake. These loading conditions were evaluated as follows:

a. Deadweight - The pipe deadweight loading was analyzed including the effect of the preloading of the spring hanger supports. The spring hanger preloads were obtained from installation drawings supplied by the hanger manufacturer. The effects of snubbers and seismic constraints, which are not applicable to a static analysis, were not included in the deadweight analysis.

b. Pressure - The operating system pressure stresses were obtained by hand calculations. The circumferential pressure stress is determined by

$$\sigma = \frac{PR_i}{t}$$

and the longitudinal pressure stress is determined from

$$\sigma = \frac{PR_i^2}{(R_o^2 - R_i^2)}$$

where:

P = system pressure
R_i = pipe inside radius
R_o = pipe outside radius
t = pipe wall thickness.

c. Safe Shutdown Earthquake - The piping response to a postulated safe shutdown earthquake (SSE) was obtained by exciting the piping system with the appropriate acceleration response spectra. The analyses used the amplified response spectra obtained from the bounding analyses of Reference B-2, "NMP-1 Floor Acceleration Response Spectra," by URS/Blume. The floor response spectra are based on a Regulatory Guide 1.60 ground motion spectra normalized to a 0.11g zero period acceleration (ZPA) ground motion. This ZPA is in accordance with the NMP-1 design basis given in the NMP-1 FSAR. More realistic response spectra are now being developed for NMP-1 as part of the seismic re-evaluation program. The response spectra used in this analysis are upper-bound values enveloping the expected finalized spectrum. An envelope of floor response spectra covering all building elevations with piping system supports was used. Figures B-11 through B-15 show the response spectra used for each system. Spectral damping values were obtained from Regulatory Guide 1.61 (2% critical damping for pipe 12" diameter or less, 3% for pipe greater than 12" diameter).

ANSYS was used to generate modal responses for seismic accelerations in the vertical and two horizontal directions. The individual modal results for each acceleration direction were combined in accordance with the rules for closely spaced modes presented in Regulatory Guide 1.92. Modes with natural frequencies up to 33 Hz were considered.

Results for each of the three acceleration directions were combined by the square root sum of the squares (SRSS) method.

4. Results

The results of individual loading conditions were combined by absolute sum to determine stress results for service level D conditions. The maximum stress for each pipe size was determined by absolute summing the bending and axial components of stress. Stresses in pipe sections inside the drywell and in the empty feedwater recirculation line were not included in the analysis since only break locations in pressurized portions of the systems outside the drywell are involved in the leak-before-break analysis. The magnitude and location of the maximum stresses in each piping system are summarized in Table B-2 and described below:

a. Main Steam Piping - The maximum Level D stresses for the 16", 18" and 24" piping occur at the following locations: (1) the turbine bypass - main steam connection tee, (2) the inlet to the turbine-stop and control valve manifold and (3) at anchor 02-NM-A1 just below the external main steam isolation valves. As shown in Table B-2, the total stress at these locations is about 16-17 ksi, with seismic stresses dominating.

b. Emergency Condenser Piping - The maximum stresses (outside containment) in each of these systems occur at snubbers 39-HS-3 and 4 (node 34) in the condensate return system and snubbers 39-HS-14 and

15 (node 52) in the steam supply piping. These stresses, which occur due to bending around the snubber attachments under seismic load, are about 23 ksi and 21 ksi for the steam and condensate lines, respectively.

c. Reactor Feedwater - the locations of maximum stress for the 14", 16", and 18" piping, occur at: (1) the 18" pipe - 14" reducer (node 22) on the extension to the feedwater recirculation line (system 49), (2) node 16, near pipe hanger 30-H4, and (3) node 80, the attachment of pipe hanger 30-H13. These stresses, due primarily to seismic accelerations, are about 24 ksi, 20 ksi and 25 ksi for the 14", 16" and 18" piping, respectively.

d. Reactor Water Cleanup - The maximum total stress of about 14 ksi occurs at the connection to heat exchanger ND-03 (node 71).

References

B-1 NRC letter L-505-81-12-015 dated December 4, 1984 to Consumers Power Corporation, with enclosures.

B-2 "Nine Mile Point Unit 1, Floor Acceleration Response Spectra" (Draft), by URS/J. A. Blume and Associates, transmitted to Niagara Mohawk Power Corporation November 23, 1982.

TABLE B-1

MATERIAL + PHYSICAL PROPERTIES

SYSTEM	MATERIAL	OD (in)	WALL THICKNESS (in)	OPERATING TEMPERATURE (°F)	E (psi)	WEIGHT (lb/ft) (1)	RADII OF CURVATURE (in)
Main Steam	A106, Gr B A106, Gr B A106, Gr B	16 18 24	1.031 1.156 1.219	550 550 550	27.0E6 27.0E6 27.0E6	187.1 233.0 330.7	24,81 27 36,120
Reactor Water Clean-up	A106, Gr B	6.625	0.432	500	27.3E6	46.8	6,9,30
Reactor Feedwater	A106, Gr B A106, Gr B A106, Gr B A106, Gr B	14 14 16 18	0.375 0.937 1.031 1.156	150 360 360 360	29.1E6 27.9E6 27.9E6 27.9E6	113.3 175.3 223.6 282.4	21 - 24,80 18
Emergency Condenser Steam Supply	A376, Type 304 A376, Type 304	10.75 12.75	0.522 0.622	550 550	25.4E6 25.4E6	72.6 98.8	15,48 18,60
Emergency Condenser Condensate Return	A376, Type 304 A376, Type 304	10.75 12.75	0.522 0.622	550 550	25.4E6 25.4E6	95.0 130.2	15,48 -

ν = Poisson's Ratio = 0.3 for All Cases

NOTE:

(1) Weight includes insulation, fluid and pipe wall.

TABLE B-2

MAXIMUM STRESSES

SYSTEM	OD (in)	LOCATION(1) (node)	DEADWEIGHT		SSE		σ_p(4) (ksi)	σ_T(5) (ksi)
			σ_a(2) (ksi)	σ_b(3) (ksi)	σ_a(2) (ksi)	σ_b(3) (ksi)		
Main Steam	16	20	0.0	1.1	0.3	12.0	3.3	16.8
	18	138	0.0	0.5	0.4	12.2	3.3	16.4
	24	270	0.1	0.6	0.2	12.4	4.4	17.7
Emer Cond Steam	12.75	52	0.0	0.3	0.7	17.6	4.5	23.2
Emer Cond Condensate	10.75	34	0.2	1.1	0.2	15.6	4.5	21.3
Reactor Feedwater	14	22	0.0	1.0	0.5	20.0	3.1	24.3
	16	16	0.0	0.5	0.2	16.0	3.2	19.8
	18	80	0.0	0.7	1.4	19.9	3.3	25.3
Reactor Water Cleanup	6.625	71	0.1	8.3	0.1	3.0	3.2	14.0

NOTES:

1. Node locations are shown on Figures B-2, B-4, B-6, B-8, and B-10.
2. Stress resulting from axial loads.
3. Bending stress resulting from moment loads.
4. Longitudinal pressure stress.
5. Total stress = deadweight axial plus bending and SSE axial plus bending and longitudinal pressure stress.

MPR ASSOCIATES
F-85-45-3
6/13/84

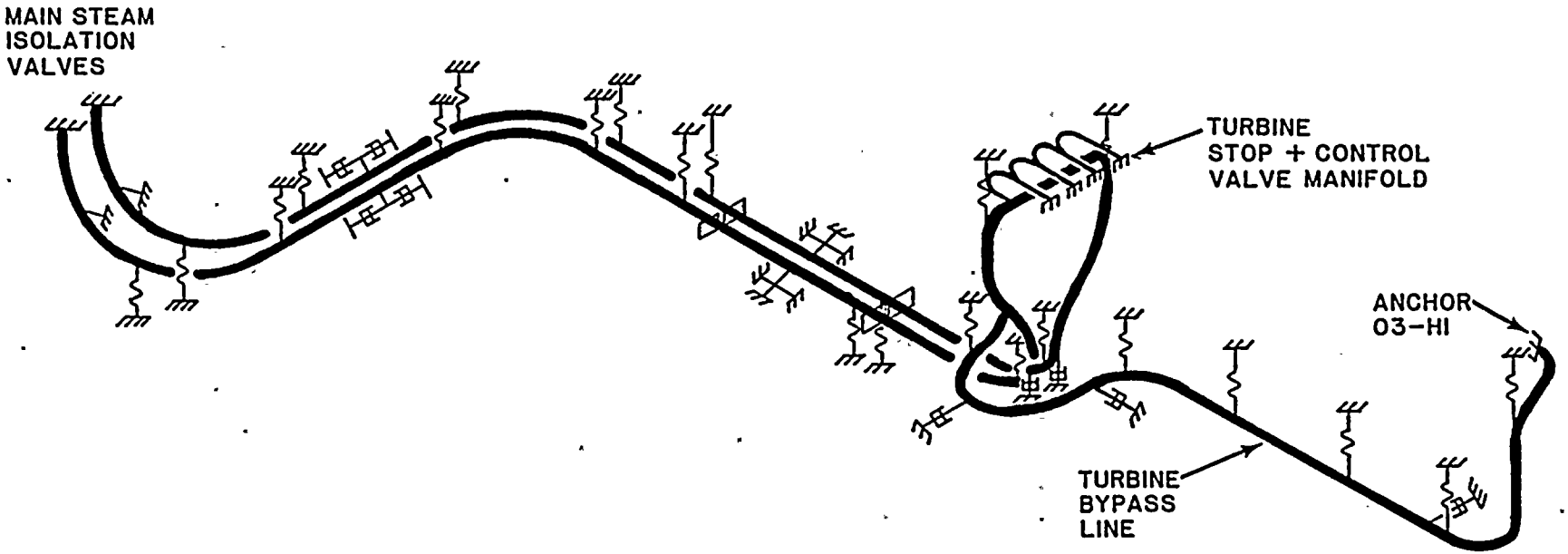

MAIN STEAM

FIGURE B-1

MPR ASSOCIATES
F-85-45-15
7/8/84

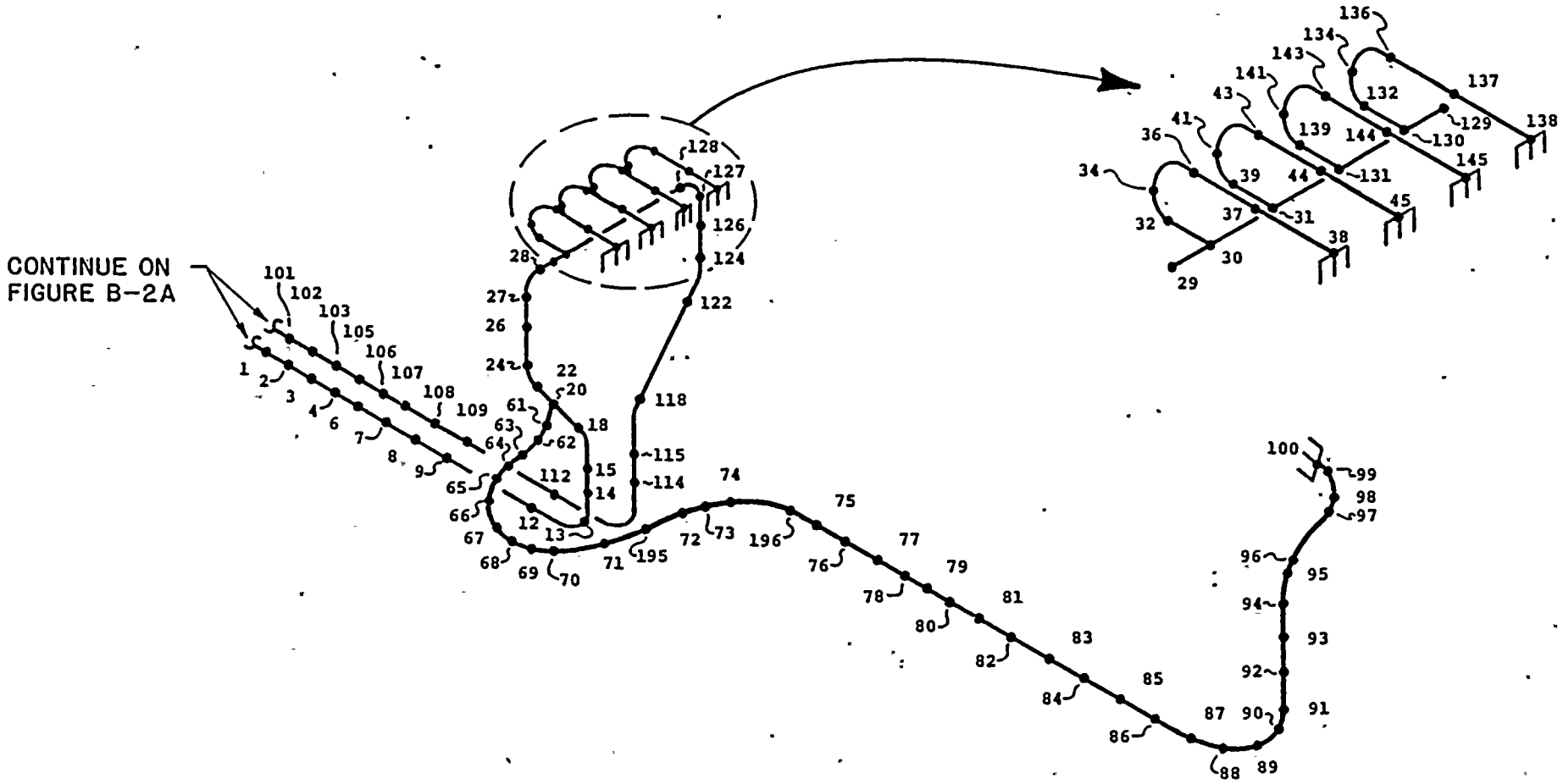

MAIN STEAM
FINITE ELEMENT MODEL
FIGURE B-2

MPR ASSOCIATES
F-85-45-15
7/8/84

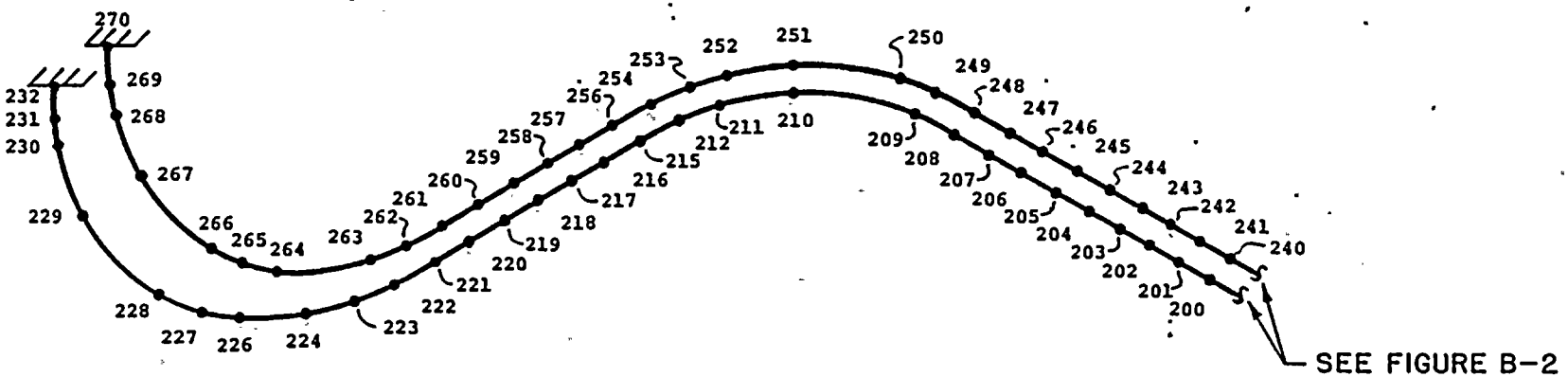

MAIN STEAM
FINITE ELEMENT MODEL

FIGURE B-2A

MPR ASSOCIATES
F-65-45-1
6/13/84

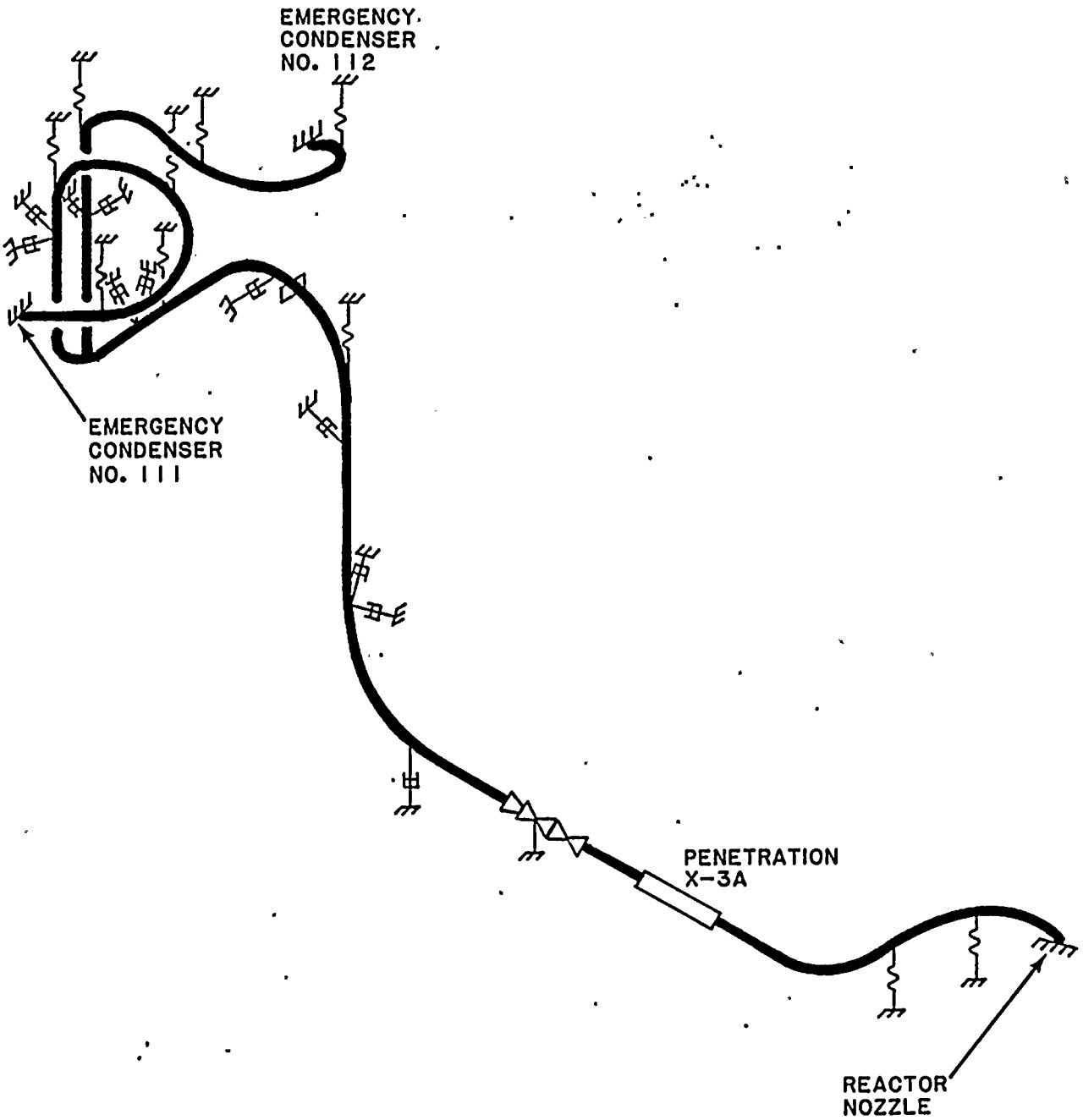

EMERGENCY CONDENSER STEAM SUPPLY

FIGURE B-3

MPR ASSOCIATES
F-85-45-13
7/8/84

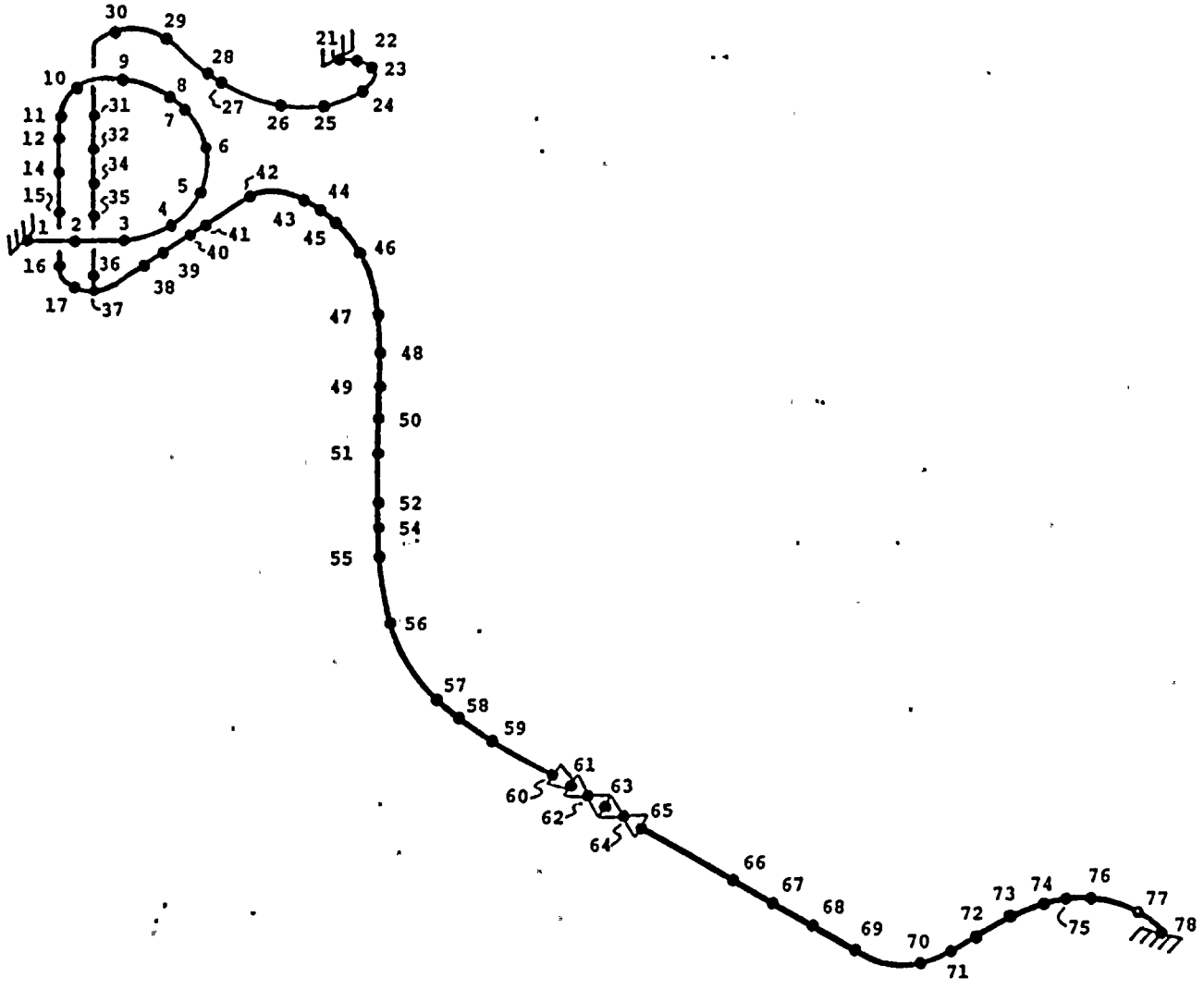

EMERGENCY CONDENSER STEAM SUPPLY
FINITE ELEMENT MODEL

FIGURE B-4

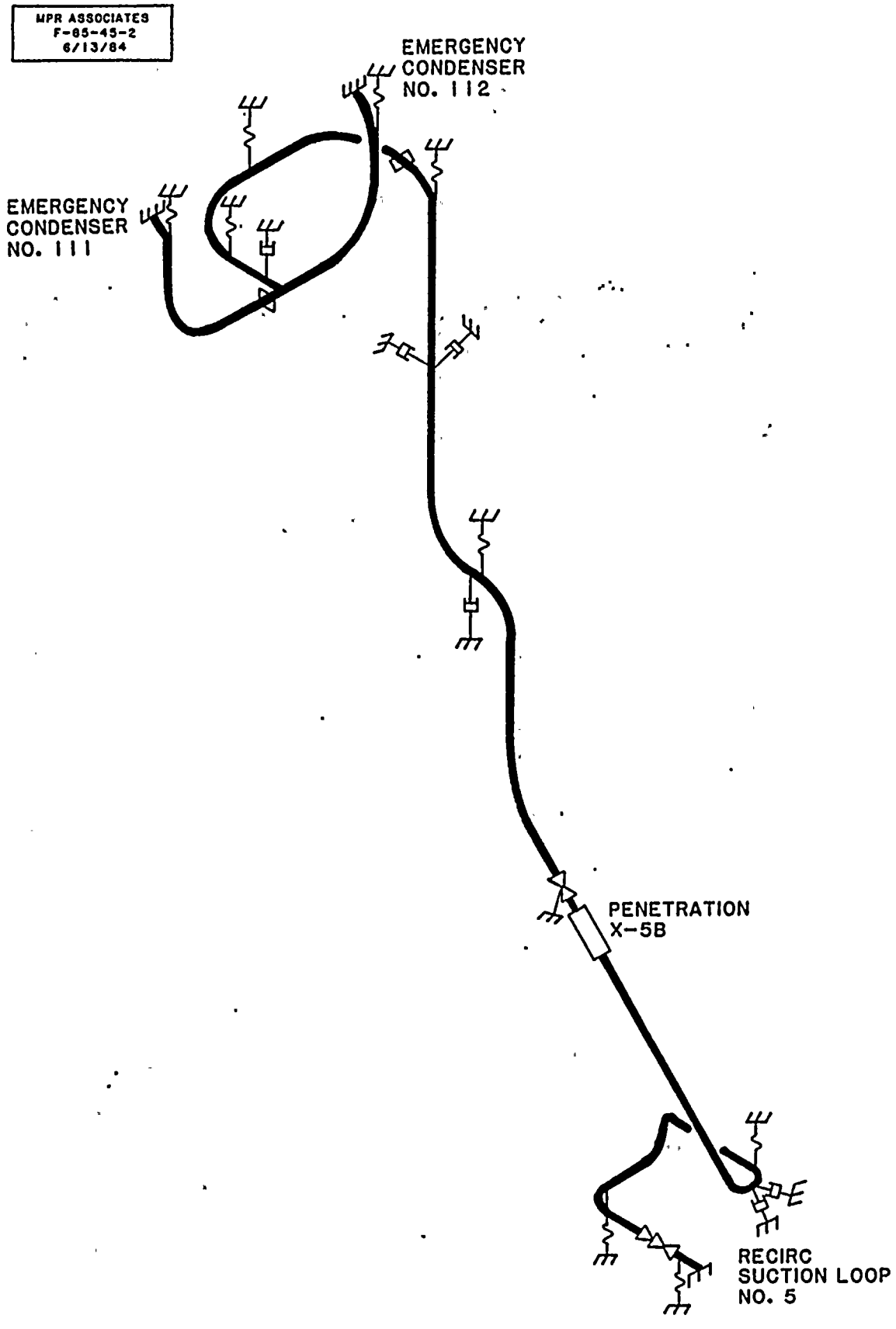

EMERGENCY CONDENSER CONDENSATE RETURN

FIGURE B-5

MPR ASSOCIATES
F-85-45-12
7/8/84

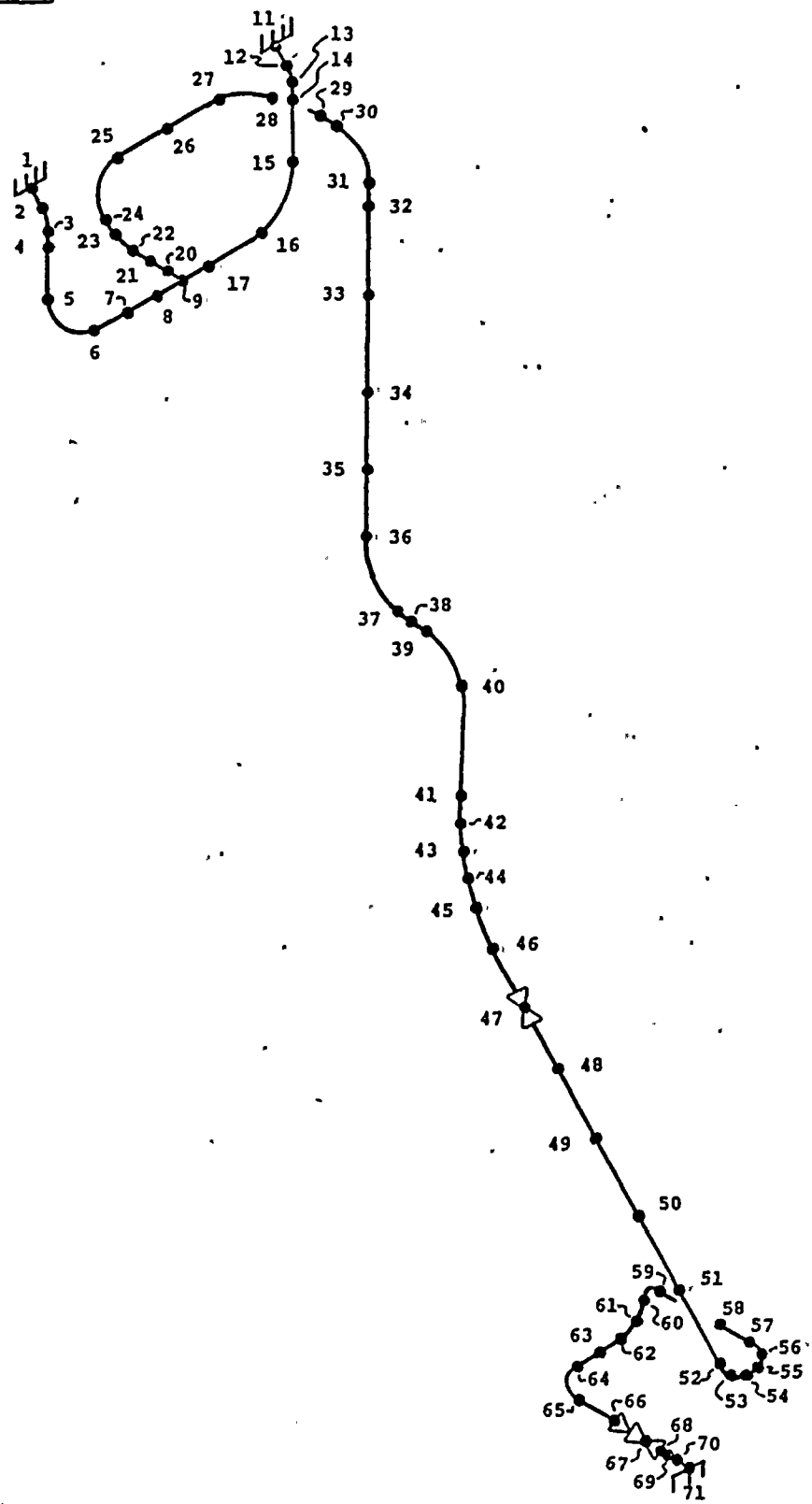

EMERGENCY CONDENSER CONDENSATE RETURN
FINITE ELEMENT MODEL

FIGURE B-6

MPR ASSOCIATES
F-85-45-4
6/13/84

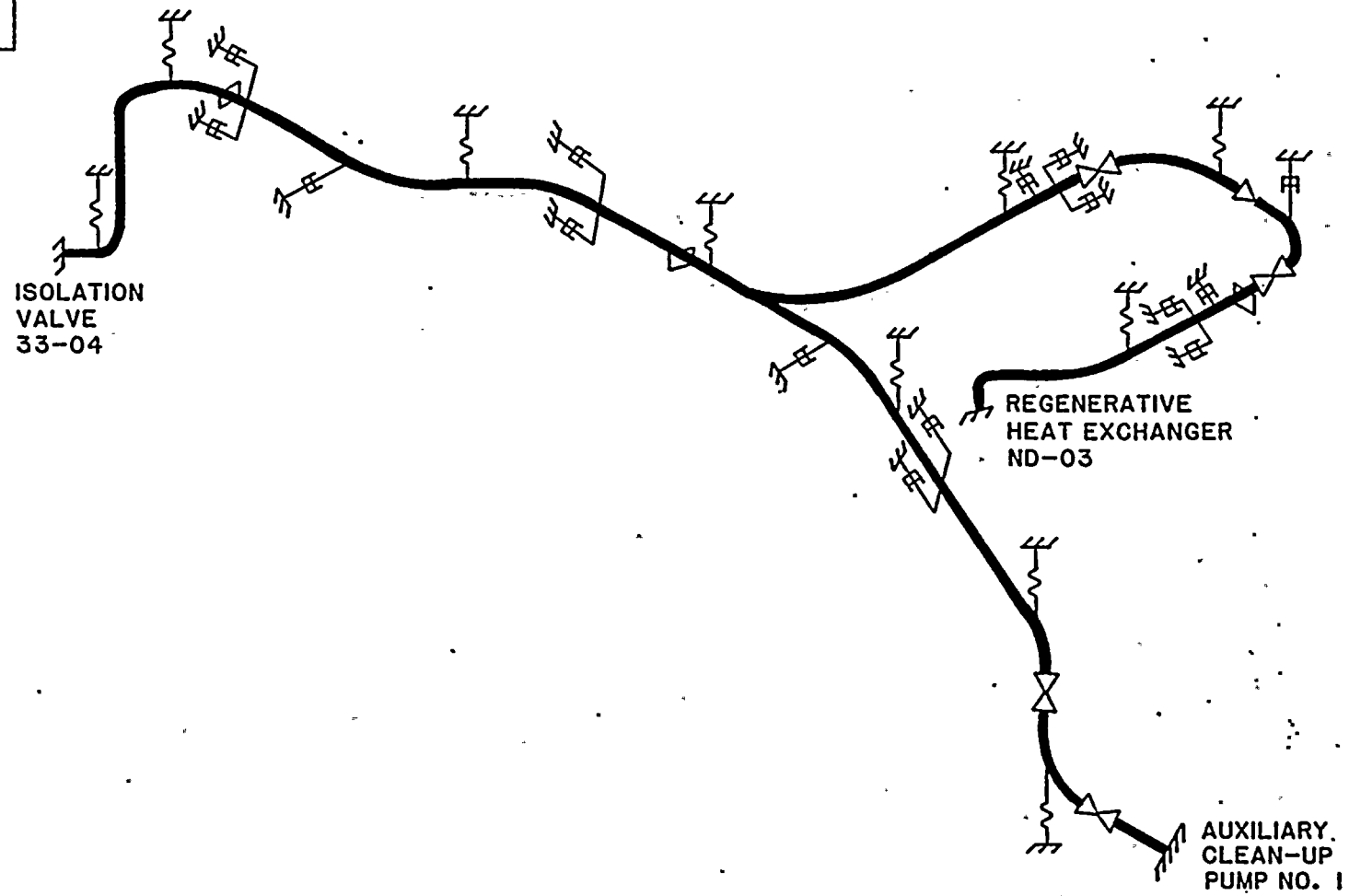

REACTOR WATER CLEAN-UP

FIGURE B-7.

MPR ASSOCIATES
F-85-45-14
7/8/84

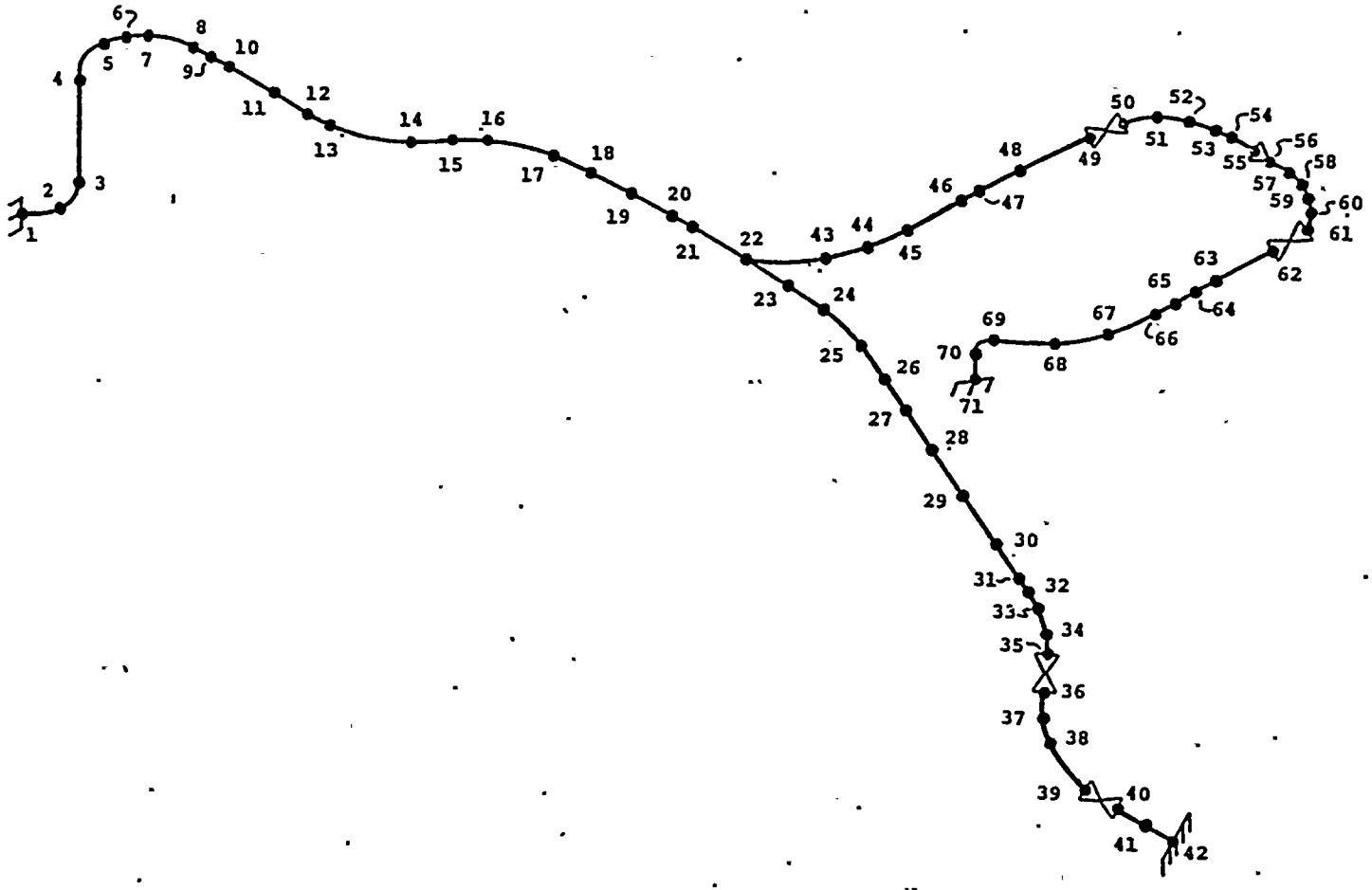

REACTOR WATER CLEAN-UP
FINITE ELEMENT MODEL
FIGURE B-8

MPR ASSOCIATES
F-85-45-5
6/13/84

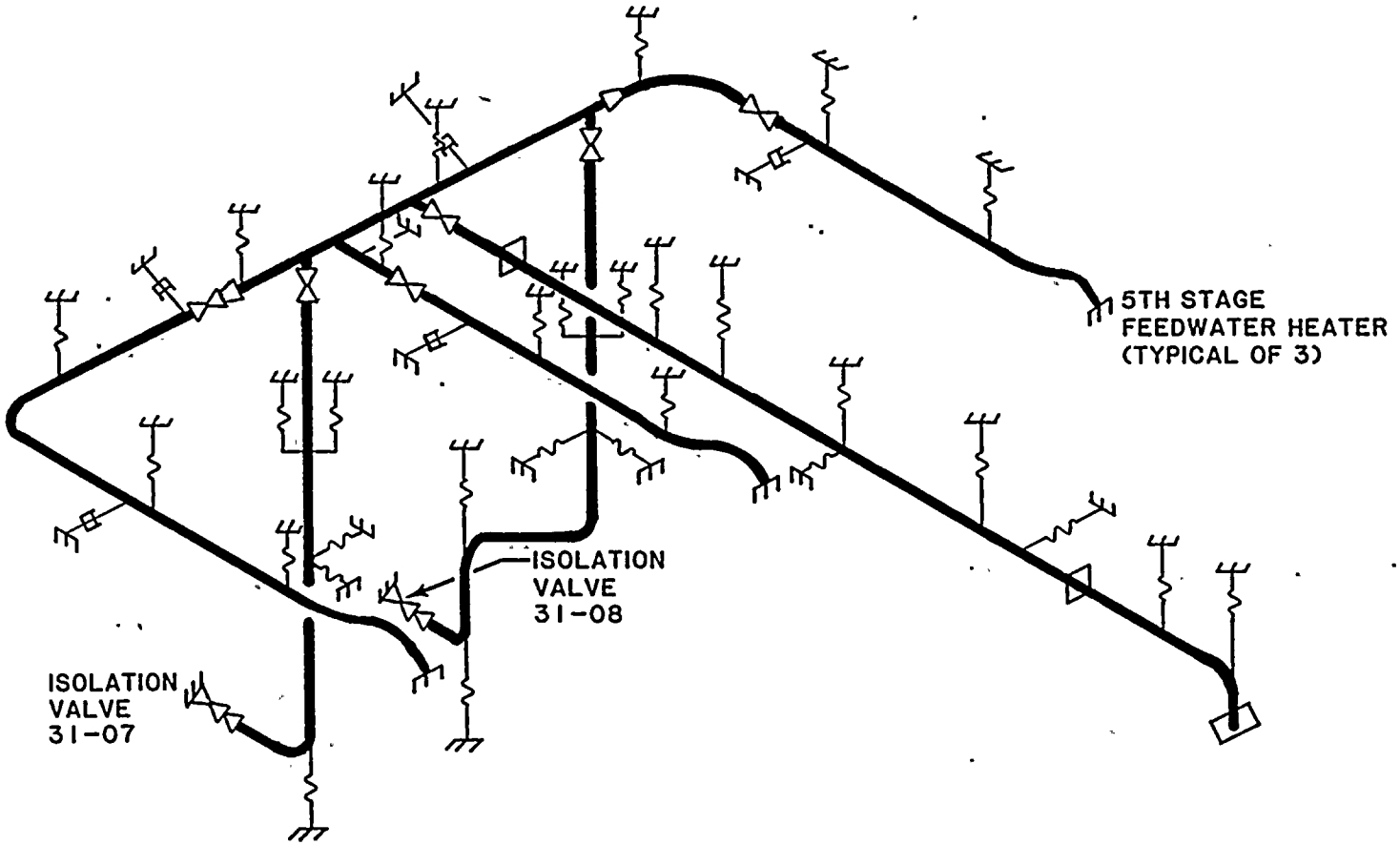

REACTOR FEEDWATER

FIGURE B-9

MPR ASSOCIATES
F-85-45-11
7/8/84

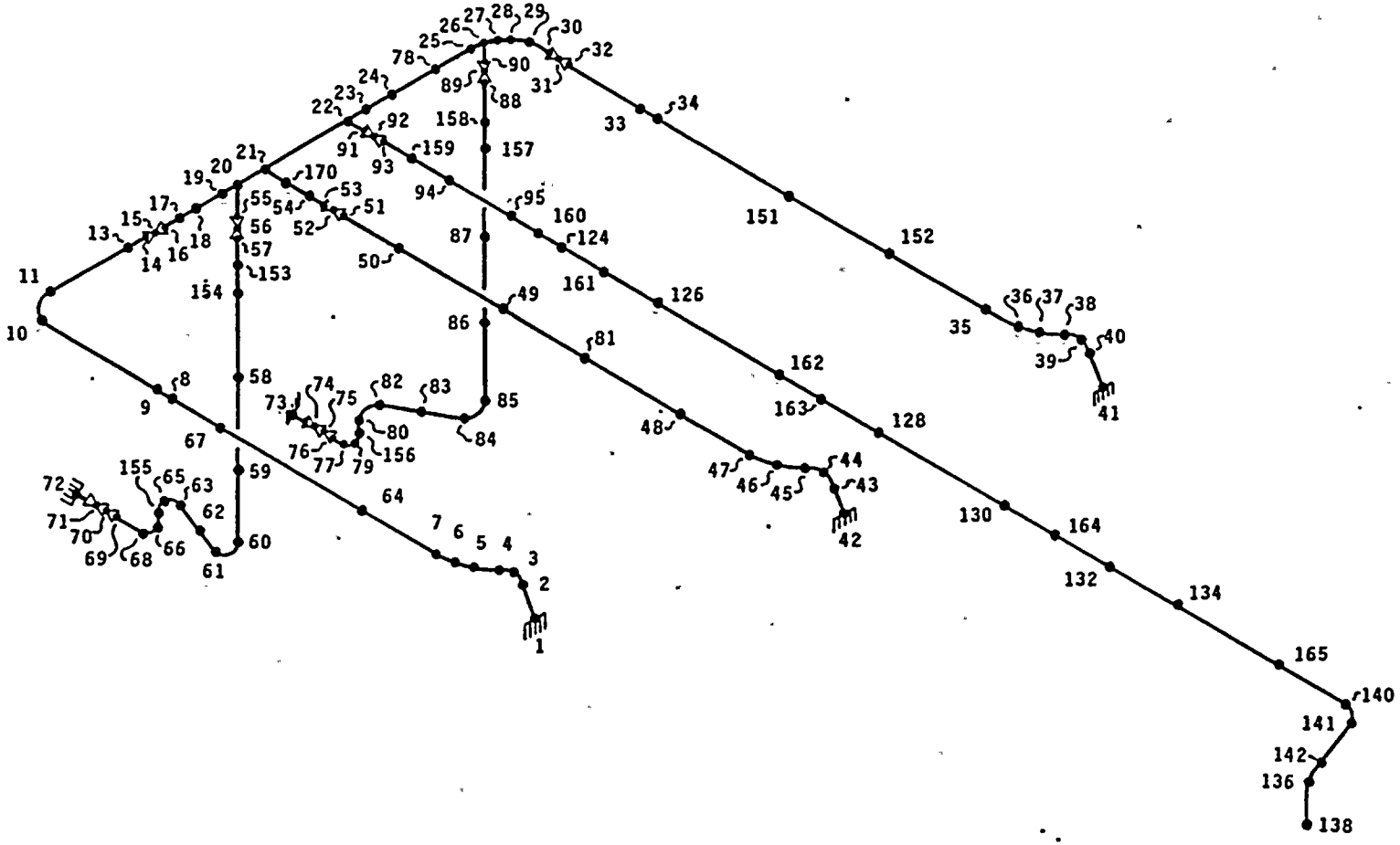

REACTOR FEEDWATER
FINITE ELEMENT MODEL

FIGURE B-10

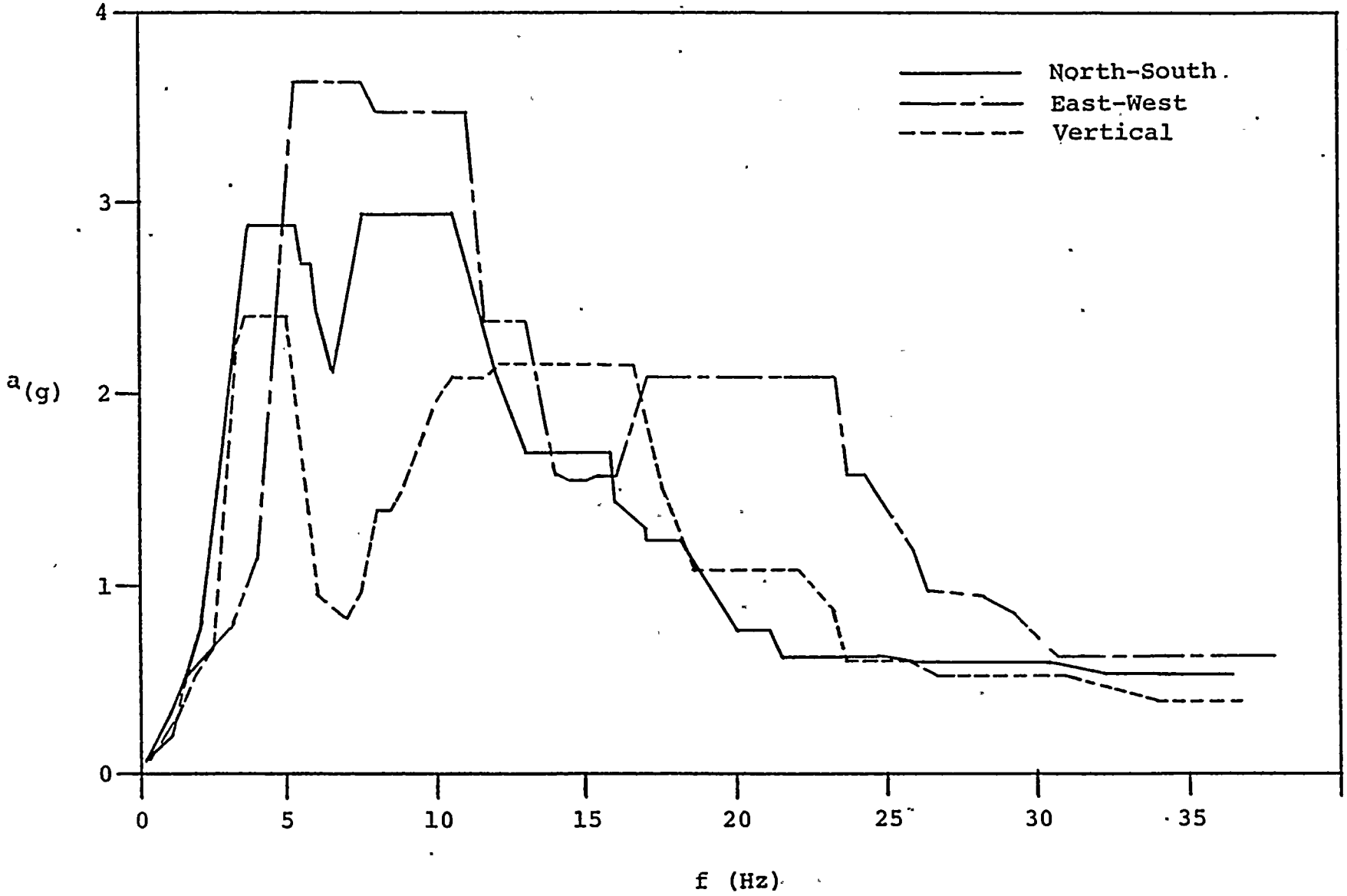

MAIN STEAM
FREQUENCY RESPONSE SPECTRA
FIGURE B-11

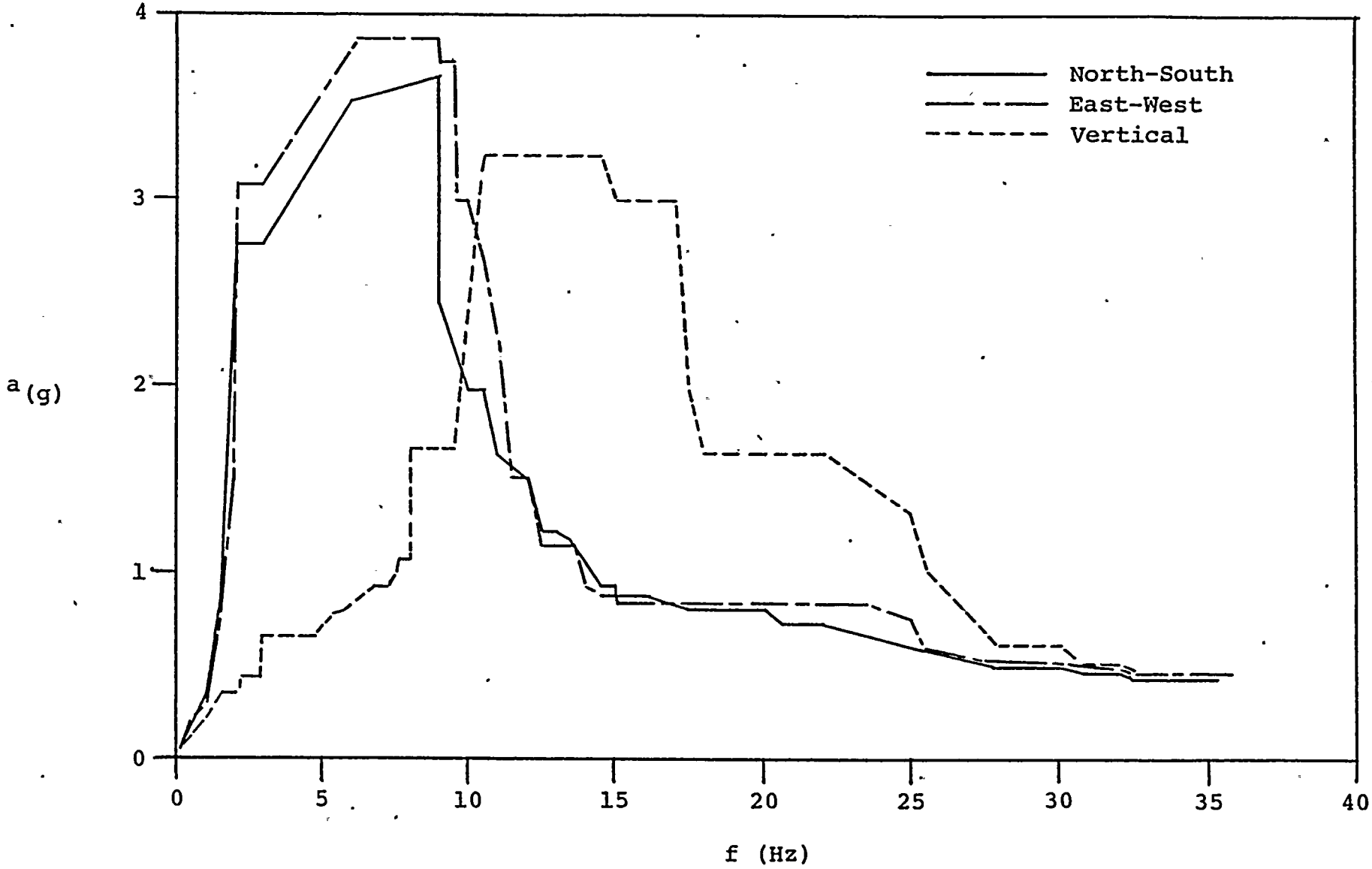

EMERGENCY CONDENSER STEAM SUPPLY
FREQUENCY RESPONSE SPECTRA
FIGURE B-12

MPR ASSOCIATES
F-85-45-10
7/3/84

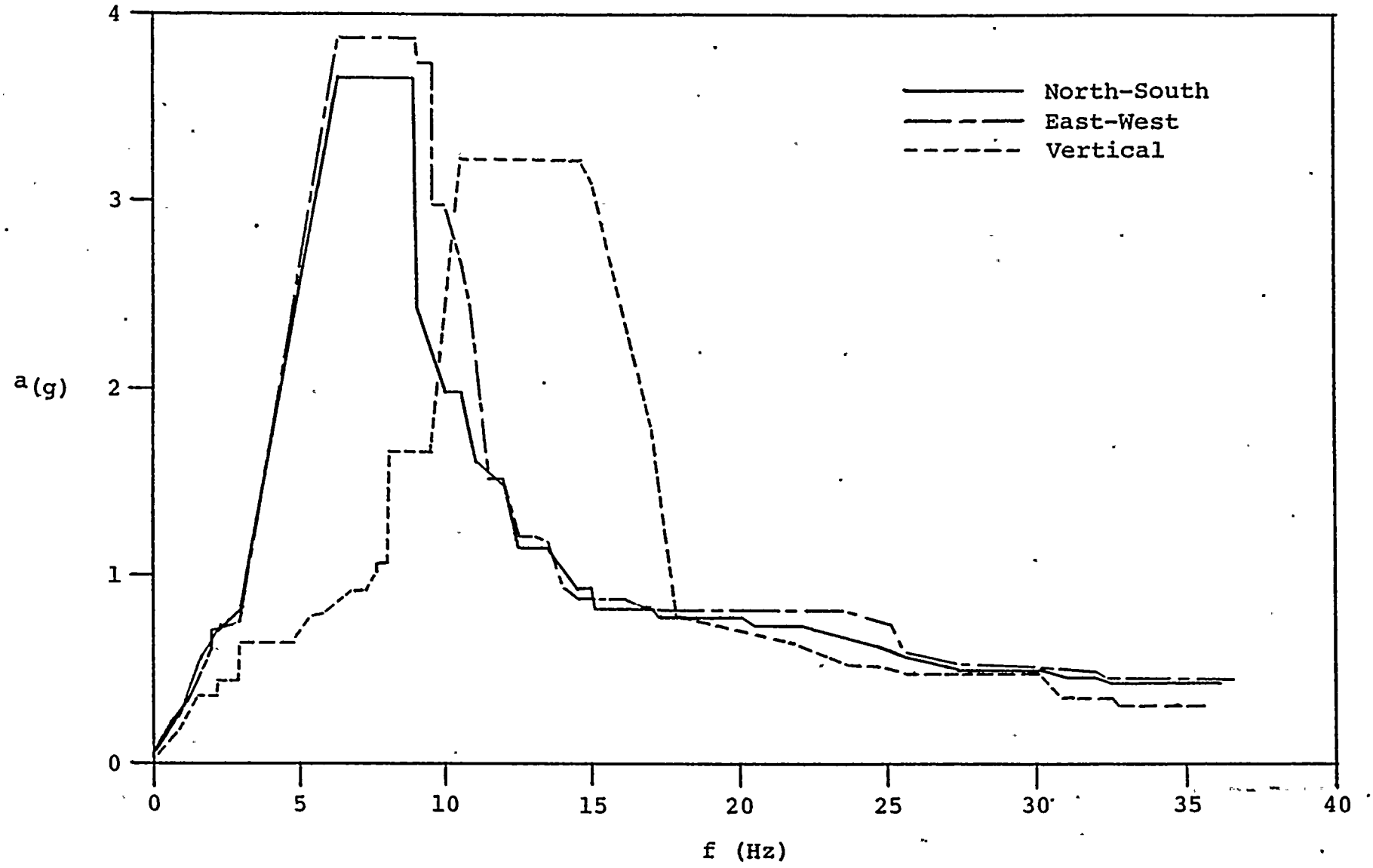

EMERGENCY CONDENSER CONDENSATE RETURN
FREQUENCY RESPONSE SPECTRA
FIGURE B-13

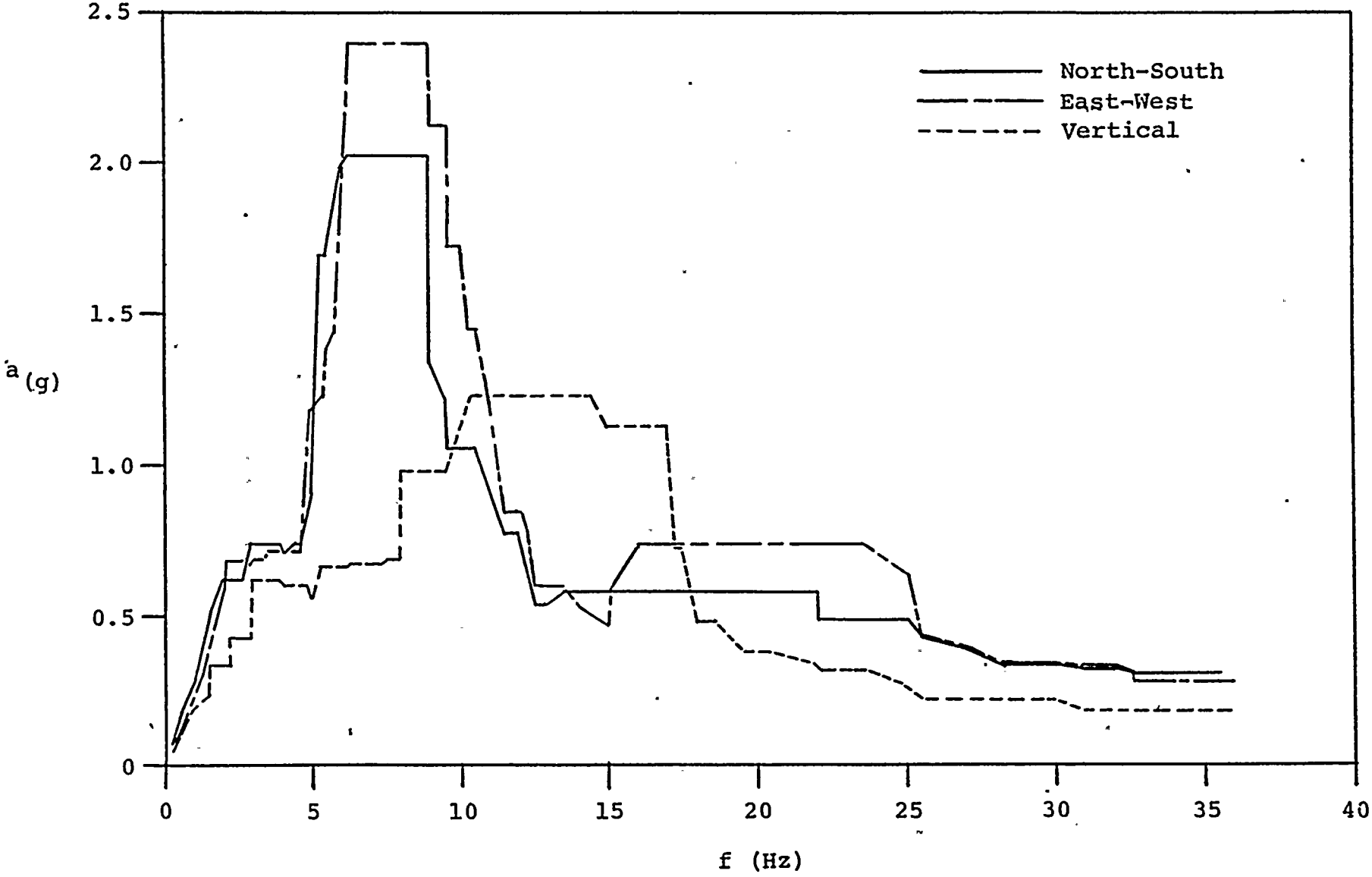

REACTOR WATER CLEAN-UP
FREQUENCY RESPONSE SPECTRA
FIGURE B-14

MPR ASSOCIATES
F-85-45-7
7/3/84

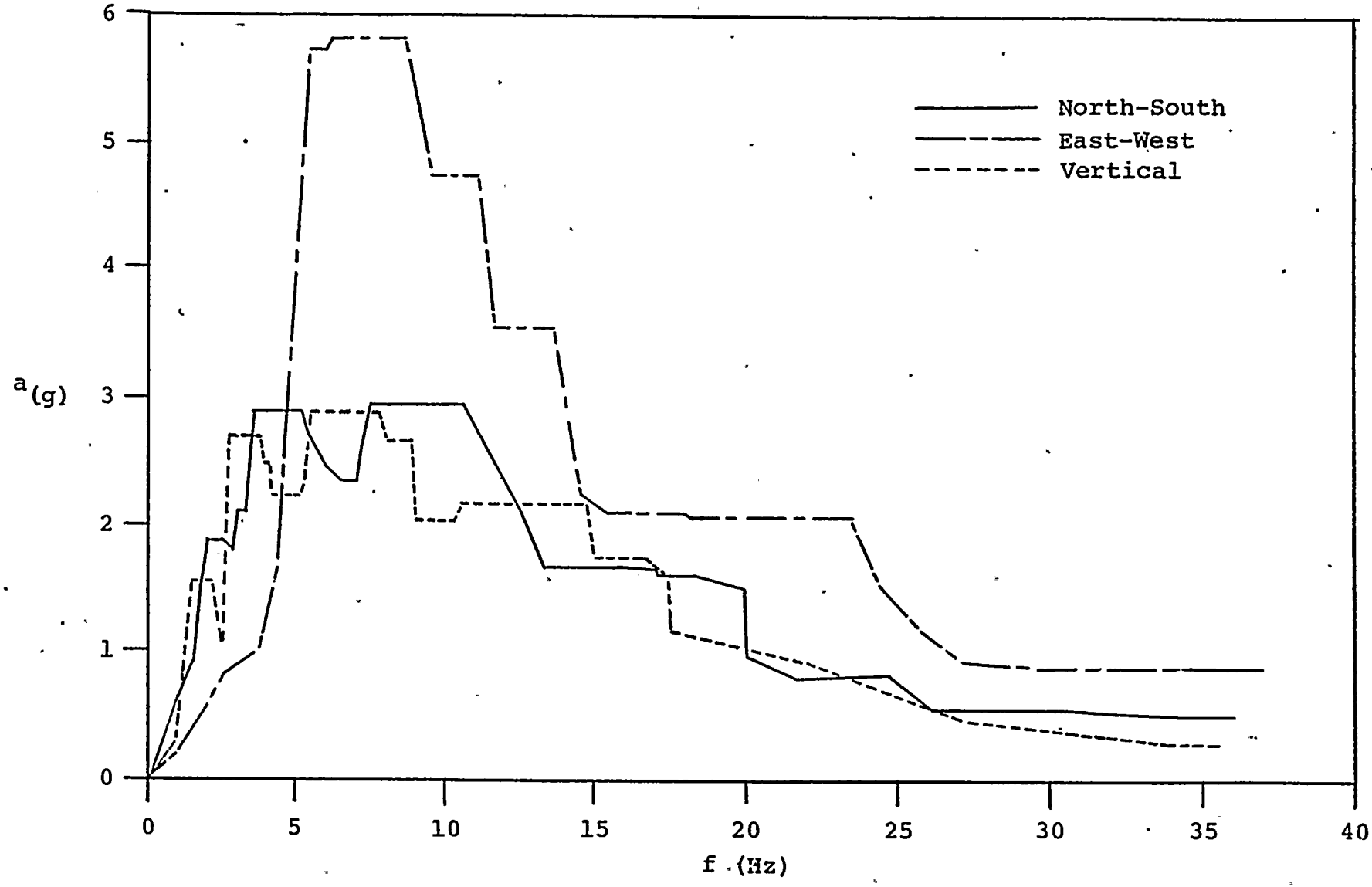

REACTOR FEEDWATER
FREQUENCY RESPONSE SPECTRA
FIGURE B-15

Appendix C

J-INTEGRAL THEORY

To satisfy the leak-before-break criteria presented in Reference C-1, it is necessary to show that the applied J-integral, J_{app}, is less than J_{IC} (a material property) for a one gallon per minute (gpm) plus 2t crack size under Level D loading conditions. Described below are the methods by which J_{app} was calculated for (1) longitudinal cracks, (2) circumferential cracks, and (3) circumferential cracks under plastic loads.

1. Longitudinal Cracks

In the linear elastic range, J_{app} is related to K, the stress intensity factor from linear elastic fracture mechanics (LEFM), by the relation, $J = K^2/E$, where E is the material elastic modulus. The stress intensity factor, K, is calculated from traditional LEFM methods $K = \sigma \sqrt{\pi a} f$, where σ is the stress acting on the crack, a is one-half the crack length and f is a geometry factor, available from Reference C-2. The only significant stress acting on a longitudinally oriented pipe crack is the piping internal pressure. Hoop stress due to internal pressure is calculated from $\sigma = PR_i/t$, where P is the internal pressure, R_i is the pipe inside radius and t is the pipe wall thickness.

A plastic zone correction factor is used to modify the crack length in order to include the effects of plasticity near the crack tip, as suggested in Reference C-1. The effective crack length is defined as: $a = a_o + r_y$, where a_o is the actual crack length and ry is a plastic

zone correction, which is an estimate of the size of the plastic zone near the crack tip. This plastic correction is obtained through traditional LEFM methods from:

$$r_y = \frac{K^2}{2\pi\sigma_y^2},$$

where K is the applied stress intensity factor and σ_y is the material yield strength. Note that iteration is required to solve for K (and thus J). Attachment C-1 is a listing of ELASJL, a short computer program written to perform this calculation.

2. Circumferential Cracks

The applied J-integral is calculated for circumferential cracks in a manner similar to the method presented above for longitudinal cracks. LEFM solutions for the stress intensity factor, K, are determined from traditional linear elastic methods and the J-integral is found from $J = \frac{K^2}{E}$. The stress intensity factor for circumferential flaws is composed of several parts, however: $K = \Sigma\ \sigma_i\sqrt{\pi(a+r_y)}\ f_i$, where the summation is over all stresses acting on the crack (pressure, bending, tension), and f_i is a geometry factor, dependent upon the type of stress. Values for f_i are available from Reference C-2.

Unlike longitudinal flaws for which pressure is the only significant load tending to open the crack, circumferentially oriented flaws are loaded by other loads in addition to pressure. This analysis considered bending

and tensile loads resulting from deadweight and earthquake. For this load combination the plastic zone is often no longer negligible compared to the crack and the iteration procedure presented for longitudinal cracks may not converge to a solution. It is necessary to modify the plastic zone correction method in order to obtain solutions over the entire range of interest. The modified plastic zone correction chosen for circumferential flaws is one which accounts more realistically for large scale plasticity effects. It was developed recently by Tada and Paris in Reference C-3 and can be expressed:

$$r_y = \frac{K^2}{\beta \pi \sigma_y^2}$$

where β varies according to the initial crack length. In this approach, r_y is no longer an estimate of the actual plastic zone size, but rather it can be thought of as an index representing the compliance of the cracked body. When the plastic zone spreads across the remaining net ligament ahead of the crack, the compliance becomes infinitely large for non-strain hardening materials. It is possible to adjust β so that the point of "compliance instability" occurs at the limit load of the pipe, that is, at the load required to make the entire pipe cross-section plastic. (For pipes under bending, the limit moment, $Mp = 4R^2 t \sigma_y$). This determination of r_y allows calculation of K (and thus J) up to the limit load of the pipe. A computer program, ELASJC, was written to perform this calculation and is listed in Attachment C-2.

3. Plastic Loads

When applied loads exceed the limit load discussed above, no solution for J is possible using plastic zone correction methods. In this case, it is necessary to use elastic-plastic fracture mechanics (EPFM) methods which are developed specifically for plastic cross-sections. The method used to calculate J under plastic loads is taken from References C-4 through C-7. The J-integral is expressed as follows:

$$J = f_1(a_e)\,\frac{M^2}{E} + \alpha\,\sigma_o\,\varepsilon_o\,ch_1(a/b,n)\left(\frac{M}{Mo}\right)^{n+1},$$

where the first term is the elastic contribution to J, the second term is the plastic contribution, and the following are defined for a cracked pipe:

$f_1(a_e)$ = a geometry correction factor calculable from traditional LEFM solutions.

a_e = pseudo-plastic zone corrected crack length using the methods from Reference C-4.

M = one-half the moment (per unit thickness) applied to the pipe.

E = modulus of elasticity.

α, n are the coefficients for a Ramberg-Osgood fit of the material stress-strain curve.

σ_o = yield strength.

$\varepsilon_o = \sigma_o/E$

a = one-half circumferential crack length.

$b = \pi R$

$c = b-a$

h_1 (a/b, n) = tabulated function based on finite element J-integral modeling of cracked bodies.

M_o = one-half the moment required to make the pipe cracked cross-section fully plastic assuming elastic-perfectly plastic behavior.

J is obtained using solutions for a single edge cracked plate (SECP) model, which are then corrected with geometry correction factors to obtain J solutions for pipe. This calculation was performed using a computer program, JINT, which is listed in Attachment C-3.

References

C-1 NRC letter L505-81-12-015 dated December 4, 1981 to Consumers Power Corporation, with enclosures.

C-2 H. Tada, "The Effects of Shell Corrections on Stress Intensity Factors and the Crack Opening Area of a Circumferential and a Longitudinal Through Crack in a Pipe," NUREG/CR-3464, The Application of Fracture Proof Design Methods Using Tearing Instability Theory to Nuclear Piping Postulating Circumferential Throughwall Cracks.

C-3 H. Tada and P. Paris, "Estimation Procedures for Load-Development Relation and J-integral for Entire Range of Elastic-Plastic Loading of Circumferentially Cracked Pipes," NUREG/CR-3464.

C-4 V. Kumar, M.D. German and C. F. Shih, EPRI NP 1931, "An Engineering Approach to Elastic-Plastic Fracture Analysis," July 1981.

C-5 M. D. German, W. R. Anders, V. Kumar, C. F. Shih, H. G. DeLorenzi, and D. F. Mowbray, EPRI NP2608-LD, "Elastic-Plastic Fracture Analysis of Flawed Stainless Steel Pipes," Final Report September 1982.

C-6 Virendra Kumar and C. F. Shih, ASTM STP700, Fracture Mechanics, Proceeding of the Twelfth National Symposium on Fracture Mechanics, July 1980, p 406-438.

C-7 V. Kumar, W. W. Wilkening, W. R. Anders, M. D. German, H. G. DeLorenzi and D. F. Mowbray, "Estimation Technique for Prediction on Elastic-Plastic Fracture of Structural Components of Nuclear Systems," EPRI Contract RP 1237-1, Combined Fifth and Sixth Semiannual Report, February 1, 1981 to January 31, 1982, March 1982.

Attachment C-1

```
10 OPEN "ELASJL.OUT" FOR OUTPUT AS #1
20 KEY OFF
100 GOSUB 2000
110 GOSUB 3000
120 GOSUB 4000
130 GOSUB 5000
135 IF Q=1 OR Q1=1 THEN 100
136 PRINT :PRINT :PRINT :PRINT
137 PRINT "More complete printout is contained in file ELASJL.OUT"
140 CLOSE #1
145 SYSTEM
150 END
2000 REM
2001 CLS
2005 IF Q=1 THEN 2130
2007 IF Q1=1 THEN 2030
2010 PRINT "This program will solve for the J-integral for longitudinal"
2011 PRINT "flaws in pipe. The necessary inputs will appear on the screen"
2012 PRINT "and simply need to be input. The results will appear on the screen"
2013 PRINT "for J for each crack length analyzed. More complete printout"
2014 PRINT "information is written onto file ELASJL.OUT and may be examined"
2015 PRINT "after completion of the program.":PRINT:PRINT :PRINT
2016 PRINT "            press any key to continue...."
2017 T$=INKEY$
2018 IF T$="" THEN 2017
2020 CLS
2030 INPUT "TITLE: ";TITLE$:PRINT
2035 TITLE$=TITLE$+"  (LONG FLAW)"
2040 INPUT "MATERIAL: ";M$:PRINT
2050 INPUT "PIPE OUTSIDE DIAMETER (in): ";D:PRINT
2060 INPUT "WALL THICKNESS (in): ";T:PRINT
2070 INPUT "SYSTEM PRESSURE (psi): ";P:PRINT
2074 PI=3.1416:K0=0
2080 R=(D-2*T)/2
2090 SIGP=P*R/T
2110 IF LEFT$(M$,1)="C" THEN SIGY=27100:E=2.7E+07:M$="CARBON STEEL":GOTO 2130
2120 SIGY=23000:E=2.56E+07:M$="STAINLESS STEEL"
2130 INPUT "INITIAL CRACK LENGTH (in): ";A0:PRINT
2140 RETURN
3000 REM
3010 REM
3020 A=A0/2
3025 LAMBDA=A/SQR((R+T/2)*T)
3030 IF LAMBDA<1 THEN F=SQR(1+1.25*LAMBDA^2) ELSE F=.6+.9*LAMBDA
3040 K=SIGP*F*SQR(PI*A)
3050 IF ABS(K-K0)<10 THEN J=K*K/E:RETURN
3060 A=A0/2+K*K/(2*PI*SIGY*SIGY)
3070 IF A>10*A0 THEN CONVERG=1:RETURN
3080 K0=K
3090 GOTO 3025
4000 REM
4010 REM
4020 CLS
4025 PRINT #1,CHR$(12)
4030 PRINT #1,TITLE$:PRINT #1,B$
4040 PRINT #1,M$:PRINT #1,B$
4050 PRINT #1,"PIPE DIAMETER=  ";:PRINT #1,USING "##.###";D;:PRINT #1," in"
```

```
4060 PRINT #1,"WALL THICKNESS= ";:PRINT #1,USING " #.###";T;:PRINT #1," in"
4070 PRINT #1,B$
4080 PRINT #1,"PRESSURE=         ";:PRINT #1,USING " ####.#";P;:PRINT #1," psi"
4090 PRINT #1,"PRESSURE STRESS= ";:PRINT #1,USING "#####.#";SIGP;:PRINT #1," psi
"
4100 PRINT #1,B$
4110 PRINT #1,"INITIAL CRACK LENGTH=    ";:PRINT #1,USING "###.##";A0;:PRINT #1,"
 in"
4112 PRINT "INITIAL CRACK LENGTH=    ";:PRINT USING "###.##";A0;:PRINT " in"
4113 PRINT :PRINT :PRINT
4115 IF CONVERG=1 THEN 4170
4120 PRINT #1,"EFFECTIVE CRACK LENGTH= ";:PRINT #1,USING "###.##";2*A;:PRINT #1,
" in"
4130 PRINT #1,B$
4140 PRINT #1,"J= ";:PRINT #1,USING "####.#";J;:PRINT #1," in-lb/in^2"
4142 PRINT "J= ";:PRINT USING "####.#";J;:PRINT " in-lb/in^2"
4150 FOR I=1 TO 5:PRINT #1,B$:NEXT I
4160 RETURN
4170 FOR I=1 TO 3:PRINT #1,B$:NEXT I
4180 PRINT #1,"For the above conditions, this problem has no solution"
4182 PRINT "For the above conditions, this problem has no solution"
4190 PRINT
4195 CONVERG=0
4200 RETURN
5000 REM
5010 REM
5020 FOR I=1 TO 5:PRINT :NEXT I
5030 INPUT "another crack length ";Q$
5040 IF Q$="Y" THEN Q=1 :RETURN
5042 Q=0
5044 PRINT :PRINT :INPUT "start again from beginning";Q1$
5046 IF Q1$="Y" THEN Q1=1:ELSE Q1=0
5050 RETURN
```

Attachment C-2

```
5 OPEN "ELASJC.OUT" FOR OUTPUT AS #1
7 KEY OFF
10 DEF FNF(T)=1+8*(T/PI)^2.5
20 DEF FNG(T)=T*FNF(T)^2
30 DEF FNGP(T)=(FNG(T*1.01)-FNG(T))/(.01*T)
100 GOSUB 6000
250 GOSUB 3000
260 GOSUB 4000
265 IF CONVERG=1 THEN 280
270 GOSUB 5000
280 GOSUB 7000
290 GOSUB 8000
295 IF Q=1 OR Q1=1 THEN 100
300 CLOSE #1
305 PRINT :PRINT :PRINT :PRINT
306 PRINT "More complete printout is contained in file ELASJC.OUT"
308 SYSTEM
310 END
3000 REM
3010 REM
3020 REM
3030 DELTA=PI/8
3040 THETAE=THETA0+DELTA
3050 IF ABS(THETAE-THETAE0)<.0001 THEN GOTO 3090
3060 DELTA=FNG(THETAE)/FNGP(THETAE)
3070 THETAE0=THETAE
3080 GOTO 3040
3090 SP=(COS(THETA0/2)-SIN(THETA0)/2)*4/PI
3100 ALPHA=FNGP(THETAE)*SP^2
3110 RETURN
4000 REM
4010 REM
4020 THETA=THETA0
4030 SIGMA=SIGB+SIGT+SIGP
4040 KP=SIGMA*FNF(THETA)*SQR(PI*R*THETA)
4050 IF ABS(KP-KP0)< 10 THEN RETURN
4060 THETA=THETA0+KP^2/(PI*R*ALPHA*SIGY^2)
4065 IF THETA>2*PI THEN CONVERG=1:RETURN
4070 KP0=KP
4080 GOTO 4040
5000 REM
5010 REM
5020 REM
5030 REM
5040 TP=THETA/PI
5050 FT=1+7.5*TP^1.5-15*TP^2.5+33*TP^3.5
5060 FB=1+6.8*TP^1.5-13.6*TP^2.5+20*TP^3.5
5065 LAMBDA=R*THETA/SQR(R*T)
5070 IF LAMBDA<1 THEN FP=SQR(1+.3225*LAMBDA^2) ELSE FP=.9+.25*LAMBDA
5080 K=(SIGB*FB+SIGT*FT+SIGP*FP)*SQR(R*PI*THETA)
5090 J=K*K/E
5100 RETURN
6000 REM
6001 CLS
6002 IF Q=1 THEN 6120
6003 IF Q1=1 THEN 6065
6005 PRINT "This program will solve for the J-integral for circumferential"
```

```
6005 PRINT "This program will solve for the J-integral for circumferential"
6006 PRINT "flaws in pipe. The necessary inputs will appear on the screen"
6007 PRINT "and simply need to be input. The results will appear on the screen"
6008 PRINT "for J for each crack length analyzed. More complete printout"
6009 PRINT "information is written onto file ELASJC.OUT and may be examined"
6010 PRINT "after completion of the program.":PRINT :PRINT :PRINT
6011 PRINT "            press any key to continue...."
6012 T$=INKEY$
6013 IF T$="" THEN 6012
6019 THETAE0=0
6020 KP0=0
6030 PI=3.1415
6040 B$=" "
6060 CLS
6065 INPUT "TITLE: ";TITLE$:PRINT
6066 TITLE$=TITLE$+"  (CIRCUM FLAW)"
6067 INPUT "PIPE MATERIAL: ";M$:PRINT
6070 INPUT "PIPE DIAMETER  (IN) : ";D:PRINT
6080 INPUT "WALL THICKNESS  (IN) : ";T:PRINT
6090 INPUT "BENDING STRESS  (PSI) : ";SIGB:PRINT
6100 INPUT "AXIAL STRESS  (PSI) : ";SIGT:PRINT
6110 INPUT "SYSTEM PRESSURE  (PSI) : ";P:PRINT
6114 IF LEFT$(M$,1)="C" THEN SIGY=27100:E=2.7E+07:M$="CARBON STEEL":GOTO 6116
6115 SIGY=23000:E=2.56E+07:M$="STAINLESS STEEL"
6116 R=(D-T)/2
6117 SIGP=P*(R-T/2)^2/(2*R*T)
6120 INPUT "INITIAL CRACK LENGTH  (IN) : ";A0:PRINT
6160 THETA0=A0/(2*R)
6180 RETURN
7000 REM
7010 REM
7020 CLS
7025 PRINT #1,CHR$(12)
7030 PRINT #1,TITLE$:PRINT #1,B$
7040 PRINT #1,M$:PRINT #1,B$
7050 PRINT #1,"PIPE DIAMETER=  ";:PRINT #1,USING "##.### ";D;:PRINT #1," in"
7060 PRINT #1,"WALL THICKNESS= ";:PRINT #1,USING " #.### ";T;:PRINT #1," in"
7070 PRINT #1,B$
7080 PRINT #1,"BENDING  STRESS= ";:PRINT #1,USING "#####.#";SIGB;:PRINT #1," psi
"
7090 PRINT #1,"AXIAL  STRESS=  ";:PRINT #1,USING "#####.#";SIGT;:PRINT #1," psi
"
7100 PRINT #1,"PRESSURE STRESS= ";:PRINT #1,USING "#####.#";SIGP;:PRINT #1," psi
"
7110 PRINT #1,B$:A=2*R*THETA
7120 PRINT #1,"INITAL  CRACK  LENGTH=  ";:PRINT #1,USING "##.##";A0;:PRINT #1,"
in"
7123 PRINT "INITAL  CRACK  LENGTH=  ";:PRINT USING "##.##";A0;:PRINT " in"
7124 PRINT
7125 IF CONVERG=1 THEN 7170
7130 PRINT #1,"EFFECTIVE CRACK LENGTH= ";:PRINT #1,USING "##.##";A;:PRINT #1," i
n"
7140 PRINT #1,B$
7148 PRINT "J= ";:PRINT USING "#####.#";J;:PRINT " in-lb/in^2"
7149 PRINT #1,"J= ";:PRINT #1,USING "#####.#";J;:PRINT #1," in-lb/in^2"
```

```
7150 FOR I=1 TO 5 :PRINT #1,B$ :NEXT I
7155 PRINT :PRINT :PRINT :PRINT
7160 RETURN
7170 PRINT #1,B$:PRINT #1,B$:PRINT #1,B$
7180 PRINT #1,"For the above conditions, this problem has no solution"
7185 PRINT  "This initial crack length does not converge for this situation"
7190 PRINT :PRINT :PRINT:CONVERG=0
7195 FOR I=1 TO 5 :PRINT #1,B$ :NEXT I
7200 RETURN
8000 REM
8010 REM
8020 INPUT "another crack length";Q$
8030 IF Q$="Y" THEN Q=1:RETURN
8033 Q=0
8035 PRINT:PRINT:INPUT "start again from beginning";Q1$
8040 IF Q1$="Y" THEN Q1=1:ELSE Q1=0
8050 RETURN
```

Attachment C-3

```
90 KEY OFF
100 FLAG=0
105 CLS
110 INPUT "SYSTEM NAME..";N$
120 INPUT "MATERIAL  (C/S)";M$
130 IF M$="C" THEN M$="CARBON STEEL":S0=27100!:E=2.7E+07:AL=1.94:N=4.42:GOTO 150

140 M$="STAINLESS STEEL":S0=23000!:E=2.56E+07:AL=2.13:N=3.79
150 E0=S0/E
160 CLS
170 INPUT "PIPE DIAMETER";D
180 INPUT "WALL THICKNESS";T
190 R=D/2
200 I=3.1416*(R^4-(R-T)^4)/4
210 PRINT
220 INPUT "FLAW SIZE (WHOLE PIPE)";A
230 A=A/2
240 IF FLAG=1 THEN 260
250 INPUT "LEVEL D STRESS";SD
253 IF M$="CARBON STEEL" THEN H1=.677:GOTO 260
255 INPUT "EMER COND STEAM ";Q$
257 IF Q$="Y" THEN H1=.74 ELSE H1=.693
260 CLS
270 B=3.1416*R
280 C=B-A
290 G=2*A/D
300 Z=A/B
320 GOSUB 1000
330 X1=R/T
340 X=A/SQR(R*T)
350 A1=.2*X1+1
360 B1=9.000001E-02*X1+.75
370 C1=.0035*X1+8.250001E-02
380 CF=B1-C1*(X-A1)*(X-A1)
390 M=I*SD/(2*R)
400 TRIG=COS(G/2)-.5*SIN(G)
410 MO=2*SO*R*R*T*TRIG
420 MM0=M/MO
430 PHI=1/(1+MM0*MM0)
440 RY1=(PHI/6.283)*((N-1)/(N+1))
450 JEL=CF*F1*((M/T)^2)/E
460 KEL=SQR(JEL*E)
470 RY2=(KEL/SO)^2
480 RY=RY1*RY2
490 A=A+RY
500 Z=A/B
510 GOSUB 1000
520 JEL=CF*F1*((M/T)^2)/E
530 JP=CF*AL*SO*EO*C*H1*MM0^(N+1)
540 J=JEL+JP
545 LPRINT CHR$(12)
550 LPRINT N$
560 LPRINT
570 LPRINT M$
580 LPRINT
```

```
590 LPRINT "PIPE DIAMETER= ";:LPRINT USING " ##.###";D;:LPRINT " in"
600 LPRINT "WALL THICKNESS=";:LPRINT USING " ##.###";T;:LPRINT " in"
610 LPRINT
620 LPRINT "INITIAL FLAW SIZE=";:LPRINT USING " ##.###";2*(A-RY);:LPRINT " in"
625 PRINT "INITIAL FLAW SIZE=";:PRINT USING " ##.###";2*(A-RY);:PRINT " in"
630 LPRINT "EFFECTIVE FLAW SIZE=  ";:LPRINT USING " ##.###";2*A;:LPRINT " in"
640 LPRINT
650 LPRINT "STRESS=";:LPRINT USING " #####.#";SD;:LPRINT " psi"
660 LPRINT
670 LPRINT "J=";:LPRINT USING " #####.#";J;:LPRINT " in-lb/in^2"
675 PRINT :PRINT :PRINT "J=";:PRINT USING " #####.#";J;:PRINT ", in-lb/in^2"
680 LPRINT
690 PRINT:PRINT :PRINT :PRINT
700 INPUT "     another flaw";F$
710 IF F$="Y" THEN FLAG=1:CLS:GOTO 220
715 SYSTEM
720 END
1000 F=1.122-1.4*Z+7.33*Z*Z-13.08*Z^3+14*Z^4
1010 F1=36*3.1416*A*F*F/B^4
1020 RETURN
```

Appendix D

TEARING STABILITY THEORY

The criteria for stability of a cracked pipe under large loads were developed briefly by Paris in a recent paper, Reference D-1. These general criteria, which involve only considerations of simple moment balance, can be extended and applied to a cracked section whose J-integral is known as a function of crack size and hinge angle. These new criteria can be further modified to use the crack size and applied moment as independent variables, since most expressions of the J-intergal and cracked section compliance use these as independent variables.

Along the lines presented by Paris in Reference D-1, consider a fixed-ended beam with a crack at its midpoint as shown in Figure D-1. This fixed-end condition will later be relaxed; however, including it now simplifies understanding of the stability process. Assume that loads in the piping system (which is represented by the beam) are distributed arbitrarily and represent hanger loads, fixed support loads and inertial loads (e.g., earthquake). These loads are represented by point loads P1, P2, P3 in Figure D-1, but distributed loads are also implied.

Assume the crack is heavily loaded and the remaining section at the crack is carrying a plastic moment, Mp. If the crack grows, the moment carried by the net section is reduced by an amount dMp and the hinge angle, ϕ, at the crack increases an amount $d\phi$. For stability, the moment change, dMp, must be picked up by the rest of the system. In that case, the final state in Figure D-1 is reached with a new moment carried by the cracked section, Mp - dMp, and new hinge angle, $\phi + d\phi$.

As Paris points out, stability is implied when the moment rate of change (with respect to hinge angle) in the cracked section is less than the moment rate of change (with respect to hinge angle) that the rest of the system can pick up:

$$-\frac{dM_p}{d\varphi} < \left.\frac{dM}{d\varphi}\right|_{system} \qquad \text{Stability Condition}$$

Departing from Paris' assumptions in Reference D-1, it is not assumed $\left.\frac{dM}{d\phi}\right|$system is related to the stiffness of a fixed-ended beam with length L and moment of inertia I. Rather, since it is possible from finite element modeling of a piping system to directly calculate $\left.\frac{dM}{d\phi}\right|$system at any node point, we assume $\left.\frac{dM}{d\phi}\right|$system is known. This derivative, $\left.\frac{dM}{d\phi}\right|$ system, is the the system stiffness, K_ϕ. For these conditions, stability can be characterized as follows:

$$-\frac{dM_p}{d\varphi} < K_\varphi \qquad \underline{\text{Stable}}$$

$$-\frac{dM_p}{d\varphi} > K_\varphi \qquad \underline{\text{Unstable}}$$

In order to apply this stability criteria to an actual pipe with an assumed flaw, the relationship between moment carrying capability, hinge angle and crack size must be known for a pipe section with, in the case of interest, a through wall circumferentially oriented flaw. This will allow calculation of $\frac{dMp}{d\phi}$ for arbitrary loading and crack size. Laboratory tests of cracked pipe sections could be used to <u>measure</u> $\frac{dMp}{d\phi}$, but such tests, in general, are too expensive to be practical for every flaw size and pipe size of interest.

The historical approach to this problem has been to calculate the compliance of the cracked section, assuming some sort of material stress-strain relation (e.g., elastic-perfectly plastic, power law hardening, etc.). In order to calculate $\frac{dMp}{d\phi}$, however, it is necessary to introduce another function that details the state of stress at the flaw tip. This function, called the "J-integral" (or simply "J") represents the strength of the stress field's rise to infinity at the flaw tip. The concepts of "J" and "J-controlled crack growth" were developed by Rice in the 1960's. Assume that, like the plastic moment-carrying capability of the flaw, J is a function of the crack size, a, and hinge angle:

$$Mp = Mp(a,\phi) \tag{1}$$

$$J = J(a,\phi) \tag{2}$$

Using Rice's energy definition of J, it can be written:

$$J = \frac{-1}{t} \int_0^{\varphi} \frac{\partial M_\rho}{\partial a}\Big)_\varphi d\varphi \tag{3}$$

where t is the pipe wall thickness.

It is important to note one further property of J: for a growing crack, the quantity $\frac{dJ}{da}$ (i.e., the <u>total</u> variation of J with respect flaw size) is a material property, and under conditions of significant crack growth (i.e., greater than 0.1" or so), it is a constant independent of what type of specimen is used to measure it. Therefore, laboratory tests on small compact tension specimens of the appropriate

material can be used to determine $\frac{dJ}{da}$ for appropriate temperatures. $\frac{dJ}{da}$ is a measure of the plastic tearing resistance of the material.

Returning to the stability problem, it is desired to calculate $\frac{dMp}{d\phi}$ (i.e., the <u>total</u> variation in cracked section moment with hinge angle), allowing the crack size to vary.

Differentiating equation (1)

$$dM_p \approx \left(\frac{\partial M_p}{\partial a}\right)_\varphi da + \left(\frac{\partial M_p}{\partial \varphi}\right)_a d\varphi \qquad (4)$$

Differentiating J, from equation (3)

$$dJ = -\frac{1}{t}\left(\frac{\partial M_p}{\partial a}\right)_\varphi + \left(\frac{\partial J}{\partial a}\right)_\varphi da \qquad (5)$$

Note at this point that Paris ignores the second term in (5), claiming that it is small under conditions where J is valid (small crack growth compared to pipe circumference). Because this term turns out not to be small, and it is necessary to retain the term for mathematical consistency, this derivation retains it.

Dividing (4) by $d\phi$,

$$\frac{dM_p}{d\varphi} = \left(\frac{\partial M_p}{\partial a}\right)_\varphi \frac{da}{d\varphi} + \left(\frac{\partial M_p}{\partial \varphi}\right)_a \qquad (6)$$

Since "a" and "ϕ" are assumed to be independent variables, the quantity $\frac{da}{d\phi}$ is undefined. For this reason, a new relationship between a and ϕ, offered by J, is needed. This

relationship will eventually be related to the $\frac{dJ}{da}$ material property, which is physically real.

Solving (5) for $d\phi$, find that

$$d\varphi = \frac{\left(\frac{\partial J}{\partial a}\right)_\varphi da - dJ}{\frac{1}{t}\left(\frac{\partial M_p}{\partial a}\right)_\varphi}$$

and substituting this into (6) for $d\phi$:

$$\frac{dM_p}{d\varphi} = \frac{1}{t}\left(\frac{\partial M_p}{\partial a}\right)_\varphi^2 \frac{da}{\left(\frac{\partial J}{\partial a}\right)_\varphi da - dJ} + \left(\frac{\partial M_p}{\partial \varphi}\right)_a$$

or

$$\frac{dM_p}{d\varphi} = \frac{1}{t}\left(\frac{\partial M_p}{\partial a}\right)_\varphi^2 \left[\left(\frac{\partial J}{\partial a}\right)_\varphi - \frac{dJ}{da}\right]^{-1} + \left(\frac{\partial M_p}{\partial \varphi}\right)_a \quad (7)$$

Under conditions of flaw growth, as has already been noted, $\frac{dJ}{da}$ is a material property, now referred to as $\frac{dJ}{da}_{MAT}$. The quantity $\frac{E}{\sigma_o^2}\frac{dJ}{da}_{MAT}$ (a dimensionless form of $\frac{dJ}{da}_{MAT}$) is called "T_{MAT}" or the tearing modulus.

$$T_{MAT} = \frac{E}{\sigma_o^2}\left.\frac{dJ}{da}\right|_{MAT} \quad (8)$$

Using (8) in (7),

$$\frac{dM_p}{d\varphi} = \frac{1}{t}\left(\frac{\partial M_p}{\partial a}\right)_\varphi^2 \left[\left(\frac{\partial J}{\partial a}\right)_\varphi - \frac{\sigma_o^2}{E} T_{MAT}\right]^{-1} + \left(\frac{\partial M_p}{\partial \varphi}\right)_a \quad (9)$$

Using the stability criteria, $-\frac{dMp}{d\phi} < K_\phi$

$$-\frac{1}{t}\left(\frac{\partial Mp}{\partial a}\right)_\varphi^2\left[\left(\frac{\partial J}{\partial a}\right)_\varphi - \frac{\sigma_o^2}{E}T_{MAT}\right]^{-1} - \left(\frac{\partial Mp}{\partial \varphi}\right)_a < K_\varphi$$

or, solving for T_{MAT}:

$$T_{MAT} > \frac{E}{\sigma_o^2}\frac{1}{t}\left(\frac{\partial Mp}{\partial a}\right)_\varphi^2\left[K_\varphi + \left(\frac{\partial Mp}{\partial \varphi}\right)_a\right]^{-1} + \frac{E}{\sigma_o^2}\left(\frac{\partial J}{\partial a}\right)_\varphi \quad (10)$$

This equation says that a measured material property, T_{MAT}, must be greater than some calculated function of flaw size, applied moment and piping system stiffness in order for the crack to be stable. The quantities $Mp(a,\phi)$ and $J(a,\phi)$ have been calculated by others for various flaw geometries in pipes, and other shapes, using several assumptions regarding strain hardening behavior. The exact expressions for these terms in (10) is a separate calculation shown in Appendix E.

It is desired to re-cast equation (10) in terms of the independent variables a and Mp, rather than a and ϕ . This is done because most calculations for J are done in terms of J(a, Mp). Further, in the "a, Mp" system, a particularly simple expression for T_{MAT} (i.e., equation 10) exists for the condition $K_\phi = 0$. It is known intuitively that if $K_\phi = 0$, the cracked section is dead loaded. Under these conditions, it is evident that

$$T_{MAT}(K_\varphi = 0) > \frac{E}{\sigma_o^2}\left(\frac{\partial J}{\partial a}\right)_{M_p} ;$$

that is, the applied moment does not change if the crack grows. After transposing equation (10) to the "a, Mp" variable system, the stability condition $T_{MAT} = \frac{E}{\sigma_{o^2}} \frac{dJ}{da}_{Mp}$ is expected when $K\phi = 0$.

Recasting the problem in the "a, Mp" variable system:

$$J := J(a, Mp)$$

$$\phi = \phi(a, Mp)$$

$$J = \frac{1}{t} \int_0^{Mp} \frac{\partial \varphi}{\partial a}\Big)_{Mp} dMp$$

(Reformulation of Rice's Energy Integral - see Reference D-2)

The expression $\frac{\partial Mp}{\partial a}\Big)_{\phi}$ in (10) is readily found in this new system by noting that in this derivative, ϕ, is a constant. That is,

$$d\varphi = 0 = \frac{\partial \varphi}{\partial a}\Big)_{Mp} da + \frac{\partial \varphi}{\partial Mp}\Big)_{a} dMp$$

or

$$\frac{\partial Mp}{\partial a}\Big)_{\varphi} = -\left(\partial\varphi/\partial a\right)_{Mp} \Big/ \left(\partial\varphi/\partial Mp\right)_{a} \qquad (11)$$

In addition, the term $\frac{\partial Mp}{\partial \phi}\Big)_{a}$ in (10) is simply

$$\frac{\partial Mp}{\partial \varphi}\Big)_{a} = 1 \Big/ \left(\partial\varphi/\partial Mp\right)_{a} \qquad (12)$$

Finally, the term $\left.\frac{\partial J}{\partial a}\right)_{\phi}$ can be found from:

$$0 = d\varphi = \left.\frac{\partial \varphi}{\partial a}\right)_{M_p} da + \left.\frac{\partial \varphi}{\partial M_p}\right)_{a} dM_p$$

or

$$\left. dM_p \right)_{\varphi} = - \left[\left(\partial \varphi / \partial a \right)_{M_p} / \left(\partial \varphi / \partial M_p \right)_a \right] da \qquad (13)$$

Now

$$dJ = \left.\frac{\partial J}{\partial a}\right)_{M_p} da + \left.\frac{\partial J}{\partial M_p}\right)_{a} dM_p \qquad (14)$$

At ϕ = const, use (13) in (14) for dMp

$$\left. dJ \right)_{\varphi} = \left.\frac{\partial J}{\partial a}\right)_{M_p} da - \left.\frac{\partial J}{\partial M_p}\right)_{a} \left[\left(\partial \varphi / \partial a \right)_{M_p} / \left(\partial \varphi / \partial M_p \right)_a \right] da$$

Finally,

$$\left.\frac{\partial J}{\partial a}\right)_{\varphi} = \left.\frac{\partial J}{\partial a}\right]_{M_p} - \left[\left(\partial \varphi / \partial a \right)_{M_p} / \left(\partial \varphi / \partial M_p \right)_a \right] \left.\frac{\partial J}{\partial M_p}\right)_{a} \qquad (15)$$

Substituting equations (11), (12) and (15) into (10) converts (10) to the "a, M" system:

$$T_{MAT} > \frac{E}{\sigma_0^2}\,\frac{1}{t}\left[\left(\partial\varphi/\partial a\right)_{M_p} / \left(\partial\varphi/\partial M_p\right)_a\right]^2 \cdot \left[K_\varphi + 1/\left(\partial\varphi/\partial M_p\right)_a\right]^{-1} +$$

$$+ \frac{E}{\sigma_0^2}\left\{\left(\frac{\partial J}{\partial a}\right)_{M_p} - \left[\left(\partial\varphi/\partial a\right)_{M_p} / \left(\partial\varphi/\partial M_p\right)_a\right]\left(\frac{\partial J}{\partial M_p}\right)_a\right\} \qquad (16)$$

Evaluating this equation at the limit $K_\phi = 0$:

$$T_{MAT} > \frac{E}{\sigma_0^2}\,\frac{1}{t}\left[\left(\partial\varphi/\partial a\right)_{M_p} / \left(\partial\varphi/\partial M_p\right)_a\right]^2 \cdot \left[1/\left(\partial\varphi/\partial M_p\right)_a\right]^{-1} +$$

$$+ \frac{E}{\sigma_0^2}\left\{\left(\frac{\partial J}{\partial a}\right)_{M_p} - \left[\left(\partial\varphi/\partial a\right)_{M_p} / \left(\partial\varphi/\partial M_p\right)_a\right]\left(\frac{\partial J}{\partial M_p}\right)_a\right\}$$

Rearranging terms and simplifying:

$$T_{MAT} > \frac{E}{\sigma_0^2}\left\{\left(\frac{\partial J}{\partial a}\right)_{M_p} + \frac{1}{t}\left[\left(\partial\varphi/\partial a\right)_{M_p} / \left(\partial\varphi/\partial M_p\right)_a\right] \times \right.$$

$$\left. \times \left[\left(\partial\varphi/\partial a\right)_{M_p} - t\left(\frac{\partial J}{\partial M_p}\right)_a\right]\right\}$$

Focusing on the terms inside the second square brackets:

$$\frac{\partial \varphi}{\partial a}\Big)_{M_p} - t\,\frac{\partial J}{\partial M_p}\Big)_a$$

and examining the integral expression for J on page D-7, one sees that

$$\frac{\partial J}{\partial M_p}\Big)_a = \frac{1}{t}\,\frac{\partial \varphi}{\partial a}\Big)_{M_p}$$

The terms in square brackets cancel and

$$T_{MAT} > \frac{E}{\sigma_0^2}\,\frac{\partial J}{\partial a}\Big)_{M_p}$$ as expected.

References:

D-1 Paul C. Paris "Fracture Proof Design and Analysis of Nuclear Piping," NUREG CR 3464, Sept. 1983

D-2 J. W. Hutchinson and P. C. Paris, "Stability Analysis of J-Controlled Crack Growth," ASTM STP 668, 1979, p 37-64.

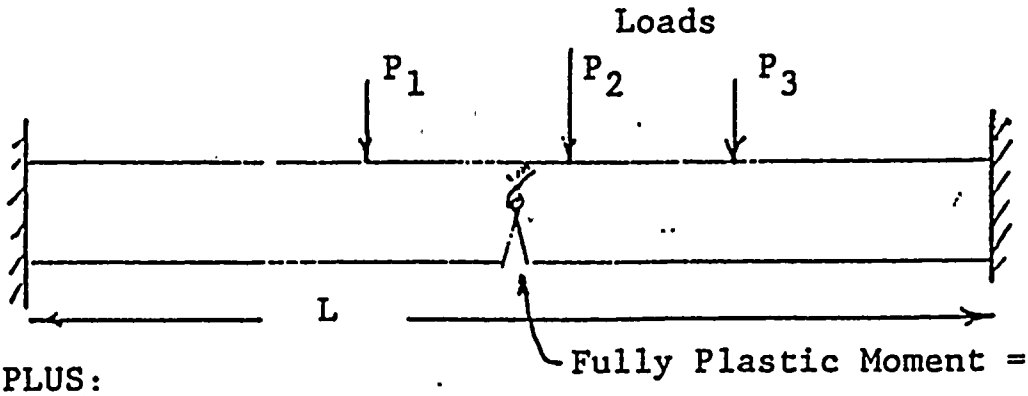

Figure 1a (Original State)

PLUS:

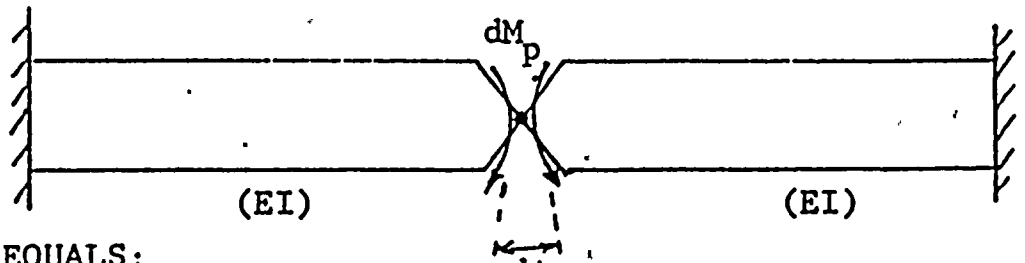

Figure 1b (Changes)

EQUALS:

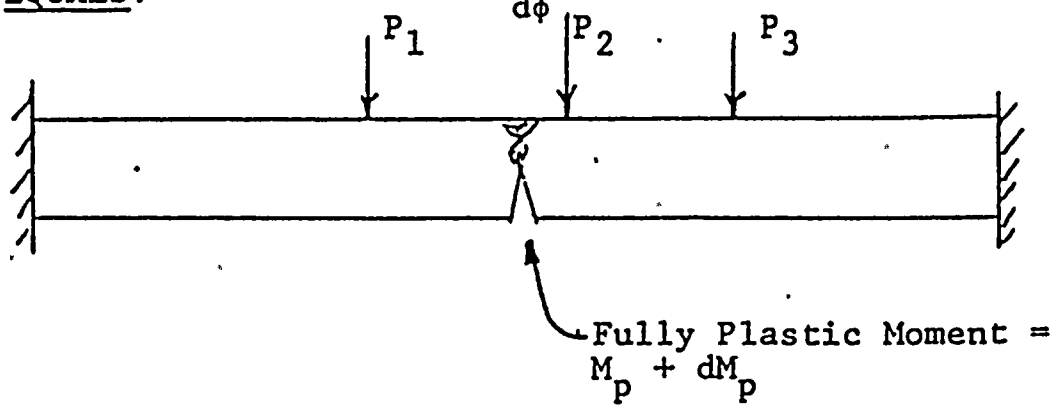

Figure 1c (Final State)

Figure D-1

Appendix E

APPLICATION OF TEARING STABILITY THEORY TO STRAIN HARDENING MATERIAL

In order to apply the tearing stability theory developed in Appendix D to real piping systems, it is necessary to evaluate in detail the various terms that appear in the tearing instability equation developed in Appendix D. Expressions for the J-integral and the plastic hinge angle for a single edge cracked plate have been developed by GE, Reference E-1, for the case of pure moment loading. Correction factors needed to relate these quantities to those for a cracked pipe (curvature effects factors) were developed by GE and applied by MPR in Reference E-2. Tearing stability calculations involve derivatives of J and the hinge angle, Φ, with respect to the crack size and applied moment. These derivatives will be taken explicitly.

For strain hardening materials that obey Ramberg-Osgood power law hardening,

$$\varepsilon/\varepsilon_o = \sigma/\sigma_o + \alpha(\sigma/\sigma_o)^n;$$ where α, n are material constants,

the J-integral and hinge angle can be expressed as follows (Reference E-1):

$$J = f_1(a)\frac{M^2}{E} + \alpha\sigma_o\varepsilon_o ch_1(a/b,n)(M/M_o)^{n+1}$$

$$\Phi = f_3(a)\frac{M}{E} + \alpha\varepsilon_o h_3(a/b,n)(M/Mo)^n$$

The first term in each expression is the elastic contribution and the second is the plastic contribution. Elastic solutions for J (that is, K^2/E) and the hinge angle are tabulated in handbooks, such as Reference E-3. From Reference E-3, for a single edge cracked plate of width b, crack depth a and thickness t, the elastic solution is found in the functions f_1 and f_3:

$$f_1 = \frac{36\pi a}{t^2 b^4} F^2$$

$$f_3 = \frac{24}{t b^2} S,$$

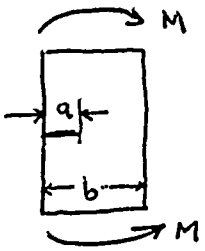

$$F(a/b) = 1.122 - 1.4\,a/b + 7.33(a/b)^2 - 13.08(a/b)^3 + 14.0(a/b)^4$$

$$S(a/b) = \left[\frac{a/b}{1-a/b}\right]^2 \left[5.93 - 19.69(a/b) + 37.14(a/b)^2 - 35.84(a/b)^3 + 13.12(a/b)^4\right]$$

Plastic contributions to J and Φ depend on the material constants α and n, yield stress σ_o, yield strain $\varepsilon_o = \sigma_o/E$, a tabulated function of a/b and n (h_1 or h_3) and the ratio of applied moment to the moment at which the cracked section goes completely plastic, Mo. Values of h_1 and h_3 are tabulated in Reference E-1:

h_1, h_2, h_3, AND h_5 FOR A SECP IN PLANE STRESS UNDER PURE BENDING

		n = 1	n = 2	n = 3	n = 5	n = 7	n = 10	n = 13	n = 15
a/b = 1/8	h_1	0.730	0.721	0.714	0.662	0.610	0.538	0.443	0.403
	h_2	7.306	7.118	6.947	6.273	5.639	4.827	3.926	3.527
	h_3	0.408	-0.128	-0.042	0.050	0.237	0.475	0.496	0.547
	h_5	0.000	0.482	0.415	0.338	0.286	0.226	0.171	0.147
a/b = 1/4	h_1	0.961	0.891	0.816	0.701	0.620	0.536	0.476	0.444
	h_2	6.136	5.211	4.567	3.659	3.089	2.562	2.228	2.060
	h_3	1.141	1.093	1.220	1.291	1.234	1.091	0.961	0.890
	h_5	0.000	0.764	0.647	0.507	0.427	0.359	0.316	0.295
a/b = 3/8	h_1	1.058	0.914	0.809	0.668	0.575	0.479	0.407	0.368
	h_2	5.494	4.150	3.417	2.590	2.133	1.719	1.440	1.294
	h_3	1.947	1.847	1.759	1.513	1.253	1.004	0.838	0.752
	h_5	0.000	0.908	0.738	0.562	0.470	0.387	0.329	0.298

Mo for the single edge cracked plate is defined from:

$$Mo = .267\ \sigma_o c^2 t, \text{ where } c = a - b$$

However, GE recommends using Mo for the equivalent 1/2 pipe:

$$Mo = 2R^2 t\sigma_o\ (\cos \gamma/2 - 1/2 \sin \gamma).$$

R is the pipe radius and γ is 1/2 the crack angle:

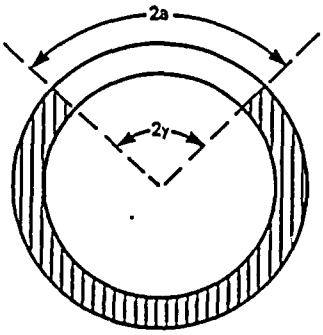

$\gamma = a/R$

a = 1/2 crack size,

The geometric relation between the single edge cracked plate and the pipe is shown below.

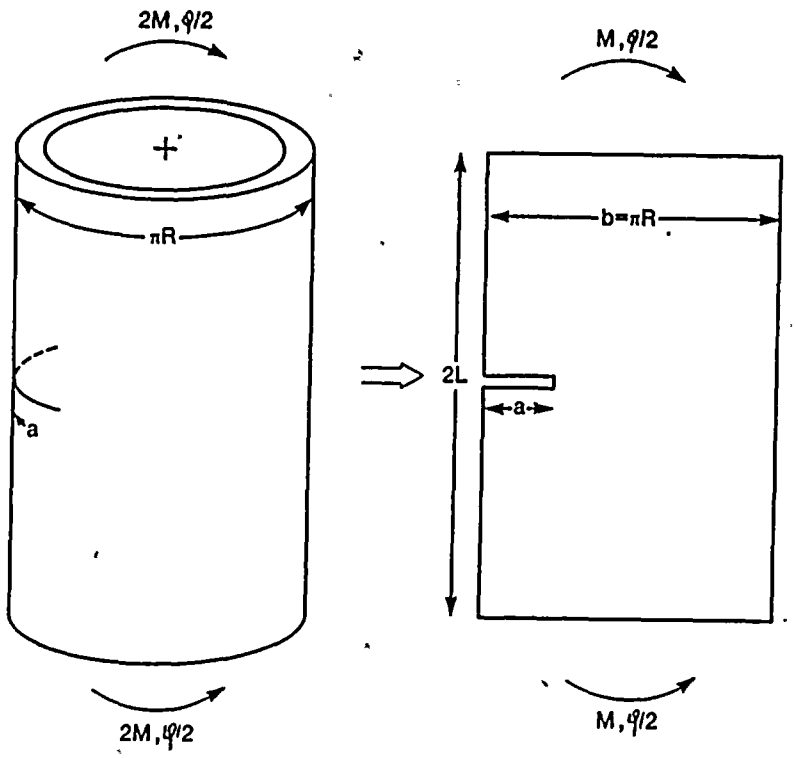

Note that the total hinge angle is Φ in both cases. GE in Reference E-4 developed one further correction factor to accomplish the plate-to-pipe transformation: 3-D finite element solutions (elastic) for J and Φ were ratioed to develop plate-to-pipe correction factors that are <u>assumed</u> to also apply plastically:

$$J_{pipe} = CF_1 \, J_{SECP}$$

$$\Phi_{pipe} = CF_2 \, \Phi_{SECP}$$

The correction factor CF_1 was developed for a range of a/b and R/t values, and was found in Reference E-2 to be expressible as a quadratic in the parameter $a/\sqrt{Rt} = X$:

$$CF_1 = B - C(X-A)^2,$$

where

$$A = .2 \; R/t + 1$$

$$B = .09 \; R/t + .75$$

$$C = .0035 \; R/t + .0825.$$

The correction factor, CF_2, was never quantified by GE, but can be found from work in Reference E-5 where 3-D finite

element solutions for Φ were plotted for both the shell and plate models for a/b ratios of 1/4 and 1/8 and a presumed R/t of 10:

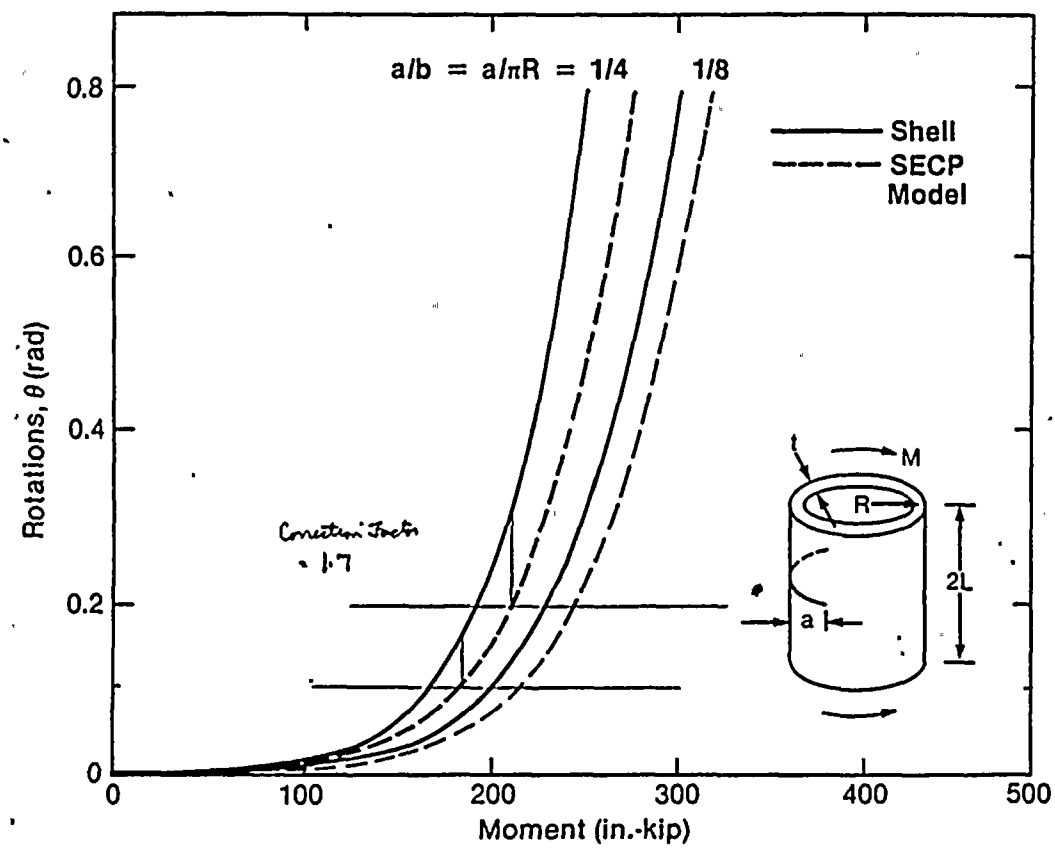

A correction factor, CF_2, of 1.7 appears appropriate for a/b = 1/4 over a range of hinge angles.

From Appendix D, the following stability criterion for plastic crack growth can be defined:

$$T_{MAT} > \frac{E}{\sigma_o^2}\frac{1}{t}\left[\left(\partial\varphi/\partial a\right)_{M_p}/\left(\partial\varphi/\partial M_p\right)_a\right]^2 \cdot \left[K_\varphi + 1/\left(\partial\varphi/\partial M_p\right)_a\right]^{-1} +$$

$$+ \frac{E}{\sigma_o^2}\left\{\left(\frac{\partial J}{\partial a}\right)_{M_p} - \left[\left(\partial\varphi/\partial a\right)_{M_p}/\left(\partial\varphi/\partial M_p\right)_a\right]\left(\frac{\partial J}{\partial M_p}\right)_a\right\}$$

The term K_Φ is developed from finite element analyses of the piping system into which the crack is embedded. Outside of this, four expressions need to be evaluated:

1. $\left(\frac{\partial\Phi}{\partial a}\right)_M$

2. $\left(\frac{\partial\Phi}{\partial M}\right)_a$

3. $\left(\frac{\partial J}{\partial a}\right)_M$

4. $\left(\frac{\partial J}{\partial M}\right)_a$

Each expression can be evaluated explicitly.

1. $\left(\frac{\partial\Phi}{\partial a}\right)_M$

Explicit derivatives of the Φ function involve the derivative of the function $h_3(a/b,n)$. However, it is found from the tabulated values of h_3 that this function varies rapidly (see Reference E-1) near crack sizes of interest ($a/b \sim .25$). Finding an accurate derivative is difficult. A better way is to use the expression relating to J to the Rice energy integral (Reference E-6):

$$J = \frac{1}{t}\int_0^M \left(\frac{\partial\Phi}{\partial M}\right)_a dM \qquad \text{(purely plastic)}$$

or

$$\frac{\partial \Phi}{\partial a})_M = t \frac{\partial J}{\partial M})_a \qquad \text{(purely plastic)}$$

This case, then, reduces to the case of evaluating expression number 4.

2. $\frac{\partial \Phi}{\partial M})_a$

$$\frac{\partial \varphi}{\partial M_p})_a = C F_2 \left[f_3/E + n \alpha \varepsilon_0 h_3 (a/b, n) \frac{1}{M} (M/M_0)^n \right]$$

3. $\frac{\partial J}{\partial a})_M$

$$\frac{\partial J}{\partial a})_{M_p} = C F_1 \left\{ \frac{df_1}{da} \frac{M^2}{E} + \alpha \sigma_0 \varepsilon_0 (M/M_0)^{n+1} \left[\left(c \frac{dh_1}{da} - h_1 \right) - c(n+1) h_1 \frac{1}{M_0} \frac{dM_0}{da} \right] \right\} + J \frac{dCF_1}{da}$$

We note from page E-2:

$$\frac{df_1}{da} = \frac{36\pi}{t^2 b^4} F^2 + \frac{72\pi a}{t^2 b^5} F F', \text{ where } F' = \frac{dF}{d(a/b)}$$

and $F' = -1.4 + 14.66(a/b) - 39.24(a/b)^2 + 56(a/b)^3$.
Also, $\frac{dh_1}{da}$ is obtainable from tabulated values of h_1. Since Mo is a function of the crack size, its derivative must be evaluated:

$$Mo = 2R^2 t \sigma_o \, (\cos \gamma/2 - 1/2 \sin \gamma); \text{ where } \gamma = a/R,$$

then,

$$\frac{1}{Mo} \frac{dMo}{da} = \frac{-1/2 \sin \gamma/2 \frac{d\gamma}{da} - 1/2 \cos \gamma \frac{d\gamma}{da}}{\cos \gamma/2 - 1/2 \sin \gamma}$$

or

$$\frac{1}{Mo}\frac{dMo}{da} = \frac{-1}{2R}\left[\frac{\sin \gamma/2 + \cos \gamma}{\cos \gamma/2 - 1/2 \sin \gamma}\right]$$

Finally, from page E-4,

$$\frac{dCF_1}{da} = 2C\ (X - A)\ \frac{dX}{da}\ , \text{ or}$$

$$\frac{dCF_1}{da} = 2C\ (X - A)\ \frac{1}{\sqrt{Rt}}$$

4. $\left.\frac{\partial J}{\partial M}\right)_a$

$$\left.\frac{\partial J}{\partial M_p}\right)_a = CF_1 \left\{ 2f_1 M/E + (n+1)\alpha \sigma_0 \varepsilon_0 C\, h_1(a/b, n)\, \frac{1}{M}\, (M/M_0)^{n+1} \right\}$$

Attachment E-1 is a list of the computer program "PIPES," which evaluates the Appendix D tearing instability criterion using the terms evaluated above.

References

E-1 V. Kumar, W. W. Wilkening, W. R. Andrews, M. D. German, H. G. deLorenzi and D. F. Mowbray, "Estimation Technique for Prediction of Elastic-Plastic Fracture of Structural Components of Nuclear Systems," Contract RP1237-1 (EPRI) Combined Fifth and Sixth Semiannual Report, February 1, 1981 to January 31, 1982.

E-2 MPR calculation "Elastic-Plastic J-Integral Program JINT," by J. E. Nestell dated 4/28/84.

E-3 H. Tada, P. Paris and G. Irwin, The Stress Analysis of Cracks Handbook (Del Research Corp., St. Louis) 1973, pp 2.13-2.14.

E-4 V. Kumar, M.D. German and C. F. Shih, "An Engineering Approach to Elastic-Plastic Fracture Analysis," EPRI NP-1931, July 1981.

E-5 M. D. German, W. R. Andrews, V. Kumar, C. F. Shih, H. G. deLorenzi, and D. F. Mowbray, "Elastic-Plastic Fracture Analysis of Flawed Stainless Steel Pipes," EPRI NP-2608LD, Final Report September 1982.

E-6 J. W. Hutchinson and P. C. Paris, "Stability Analysis of J-Controlled Crack Growth," ASTM STP 668, 1979, p. 37.

Attachment E-1

```
10 KEY OFF:CLS:COLOR 7,0,0:DEFSNG A-Z
19 PRINT "                  ************************************"
20 PRINT "                  ELASTIC-PLASTIC TEARING MODULUS THEORY"
21 PRINT "                  ************************************"
22 PRINT :PRINT "                        VERSION 1.1  (LAST MODIFIED 6/27/84)"
23 PRINT :PRINT "                         DEVELOPED BY DR. JAMES NESTELL"
24 PRINT :PRINT
26 FOR I=1 TO 11
27 PRINT :NEXT I
28 PRINT "press any key to continue....."
30 W$=INKEY$
40 IF W$="" GOTO 30
45 CLS
80 INPUT "SYSTEM NAME";N$
90 PRINT
100 INPUT "CARBON OR STAINLESS STEEL (C/S)";M$
110 FLAG=0
120 IF M$="S" GOTO 210
130 '******* MATERIAL PROPERTIES *******
140 SF=43600!
150 S0=27100!
160 E=2.7E+07
170 AL=1.94
180 N=4.42
200 GOTO 260
210 SF=42000!
220 S0=23000!
230 E=2.56E+07
240 AL=2.13
250 N=3.79
260 E0=S0/E
270 CLS
280 '******* PIPE AND FLAW GEOMETRY *******
290 INPUT "PIPE DIAMETER  (INCHES) = ";D
320 R=D/2
325 PRINT
330 INPUT "WALL THICKNESS  (INCHES) = ";T
370 I=3.1416*(R^4-(R-T)^4)/4
380 A=3.1416*R/4
390 B=4*A
400 C=B-A
410 G=3.1416/4
420 '******* TABULAR FUNCTIONS *******
430 Z=.25
440 F=1.122-1.4*Z+7.33*Z*Z-13.08*(Z^3)+14*(Z^4)
450 FP=-1.4+14.66*Z-39.24*Z*Z+56*(Z^3)
460 F1=36*3.1416*A*F*F/(B^4)
470 DF1DA=F1/A+72*3.1416*A*F*FP/(B^5)
480 Z1=(1-Z)*(1-Z)
490 S=(Z*Z/Z1)*(5.93-19.69*Z+37.14*Z*Z-35.84*(Z^3)+13.12*(Z^4))
500 Z=Z+.01
510 Z1=(1-Z)*(1-Z)
520 S1=(Z*Z/Z1)*(5.93-19.69*Z+37.14*Z*Z-35.84*(Z^3)+13.12*(Z^4))
530 SP=100*(S1-S)
540 F3=24*S/(B*B)
550 DF3DA=24*SP/(B^3)
```

```
560 IF M$="S" GOTO 620
570 H1=.734
580 H1P=-.2
590 H3=1.27
610 GOTO 670
620 H1=.771
630 H1P=-.144
640 H3=1.248
660 '******* CORRECTION FACTOR MODEL *******
670 X1=R/T
680 X=A/SQR(R*T)
690 A1=.2*X1+1
700 B1=8.999999E-02*X1+.75
710 C1=.0035*X1+.0825
720 CF=B1-C1*(X-A1)*(X-A1)
730 CFP=-2*C1*(X-A1)
740 DCFDA=(X/A)*CFP
750 '******* MO AND 1/MODMODA = M1 *******
760 TRIG=COS(G/2)-.5*SIN(G)
770 MO=2*SO*R*R*T*TRIG
780 M1=(-1/(2*R))*(SIN(G/2)+COS(G))/TRIG
790 '******* CALC DH1DA *******
800 DH1DA=(1/B)*H1P
820 CLS
830 '*******CALCULATE J INTEGRAL *******
840 INPUT "L/R =";LR
860 LEFF=R*LR
870 CLS
875 IF FLAG=1 THEN 910
880 INPUT "M/MO =";MMO
900 CLS
910 M=MO*MMO
920 JE=CF*F1*((M/T)^2)/E
930 JP=CF*AL*SO*EO*C*H1*(MMO)^(N+1)
940 J=JE+JP
950 '******* CALCULATE DJDA AT M *******
960 DJDAE=CF*DF1DA*((M/T)^2)/E
970 Y=C*DH1DA-H1-C*(N+1)*H1*M1
980 DJDAP=CF*AL*SO*EO*Y*(MMO)^(N+1)
990 DJDACF=J*DCFDA/CF
1000 DJDA=DJDAE+DJDAP+DJDACF
1010 '******* TEARING MODULUS********
1020 DJDME=2*CF*F1*M/(T*T*E)
1030 DJDMP=CF*(N+1)*AL*SO*EO*C*H1*((MMO)^(N+1))/M
1040 DJDM=DJDME+DJDMP
1050 DFCDME=1.7*F3/(T*E)
1060 DFCDMP=1.7*N*AL*EO*H3*((MMO)^N)/M
1070 DFCDM=DFCDME+DFCDMP
1090 DFCDAE=1.7*DF3DA*M/(T*E)
1100 DFCDAP=T*DJDMP
1110 DFCDA=DFCDAE+DFCDAP
1130 CONST=E/(SO*SO)
1140 RATIO=DFCDA/DFCDM
1150 KEFF=E*I/LEFF
1160 DMDF=1/DFCDM
1170 DJDAF=DJDA-RATIO*DJDM
```

```
1180 CONST1=(1/T)*CONST
1190 NUM=CONST1*RATIO*RATIO
1200 DENOM=KEFF+DMDF
1210 T1=NUM/DENOM+CONST*DJDAF
1220 '******* OUTPUT **********
1225 CLS
1230 PRINT "    PIPES     (VERSION 1.1, 6/27/84)"
1240 PRINT :PRINT
1260 C$="CARBON STEEL"
1270 S$="STAINLESS STEEL"
1280 IF M$="S" GOTO 1350
1300 PRINT N$
1310 PRINT
1320 PRINT C$
1330 GOTO 1380
1350 PRINT N$
1360 PRINT
1370 PRINT S$
1380 PRINT "D = ";D;" INCHES"
1390 PRINT "T = ";T;" INCHES"
1400 PRINT "COLLAPSE/YIELD = ";INT(100*SF/SO+.5)/100
1410 PRINT
1420 PRINT "LOAD/YIELD LOAD = ";MMO
1430 PRINT "L/R = ";LR
1440 PRINT
1450 PRINT "J = ";INT(J+.5);" IN-LB/IN**2"
1455 PRINT "T =";INT(T1+.5)
1460 PRINT "DJDA = ";INT(SO*SO*T1/E+.5);" IN-LB/IN**2-IN"
1463 HINGE=97.4*AL*EO*H3*MMO^N
1465 PRINT "HINGE ANGLE = ";:PRINT USING "##.###";HINGE;:PRINT " DEGREES"
1470 PRINT
1480 PRINT
1482 Q$=INKEY$
1484 IF Q$="" THEN 1482
1490 INPUT "ANOTHER LOAD (Y/N)";Y$
1510 IF Y$="Y" OR Y$="y" THEN FLAG=0:GOTO 870
1520 INPUT "ANOTHER L/R (Y/N)";Z$
1540 IF Z$="Y" OR Z$="y" THEN FLAG=1:GOTO 820
1545 INPUT "RESTART FROM BEGINNING  (Y/N)";Z$
1547 IF Z$="Y" OR Z$="y" THEN 45
1550 SYSTEM
1555 END
```

Appendix F

J_{IC} AND TEARING MODULUS FOR A106 GrB CARBON STEEL AND TYPE 304 STAINLESS STEEL

Values for J_{IC}, the J value corresponding to crack initiation, and T_{MAT}, the tearing resistance of a material, were obtained from test data presented in Reference F-1, which presents J vs Δa test data for A106 steel and cast stainless steel at various temperatures. Cast metal data is used for stainless steel because test data shows it has less tearing resistance than stainless steel pipe, and it is chemically similar to weld metal. It is expected that the cast material represents stainless weld metal tearing resistance properties. The approximate operating temperature of most high energy piping systems at Nine Mile Point Unit 1 is 550°F. Therefore, test data obtained at this temperature proved to be most relevant.

J_{IC} is defined at the point the J vs. Δa curve leaves the blunting line, that is, at the point of initiation of crack growth. A survey of all the test data presented in Reference F-1 and other references was conducted. As a result, the following minimum (conservative) values of J_{IC} for A106 and stainless steel weld metal were identified for use in the leak-before-break analyses:

$$\text{A106:} \quad J_{IC} = 903 \ \frac{\text{in-lb}}{\text{in}^2}$$

$$\text{304 Weld Metal:} \quad J_{IC} = 992 \ \frac{\text{in-lb}}{\text{in}^2}$$

T_{MAT} was obtained by fitting the J vs. Δa test data to obtain $\frac{dJ}{da}$ ($T = \frac{E}{\sigma_o^2} \frac{dJ}{da}$). The values of $\frac{dJ}{da}$ reported in Reference F-1 correspond to a fit of test data between crack extensions of 0.015" and 0.060". These values, however, tend to be greater than values of $\frac{dJ}{da}$ which can be obtained at crack extensions above 0.1". In fact, for crack extensions of 0.1", $\frac{dJ}{da}$ appears to be a constant, independent of further crack extension or increase in J. This phenomena was noticed in virtually all tests reported in Reference F-1. For this reason, minimum $\frac{dJ}{da}$ values fit at significant crack extensions were used. Figures F-1 and F-2 show the test data (from Reference F-1) used to fit $\frac{dJ}{da}$ for A106 carbon steel and type 304 casting material, respectively. Values for the elastic modulus and yield strength for the two materials were obtained from References F-2 and F-3, and the following values of T_{MAT} were determined:

Material	σ_o (ksi)	E (ksi)	$\frac{dJ}{da}$ (psi)	T_{MAT}
A106	27.1	27.0×10^3	5833	215
Cast Stainless	23.0	25.6×10^3	3750	182

References

F-1 NUREG/CP-0024, Vo. 3, Ninth Water Reactor Safety Research Information Meeting, Oct. 26-30, 1981, "J-R Curve Characteristics of Piping Material and Welds," J. Gudas.

F-2 1980 ASME Boiler and Pressure Vessel Code, Appendices.

F-3 Department of Defense Aerospace Structural Metals Handbook, Vol. 2, Code 1303, page 15, figure 3.03131.

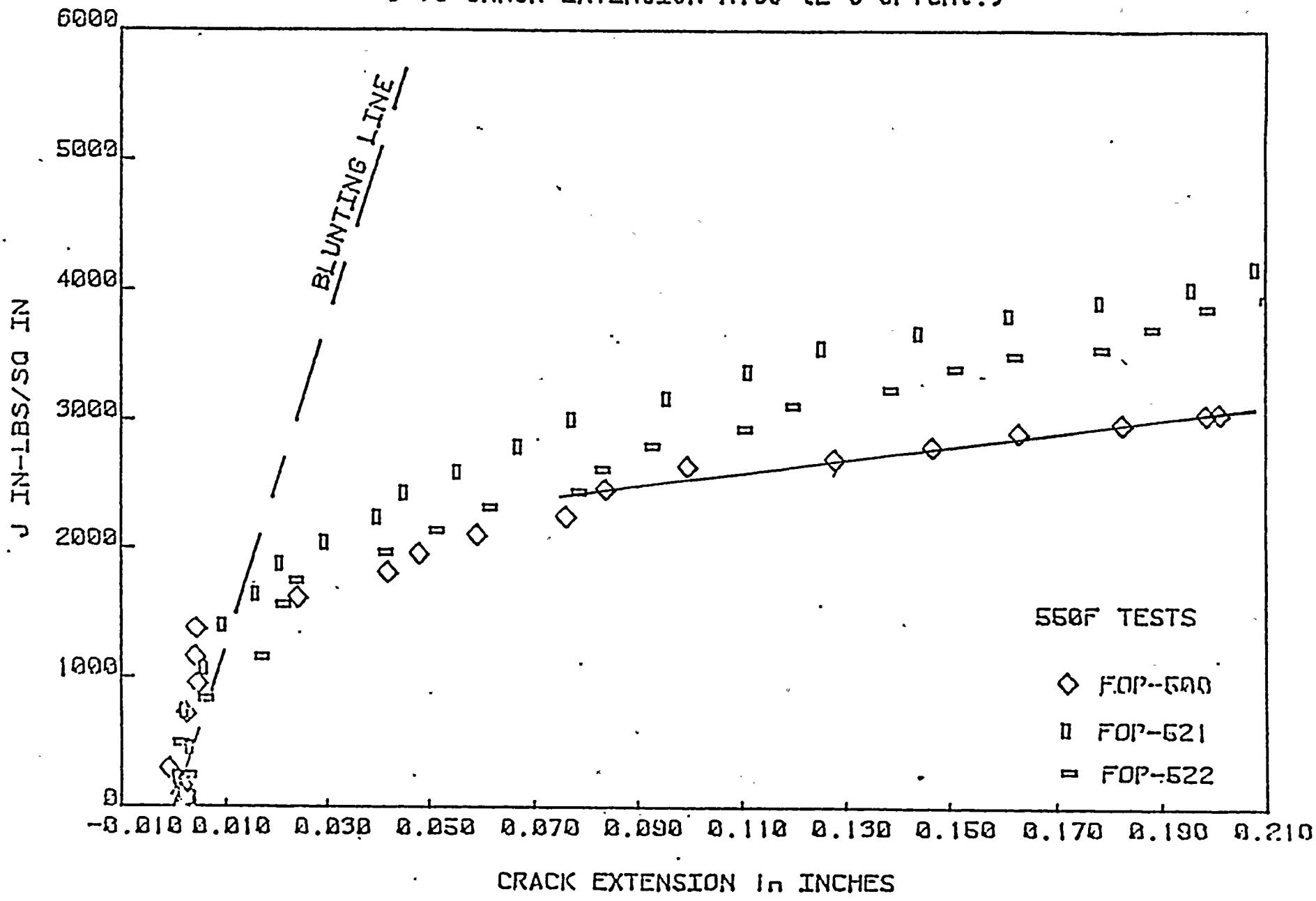
J vs CRACK EXTENSION A106 (L-C Orient.)
6000
5000
4000
3000
2000
1000
0
J IN-LBS/SQ IN
BLUNTING LINE
550F TESTS
FOP-520
FOP-521
FOP-522
-0.010
0.010
0.030
0.050
0.070
0.090
0.110
0.130
0.150
0.170
0.190
0.210
CRACK EXTENSION In INCHES

Figure F-1

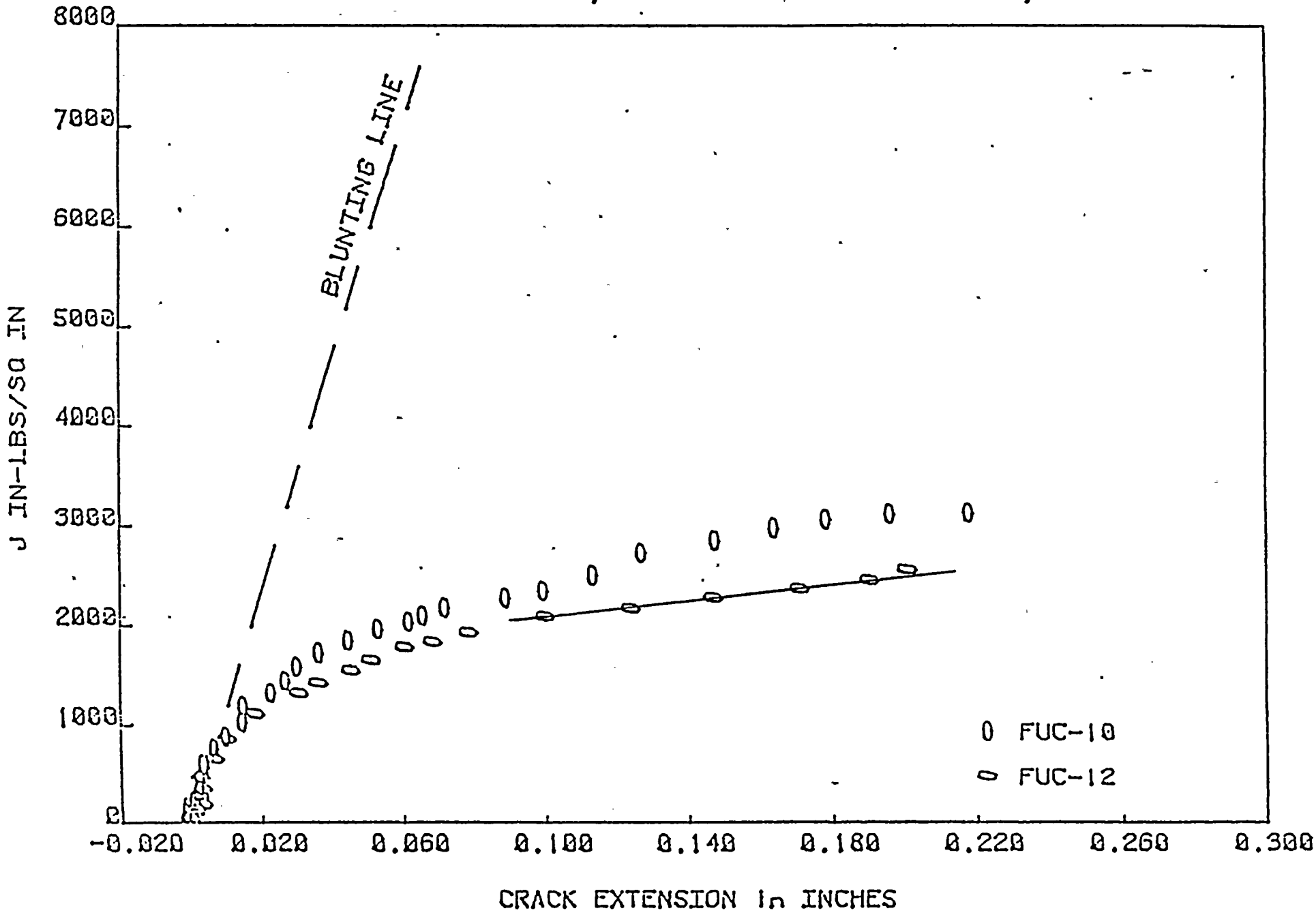
J vs CRACK EXTENSION, CF8A STAINLESS STEEL WELD,550F
8000
7000
6000
5000
4000
3000
2000
1000
0
J IN-LBS/SQ IN
BLUNTING LINE
0 FUC-10
o FUC-12
-0.020
0.020
0.060
0.100
0.140
0.180
0.220
0.260
0.300
CRACK EXTENSION In INCHES

Figure F-2